A-767

GEORGIA INSTITUTE OF TECHNOLOGY
ENGINEERING EXPERIMENT STATION
ATLANTA, GEORGIA 30332
May 4, 1964

George C. Marshall Space Flight Center
National Aeronautics and Space Administration
Huntsville, Alabama 35812

Attention: Mr. James W. Fletcher
Contracting Officer

Subject: Monthly Progress Report No. 1, Project No. A-767
Contract No. NA58-11159
"Analytical Mechanical Model for the Description of the Rotary Propellant Sloshing Motion"
Covering the Period April 1, 1964 to May 1, 1964

Gentlemen:

During the period of April 1, 1964 to May 1, 1964, all known available literature on the problem of rotary sloshing has been obtained and studied. The object of the immediate investigation was then to determine the type of nonlinearities that should be included in the analytical mechanical model. Since rotary sloshing of the fluid with a free fluid surface occurs already for a container undergoing lateral harmonic motion of small amplitudes in the immediate vicinity of the lowest antisymmetric sloshing frequency, and since usually small vibration amplitudes are encountered in actual flights of missiles and space vehicles, it was decided to include only the non-linearities due to the wave heights and fluid velocities, thus considering the excitation amplitude small compared to the tank diameter.

Rotary sloshing occurs not only in circular cylindrical containers, but also in rectangular containers, indicating that tank geometry and viscosity have only minor effects on its creation. The potential theory results can therefore be employed for the determination of the mechanical model.

Before proceeding to the description of the rotary sloshing fluid motion with an analytical mechanical model, the pressure distribution along the tank wall and container bottom has to be derived and computed. From this the liquid force and liquid moment can be obtained by integration of the appropriate pressure components along the container walls.

No difficulties have been encountered during this period.

Respectfully submitted,

Helmut F. Bauer
Project Director

HFB/c

REVIEW
PATENT 5-12 1964 BY

A-101

GEORGIA INSTITUTE OF TECHNOLOGY

ENGINEERING EXPERIMENT STATION

ATLANTA, GEORGIA 30332

June 5, 1964

George C. Marshall Space Flight Center
National Aeronautics and Space Administration
Huntsville, Alabama 35812

Attention: Mr. James W. Fletcher
Contracting Officer

Subject: Monthly Progress Report No. 2, Project No. A-767
Contract No. NA58-11159
"Analytical Mechanical Model for the Description of the Rotary Propellant Sloshing Motion"
Covering the Period May 1, 1964 to June 1, 1964

Gentlemen:

During the period of May 1, 1964 to June 1, 1964, several possible analytical models were investigated in an attempt to find a model exhibiting as nearly as possible the same non-linearities observed for the fluid at large amplitudes.

The spring mass system was abandoned because further investigation revealed that the vertical displacement of the slosh mass center of gravity could not be neglected for large amplitudes.

An investigation of the motion of the slosh mass center of gravity revealed that the motion is closely approximated by a mass point moving in a paraboloid subjected to a small harmonic displacement. Approximate solutions to the non-linear differential equation have, thus far, exhibited the desired characteristics, namely, those of a softening system for the planar oscillations, and those of a hardening system for the rotary motion.

At present, it appears that close agreement between experimental data and the analytical solution for the paraboloid model can be obtained.

Respectfully submitted,

Helmut F. Bauer
Project Director

HFB/c

GEORGIA INSTITUTE OF TECHNOLOGY
ENGINEERING EXPERIMENT STATION
ATLANTA, GEORGIA 30332
July 1, 1964

George C. Marshall Space Flight Center
National Aeronautics and Space Administration
Huntsville, Alabama 35812

Attention: Mr. James W. Fletcher
Contracting Officer

Subject: Monthly Progress Report No. 3, Project No. A-767
Contract No. NA58-11159
"Analytical Mechanical Model for the Description of the Rotary Propellent Sloshing Motion"
Covering the Period of June 1, 1964 to July 1, 1964

Gentlemen:

During the period from June 1, 1964 to July 1, 1964, the non-linear characteristics of the mass point paraboloid model were investigated. The amplitude-frequency relation showed good agreement with available experimental data for the planar motion of the fluid surface, including stability boundaries. Comparisions made with the theoretical values obtained through the inclusion of non-linear terms in the free-surface conditions also showed good agreement with the model values for both the amplitudes and stability boundaries.

In order to obtain agreement for the rotary motion, it appears necessary to also include non-linear springs which will introduce the "hardening" necessary for the desired amplitude-frequency relation.

It appears, at present, that the model thus obtained will accurately describe all observed fluid motions and will predict fluid amplitudes, forces and moments within required accuracy.

Respectfully submitted,

Helmut F. Bauer
Project Director

HFB/CDC/c

GEORGIA INSTITUTE OF TECHNOLOGY
ENGINEERING EXPERIMENT STATION
ATLANTA, GEORGIA 30332

August 5, 1964

George C. Marshall Space Flight Center
National Aeronautics and Space Administration
Huntsville, Alabama 35812

Attention: Mr. James W. Fletcher
Contracting Officer

Subject: Monthly Progress Report No. 4, Project No. A-767
Contract No. NA58-11159
"Analytical Mechanical Model for the Description of the Rotary Propellent Sloshing Motion"
Covering the Period from July 1, 1964 to August 1, 1964

Gentlemen:

The period from July 1 to August 1, 1964, was devoted principally to the incorporation of damping in the paraboloid model described briefly in previous progress letters. An investigation of the stability boundaries with damping included was conducted in order to determine, theoretically, the effect of the damping on the amplitudes and frequencies at which instability of the planar motion occurs. The results have shown that small damping does not appreciably change the stability boundaries. The stability boundaries for the undamped rotary motion of the fluid have also been determined theoretically, and an investigation of the damped rotary motion is in progress.

Equations of motion for pitching excitation have been derived and the non-linear response obtained.

All results obtained from the model equations have thus far shown good agreement with available experimental data.

Respectfully submitted,

Helmut F. Bauer
Project Director

HFB/CDC/c

GEORGIA INSTITUTE OF TECHNOLOGY
ENGINEERING EXPERIMENT STATION
ATLANTA, GEORGIA 30332
August 31, 1964

George C. Marshall Space Flight Center
National Aeronautics and Space Administration
Huntsville, Alabama 35812

Attention: Mr. James W. Fletcher
Contracting Officer

Subject: Monthly Progress Report No. 5, Project No. A-767
Contract No. NA58-11159
"Analytical Mechanical Model for the Description of the Rotary Propellent Sloshing Motion"
Covering the Period from August 1, 1964 to September 1, 1964

Gentlemen:

The period from August 1 to September 1, 1964, was devoted to an investigation of the effects of damping on the rotary motion of the propellant. The inclusion of damping in the non-linear equations necessitates the solving of four simultaneous, non-linear, algebraic equations in order to obtain the rotary response. Various iteration procedures are being used in an attempt to obtain the damped rotary response, using the undamped response as the starting point for the iteration procedure. Results, thus far, indicated that such a procedure will converge to the damped solution in frequency regions where stable rotary motion is possible.

Respectfully submitted,

Helmut F. Bauer
Project Director

HFB/CDC/c

GEORGIA INSTITUTE OF TECHNOLOGY
ENGINEERING EXPERIMENT STATION
ATLANTA, GEORGIA 30332

October 7, 1964

George C. Marshall Space Flight Center
National Aeronautics and Space Administration
Huntsville, Alabama 35812

Attention: Mr. James W. Fletcher
Contracting Officer

Subject: Monthly Progress Report No. 6, Project No. A-767
Contract No. NA58-11159
"Analytical Mechanical Model for the Description of the Rotary Propellent Sloshing Motion"
Covering the Period from September 1 to October 1, 1964

Gentlemen:

During the period September 1, to October 1, 1964, several methods were investigated for solving the similtaneous, non-linear, algebraic equations which resulted from the inclusion of damping in the differential equations of motion for the model. The Newton-Raphson method gave rapid convergence when the undamped response was used as the starting point for the iteration procedure.

A non-iterative procedure for determining the damped rotary response is, of course, desirable; consequently, various approximations which will facilitate the determining of the damped rotary amplitudes are under investigation.

Respectfully submitted,

Helmut F. Bauer
Project Director

HFB/CDC/c

GEORGIA INSTITUTE OF TECHNOLOGY
ATLANTA, GEORGIA 30332

SCHOOL OF
ENGINEERING MECHANICS

October 30, 1964

George C. Marshall Space Flight Center
National Aeronautics and Space Administration
Huntsville, Alabama 35812

Attention: Mr. James W. Fletcher
Contracting Officer

Subject: Monthly Progress Report No. 7, Project No. A-767
Contract No. NAS8-11159
"Analytical Mechanical Model for the Description of the Rotary Propellent Sloshing Motion"
Covering the Period from October 1 to November 1, 1964

Gentlemen:

During the period of October 1 to November 1, 1964, the complete mechanical analogy for the description of the liquid in a cylindrical container of circular cross section has been derived. This model describes the observed nonlinear phenomena associated with the sloshing of the liquid. The liquid in the lower part of the container follows the motion like a rigid body and is therefore described by a fixed mass with a moment of inertia. For pitching excitation about the origin, not all of the fluid is participating in the motion, but a part remains completely at rest. For this reason a frictionlessly mounted massless sphere with the moment of inertia, I_s, has been introduced. For the x- and y-direction a dashpot is connected to the sphere and to the container bottom. The slosh masses move on paraboloids and are connected with a third order spring which slides along the vertical axis.

With the help of the Lagrange equations the complete nonlinear set of equations of motion has been derived. This set consists of the force equation, moment equation, sphere equations in both directions, an infinite number of equations for the slosh masses in x-direction and in infinite number of equations for the slosh masses in y-direction.

Respectfully submitted,

Helmut F. Bauer
Project Director

HFB:bm

GEORGIA INSTITUTE OF TECHNOLOGY
ATLANTA, GEORGIA 30332

SCHOOL OF
ENGINEERING MECHANICS

December 1, 1964

George C. Marshall Space Flight Center
National Aeronautics and Space Administration
Huntsville, Alabama 35812

Attention: Mr. James W. Fletcher
Contracting Officer

Subject: Monthly Progress Report No. 8, Project No. A-767
Contract No. NAS8-11159
"Analytical Mechanical Model for the Description of the Rotary Propellent Sloshing Motion"
Covering the Period from November 1 to December 1, 1964

Gentlemen:

During the period of November 1 to December 1, 1964, the mechanical analogy has been checked for its correctness.

Furthermore some thought has been given to the technique of equivalent linearization of the nonlinear mechanical model analogy. This seems to be of importance in order to preserve the powerful methods for the solution of the systems of differential equations for the complete motion of the space vehicle, since most of the equations are given in linearized form and since at the present time only a method for the determination of the stability of the space vehicle which is based on linear theory is present at MSFC. An equivalent linear mechanical model was derived for planar motion and shall be completed in the next period.

Respectfully submitted,

Helmut F. Bauer
Project Director

HFB:bm

GEORGIA INSTITUTE OF TECHNOLOGY
ENGINEERING EXPERIMENT STATION
ATLANTA, GEORGIA 30332

January 5, 1965

George C. Marshall Space Flight Center
National Aeronautics and Space Administration
Huntsville, Alabama 35812

Attention: Mr. James W. Fletcher
Contracting Officer

Subject: Monthly Progress Report No. 9, Project No. A-767
Contract No. NA58-11159
"Analytical Mechanical Model for the Description of the Rotary Propellent Sloshing Motion"
Covering the Period from December 1, 1964 to January 1, 1965

Gentlemen:

During the period of December 1, 1964, to January 1, 1965, an equivalent linear mechanical model was derived for planar motion. The equivalent damping coefficient and equivalent spring stiffness of the mechanical model describing the nonlinear planar liquid motion have been obtained with the Kryloff and Bogoliuboff Method. The equivalent damping coefficient was obtained to be

$$\bar{c}_n = c_n (1 + \alpha_n X^2)$$

and the equivalent spring stiffness

$$\bar{k}_n = k_{on} + \alpha_n \frac{k_n}{4} X^2 + \frac{\alpha_n^2}{2} \omega_n^2 X^2$$

where X is the amplitude of the motion.

This yields from the nonlinear sloshing equation of the form

$$m_n \ddot{x}_n + c_n \dot{x}_n (1 + 4\alpha_n^2 x_n^2) + \alpha_n k_n x_n^3 + k_{on} x_n + 4\alpha_n^2 (x_n \dot{x}_n^2 + x_n^2 \ddot{x}_n) = -\ddot{x}$$

the equivalently linearized sloshing equation

$$m_n \ddot{x}_n + \bar{c}_n \dot{x}_n + \bar{k}_n x_n = -\ddot{x}$$

REVIEW
PATENT 1-16 1965 BY
FORMAT 1-16 1965 BY

which is

$$m_n \ddot{x}_n + c_n (1 + \alpha_n^2 X^2) \dot{x}_n + \left[k_{on} + \frac{\alpha_n}{2} X^2 \left(\frac{k_n}{2} + \alpha_n \omega_n^2 \right) \right] x_n = -\ddot{x}$$

No difficulties have been encountered during this period.

Respectfully submitted,

Helmut F. Bauer
Project Director

HFB/c

GEORGIA INSTITUTE OF TECHNOLOGY
ENGINEERING EXPERIMENT STATION
ATLANTA, GEORGIA 30332

February 3, 1965

George C. Marshall Space Flight Center
National Aeronautics and Space Administration
Huntsville, Alabama 35812

Attention: Mr. James W. Fletcher
Contracting Officer

Subject: Monthly Progress Report No. 10, Project No. A-767
Contract No. NA58-11159
"Analytical Mechanical Model for the Description of the Rotary Propellent Sloshing Motion"
Covering the Period from January 1, 1965 to February 1, 1965

Gentlemen:

During the period January 1, 1965 to February 1, 1965, the results of an investigation of the response of a spherical pendulum to excitation of the suspension point were compared with the results obtained for the paraboloid model. Since the pendulum has been treated as an analytical model for the linearized fluid theory, its possibility as a non-linear model was of interest. A comparison of the results obtained from the pendulum and paraboloid model with the available experimental data showed, however, that the pendulum model does not accurately predict the fluid amplitude and frequency at which instability of the planar motion occurs. Also, the amplitudes of rotary motion of the pendulum model do not agree with those observed experimentally. The paraboloid model, however, shows good agreement with experimental amplitudes and stability boundaries.

Respectfully submitted,

Helmut F. Bauer
Project Director

HFB/CDC/c

REVIEW
PATENT 2-14 1965 BY
FORMAT 2-14 1965 BY

GEORGIA INSTITUTE OF TECHNOLOGY
ENGINEERING EXPERIMENT STATION
ATLANTA, GEORGIA 30332

March 1, 1965

George C. Marshall Space Flight Center
National Aeronautics and Space Administration
Huntsville, Alabama 35812

Attention: Mr. James W. Fletcher
Contracting Officer

Subject: Monthly Progress Report No. 11, Project No. A-767
Contract No. NA58-11159
"Analytical Mechanical Model for the Description of the Rotary Propellant Sloshing Motion"
Covering the Period from February 1, 1965 to March 1, 1965

Gentlemen:

During the period of February 1, 1965 to March 1, 1965, a refined investigation of the presented mechanical model as to its solution was performed.

In the previous work that has been performed to date the approximate solution was always considered of harmonic form. The nonlinear character of the governing differential equations indicates that this assumed form of the approximate solution can be improved by the inclusion of some superharmonic terms. Thus the effect of these terms was investigated. The results of an analysis including the first odd superharmonic term exhibited that its effect is of the order of only one percent of the harmonic term. From these results it could be concluded that the amplitude of the one-term harmonic solution is of sufficient accuracy.

Respectfully submitted,

Helmut F. Bauer
Project Director

HFB/c

GEORGIA INSTITUTE OF TECHNOLOGY
ENGINEERING EXPERIMENT STATION
ATLANTA, GEORGIA 30332

April 1, 1965

George C. Marshall Space Flight Center
National Aeronautics and Space Administration
Huntsville, Alabama 35812

Attention: Mr. James W. Fletcher
Contracting Officer

Subject: Monthly Progress Report No. 12, Project No. A-767
Contract No. NA58-11159
"Analytical Mechanical Model for the Description of the Rotary Propellant Sloshing Motion"
Covering the Period from March 1, 1965 to April 1, 1965

Gentlemen:

During the period March 1, 1965 to April 1, 1965, the equations of motion of a space vehicle have been partly derived with the complete incorporation of the nonlinear model. Furthermore, various results have been checked to be made ready for the final report.

The next month's effort will be devoted to the completion of the equations of motion of a space vehicle with the nonlinear slosh model and to the simplified equations of motion in the pitch-plane with the equivalent linearized slosh model.

Respectfully submitted,

Helmut F. Bauer
Project Director

HFB/c

GEORGIA INSTITUTE OF TECHNOLOGY
ENGINEERING EXPERIMENT STATION
ATLANTA, GEORGIA 30332

May 4, 1965

George C. Marshall Space Flight Center
National Aeronautics and Space Administration
Huntsville, Alabama 35812

Attention: Mr. James W. Fletcher
Contracting Officier

Subject: Monthly Progress Report No. 13, Project No. A-767
Contract No. NA58-11159
"Analytical Mechanical Model for the Description of the Rotary Propellant Sloshing Motion"
Covering the Period from April 1, 1965, to May 1, 1965

Gentlemen:

During the period April 1, 1965 to May 1, 1965 the equations of motion of a space vehicle with the complete incorporation of the nonlinear model have been derived. They also have been presented with the equivalent linearized slosh model. Furthermore the final report has been started and shall be completed during the next month's period.

Respectfully submitted,

Helmut F. Bauer
Project Director

HFB/c

FINAL REPORT

PROJECT A-767

ANALYTICAL MECHANICAL MODEL FOR THE DESCRIPTION OF THE ROTARY PROPELLANT SLOSHING MOTION

By: Helmut F. Bauer, Charles D. Clark, and James H. Woodward

Contract NAS8-11159

Prepared for
George C. Marshall Space Flight Center
National Aeronautics and Space Administration
Huntsville, Alabama

May 31, 1965

Engineering Experiment Station
GEORGIA INSTITUTE OF TECHNOLOGY
Atlanta, Georgia

Table of Contents

List of Figures

Nomenclature

D	Dissipation function
F	Thrust
I	Moment of inertia of vehicle about mass center of vehicle
T	Kinetic energy
V	Potential energy
I_E	Moment of inertia of engine about mass center of engine
I_o	Moment of inertia of nonvibrating rigid mass about its center of mass
I_s	Moment of inertia of sphere
J_1	Bessel Function of first kind of first order
Q_i	Generalized force
Y_ν	νth bending mode in xy plane
Z_ν	νth bending mode in xz plane
a	Tank radius
g	Longitudinal acceleration
h	Liquid height
m	Total mass of vehicle
r, θ, z	Cylindrical coordinates
t	Time
c_n	Damping coefficient of nth mode
$\overline{c}_n$	Equivalent linear damping coefficient of nth mode
c_s	Damping coefficient of sphere damper
k_n	Spring constant of nth mode
$\overline{k}_n$	Equivalent linear spring constant of nth mode

ℓ_E	Distance of the mass center of engine to the swivel point
m_n	Mass of nth sloshing mode
m_o	Nonvibrating rigid mass
m_E	Total mass of engines
m_{SE}	Total mass of swivel engines
q_i	Generalized coordinate
r_{cg}	Radial displacement of the liquid center of gravity
x_{cg}	Longitudinal displacement of the liquid center of gravity
x_n, y_n, z_n	Coordinates of the nth sloshing mass
$\bar{x}$	Free fluid surface displacement, measured from the undisturbed position
y_o, z_o	Amplitude of excitation
Ω	Forcing frequency
η_n	Ratio of the forcing frequency to the nth natural frequency of the fluid
ϖ	Pitching angle
χ	Yawing angle
γ_n	Damping factor of nth mode
ϵ_n	Roots of $J_1'(\epsilon) = 0$
η_ν	Generalized coordinate of νth bending mode in the xy plane
ζ_ν	Generalized coordinate of νth bending mode in the xa plane
ω_n	Eigenfrequency of liquid
φ_o	Amplitude of rotational excitation about z-axis
χ_o	Amplitude of rotational excitation about y-axis
ψ_1, ψ_2	Rotation angles of sphere relative to tank bottom

Summary

An analytical mechanical model has been derived that describes the non-linear liquid behavior in a cylindrical container of circular cross section. The model consists of a mass with a moment of inertia rigidly connected to the container and of independently oscillating mass points for each vibration mode rolling on a guiding surface of paraboloidal form. Each of these mass points is coupled with a nonlinear spring capable of moving up and down the longitudinal axis of the container. It was found that a third order spring describes the rotary sloshing (which occurs in a forcing frequency range shortly after resonance) best. The model is simple and describes the motion of the liquid as well as points of instability very well. It exhibits quite an improved response compared to the spherical pendulum model. Since sufficient nonlinear theoretical data are not at the present time available for comparison purposes, one of the nonlinear model parameters had to be obtained from available experimental data.

An equivalent linear model was derived for the incorporation in a linear control feedback and response analysis. The equations of motion of a space vehicle were presented with a nonlinear slosh model and with equivalently linearized slosh equations.

1. Introduction

All experimental studies concerned with liquid sloshing due to lateral periodic excitations have revealed a peculiar type of liquid motion and liquid instability near the lowest resonant frequency of the fluid. It has been observed that this type of sloshing motion of the liquid also occurs in containers on non-circular cross-section as, for instance, in rectangular tanks, indicating that the container geometry is of no decisive influence on the occurance of such a motion. The essential feature of this motion is the fact that shortly before resonance the liquid ceases to oscillate about its nodal diameter which is perpendicular to the excitation direction. First an erratic motion of the free fluid surface is observed, which finally, after a further increase of excitation frequency, will exhibit a fluid motion having a rotating nodal diameter. This motion invariably occurs whether or not the liquid has any initial rotation [1]. It can, however, be initiated at any earlier excitation frequency by introducing some additional rotational motion of the liquid, as it could happen during the drainage of the container by the formation of a vortex. Since this phenomenon can nearly be eliminated by proper annular ring-baffles at the container wall which may provide appropriate damping and thus smaller surface amplitudes of the liquid, the problem is recognized as being created essentially by the non-linear effects of the fluid motion.

For a circular cylindrical container undergoing translatory excitation, Hutton [2] presented some theory about the surface motion and compared it with experimental results. No attempt, however, was made to determine the pressure distribution, the liquid force and moment. Some theoretical and experimental data concerning the response function of the fluid force

have been given by Abramson, Chu and Kana [3]. The analysis as well as the experiments show that there are three basic regions of liquid motion:

1. Stable planar motion
2. Erratic fluid surface motion in a narrow frequency band before the resonsance, i.e. unstable motion in which the motion of the nodal diameter changes constantly.
3. Stable nonplanar motion in a certain frequency band immediately above resonance.

For simplification in the treatment of the equations of motion of large liquid-propelled missiles and space vehicles, an equivalent mechanical model that should describe the motion of the liquid has to be employed. In a frequency range outside a certain domain around the resonance of the liquid the usual sloshing motion is maintained about a stationary nodal line. The response of the propellant in this frequency region can be closely predicted by linear theory, and by a mechanical model based on linearized theory [4]. This model consists essentially of a suitable mass with moment of inertia that is rigidly attached to the tank wall, and independently oscillating sloshing masses for each vibration mode which are attached through springs to the container walls. Instead of a mass-spring-system one can also employ a mathematical pendulum model. In the neighborhood of the natural frequency, however, these models cannot accurately describe the observed motion of the liquid. A first attempt was made by Berlot 5 and Freed 6 with a spherical pendulum. As is known, a spherical pendulum with sinusoidally excited support will deviate from its planar motion in the plane of excitation as soon as the excitation frequency approaches the natural frequency of the system. The linearized theory of such a parametrically excited system, however, can give only a rough representation

of the actual rotary sloshing motion of the liquid. It is able to predict only the general behavior of the motion.

Since the phenomenon involves essentially non-linear effects, an extension of the theory of the spherical pendulum [7] involving non-linear terms in the amplitude seemed logical, and it provided a fair approximation for the description of the liquid phenomenon. This non-linear analysis exhibits the same three types of motion as the liquid system. It also established [2] that the rotary motion arises as a consequence of a nonlinear coupling between liquid motion parallel and perpendicular to the plane of excitation, and that this coupling takes place through the free fluid surface waves. The results of these investigations exhibit clearly the liquid behavior in stable planar motion as to be that of a softening restoring characteristic, and that of a hardening characterisitc for non-planar motion. Experimental data reveal that the predicted non-planar motion is in poor agreement with the experimental points.

In the following, a mechanical model is derived which shall describe the motion of the liquid and the points of instability more accurately than all previous attempts. It consists of a mass having moment of inertia and rigidly attached to the container wall, and independently oscillating mass points for each vibration mode rolling on a guiding surface of paraboloidal shape. Each of these mass points is coupled with a non-linear spring capable of moving up and down the longitudinal axis of the container, providing the necessary hardening effect for the rotary sloshing. The complete mechanical model is derived and compared with available experimental results. Finally the equations of motion of a space vehicle with the nonlinear mechanical model included are derived and presented.

2. Derivation of the Mechanical Analogy

The introduction of a nonlinear spring in the usual spring-mass system describing linearized sloshing cannot account for the rotary motion and a true description of the nonlinear effects of the liquid since these types of models would neglect the important vertical displacement of the center of gravity of the liquid. Since the vertical shifting of the center of gravity of the liquid is significant for large amplitudes of the liquid surface, a pendulum performing large angular displacements would be a good first approximation for the description of the liquid. It also shows a softening restoring characteristic, thus behaving like the liquid in the container which exhibits a decrease of natural frequency with increasing wave amplitude for increasing forcing frequency below the fundamental resonance. Although the spherical pendulum yields a region of unstable motion and a domain of rotary motion and has a behavior similar to the motion of the liquid, the predicted boundaries of instability are in rather poor agreement with experimental results. For this reason, the search for a more comprehensive mechanical model was performed. In the "design" of the mechanical model, two basic features had to be observed: 1) the mechanical model should exhibit basically the same features as the liquid, i.e. it should show the same region of softening response, unstable motion, and hardening rotary motion, and, 2) it should remain simple enough not to further complicate the equations of motion of a complete space vehicle. A sliding mass point on some guiding surface with an additional nonlinear spring attached to the mass should conform to the given requirements. Since the first sloshing mode plays the predominant role in circular cylindrical containers (the masses of higher modes are all below 3% of that of the first

sloshing mode) we concentrate on the description of the liquid in that particular vibration mode.

The free fluid surface displacement as measured from the undisturbed liquid position is, for translatory excitation, given by [4] :

$$(2.1)\quad \bar{X}(r,\theta,t) = \frac{\Omega^2}{g/a}\, y_o e^{i\Omega t} \cos\theta \left\{ r/a + 2 \sum \frac{J_1(\epsilon_n\, r/a)\eta_n^2}{(\epsilon_n^2 - 1)J_1(\epsilon_n)(1 - \eta_n^2)} \right\}$$

where Ω is the forcing frequency, g the longitudinal acceleration, and x_o the forcing amplitude. The value $\eta_n = \Omega/\omega_n$ is the ratio of forcing frequency to the nth natural frequency of the liquid and a is the radius of the container. The expression ϵ_n represents the zeros of the first derivative of the Bessel function of first kind and first order ($J_1'(\epsilon_n) = 0$; $n = 1, 2, \ldots$). Representing (r/a) as a Bessel-series (Dini-Series)

$$r/a = 2 \sum \frac{J_1(\epsilon_n\, r/a)}{(\epsilon_n^2 - 1)\, J_1(\epsilon_n)}$$

and introducing it into the infinite series yields

$$\bar{X}(r,\theta,t) = \frac{2\Omega^2 y_o e^{i\Omega t}}{g/a} \cos\theta \sum \frac{J_1(\epsilon_n\, r/a)}{(\epsilon_n^2 - 1)J_1(\epsilon_n)(1 - \eta_n^2)}$$

The square of the natural circular frequency is given by

$$\omega_n^2 = (g/a)\,\epsilon_n \tanh(\epsilon_n\, h/a)$$

Retaining only the predominant first mode, the free fluid surface shape becomes

$$(2.2) \qquad \bar{X} = \bar{X}_w \frac{J_1(\epsilon_1 r/a)}{J_1(\epsilon_1)} \cos\theta$$

where $\bar{X}_w = \frac{2\Omega^2 y_o e^{i\Omega t}}{g/a(\epsilon_1^2 - 1)(1 - \eta_1^2)}$ represents the fluid amplitude at the wall of the container in the plane of excitation. From this the radial and vertical displacement of the center of gravity of the liquid is determined and yields

$$(2.3) \qquad r_{cg} = \frac{1}{\pi a^2 h} \int_o^a \int_o^{2\pi} \int_{-h/2-\bar{x}}^{h/2} r^2 \cos\theta \, dr \, d\theta \, dx = a/h\epsilon_1^2 \; \bar{X}_w$$

and

$$(2.4) \qquad x_{cg} = \frac{-1}{\pi a^2 h} \int_o^a \int_o^{2\pi} \int_{-h/2-\bar{x}}^{h/2} xr\,dr\,d\theta\,dx = -\frac{(\epsilon_1^2 - 1)}{4\,\epsilon_1^2 h} \bar{X}_w^2$$

where the integral relations

$$\int_o^a r^2 J_1(\epsilon_1 r/a)dr = \frac{a^3 J_1(\epsilon_1)}{\epsilon_1^2}$$

and

$$\int_o^a r\, J_1^2(\epsilon_1 r/a)dr = \tfrac{1}{2} a^2 \frac{(\epsilon_1^2 - 1)}{\epsilon_1^2} J_1^2(\epsilon_1)$$

have been used. Both values r_{cg} and x_{cg} are measured from the position of the center of gravity of the undisturbed liquid. Eliminating $\bar{x}_w$ from equations (2.3) and (2.4) yields the motion of the center of gravity in the form

$$(2.5) \qquad x_{cg} = -(C/2a) r_{cg}^2$$

where $C = \frac{(\epsilon_1^2 - 1)\epsilon_1^2 h}{2a}$.

The liquid in the lower part of an oscillating container behaves like a rigid body, and only that part of the liquid which is in the proximity of the surface oscillates in a manner which is dependent on the forcing frequence. Therefore, the liquid system can be described by a non-sloshing mass with moment of inertia and rigidly connected to the container and a sloshing mass point which performs oscillations while constrained by a guiding paraboloid. This system, consisting of only a mass point constrained by a paraboloid, will exhibit free rotary motion at a single frequency. No unique amplitude, however, can be determined. For this reason a nonlinear spring providing a restoring force proportional to some power of the radial displacement was introduced and provides the necessary "hardening" for the proper description of the rotary motion of the fluid. The slosh mass is attached to the spring, the other end of which is constrained to move frictionlessly up and down the center axis of the tank (Figure 1).

2.1. Nonlinear Mechanical Slosh Model for Translatory Excitation

In the following section we shall restrict our treatment to only the sloshing mass representing the first vibration mode of the liquid. The analytical model will be designed such that it will represent the same effect as the well known linear mechanical models for oscillations of small amplitude response. The sloshing part of the liquid may be represented by a liquid volume of height, h_s, corresponding to the modal sloshing mass, m_s. The ratio of the first modal sloshing mass, m_s, to the total liquid mass, m, is equal to the ratio of the height of the sloshing part of the liquid, h_s, to the total liquid height, h, i.e. [4].

$$(2.6) \quad h_s/h = m_s/m = \frac{2 \tanh(\epsilon_1 h/a)}{\epsilon_1 h/a(\epsilon_1^2 - 1)}$$

The displacement of the center of gravity of the sloshing part of the liquid is, therefore, with (2.5)

$$(2.7) \quad r_s = \frac{a}{\epsilon_1^2 h_s} \bar{X}_w = \frac{(\epsilon_1^2 - 1)\bar{X}_w}{2\epsilon_1 \tanh(\epsilon_1 h/a)}$$

and

$$x_s = -\frac{(\epsilon_1^2 - 1)\bar{X}_w^2}{4\epsilon_1^2 h_s} = -\frac{(\epsilon_1^2 - 1)^2 \bar{X}_w^2}{8a\ \epsilon_1 \tanh(\epsilon_1 h/a)}$$

which yield

$$x_s = -(C_s/2a) r_s^2$$

where $C_s = \epsilon_1 \tanh(\epsilon_1 \frac{h}{a})$. We proceed now to the derivation of the equations of motion of the slosh mass.

2.1.1. Equations of Motion

The equations of motion are derived with the help of the Lagrange equation. The above described model subjected to a translational excitation in y-direction is employed. Viscous damping is introduced by assuming that the mass point is subjected to a damping force proportional to its velocity relative to the paraboloid.

The expression for the kinetic energy is given by

$$T = \tfrac{1}{2} m_s \left[(\dot{y}_s - \Omega\, y_o \cos \Omega\, t)^2 + \dot{z}_s^2 + \dot{x}_s^2 \right]$$

or, by the introduction of the equation of constraint,

$$(2.8) \qquad f_s \equiv x_s - C_s/2a\ (y_s^2 + z_s^2) = 0\ ,$$

the kinetic energy of the slosh mass yields

$$(2.9) \qquad T = \tfrac{1}{2}m_s\ [(\dot{y}_s - \Omega\ y_o\ \cos\ \Omega\ t)^2 + \dot{z}_s^2 + \frac{C_s^2}{a^2}\ (y_s\dot{y}_s + z_s\dot{z}_s)^2]$$

The potential energy is given by

$$V = -m_s g x_s + \int_o^{r_s} k_s r_s^{2n-1}\, dr_s\ ,$$

which yields, with the equation of constraint, (2.8)

$$(2.10) \qquad V = \frac{m_s g C_s}{2a}\ (y_s^2 + z_s^2) + k_s/2n\ (y_s^2 + z_s^2)^n$$

The first term is the gravitational potential while the last term represents the energy stored in the nonlinear spring of order (2n-1).

The dissipation function is

$$D = \tfrac{1}{2}\overline{C}_s(\dot{x}_s^2 + \dot{y}_s^2 + \dot{z}_s^2)$$

and, with $\overline{C}_s = 2m_s\omega_s\gamma_s$ and the equation of constraint, becomes

$$(2.11) \qquad D = m_s\omega_s\gamma_s[\dot{y}_s^2 + \dot{z}_s^2 + \frac{c_s^2}{a^2}(y_s\dot{y}_s + z_s\dot{z}_s)^2]$$

The introduction of these expressions into the Lagrange equation

$$\frac{d}{dt}\ (\partial T/\partial\dot{q}_i) - \partial T/\partial q_i + \partial D/\partial\dot{q}_i + \partial V/\partial q_i = Q_i$$

yields, with $q_1 = y_s$ and $q_2 = z_s$, the equations of motion

$$\ddot{y}_s + 2\omega_s\gamma_s[\dot{y}_s + \frac{C_s^2}{a^2}(y_s^2\dot{y}_s + y_s z_s \dot{z}_s)] + \frac{C_s^2}{a^2}[y_s^2\ddot{y}_s + y_s\dot{y}_s^2 + y_s z_s \ddot{z}_s + y_s\dot{z}_s^2]$$

$$+ \omega_s^2[1 + \frac{k_s}{m_s\omega_s^2}(y_s^2 + z_s^2)^{n-1}]y_s = \Omega^2 y_o \cos \Omega t$$

and

$$\ddot{z}_s + 2\omega_s\gamma_s[\dot{z}_s + \frac{C_s^2}{a^2}(z_s^2\dot{z}_s + z_s y_s \dot{y}_s)] + \frac{C_s^2}{a^2}[z_s^2\ddot{z}_s + z_s\dot{z}_s^2 + z_s y_s \ddot{y}_s$$

$$+ z_s\dot{y}_s^2] + \omega_s^2[1 + \frac{k_s}{m_s\omega_s^2}(y_s^2 + z_s^2)^{n-1}]z_s = 0$$

With the dimensionless quantities

$$\eta_s = \frac{y_s}{a}, \quad \zeta_s = \frac{z_s}{a}, \quad \text{and} \quad \alpha_s = \frac{k_s a^{2n-2}}{m_s\omega_s^2},$$

the above equations of motion yield

$$\ddot{\eta}_s + 2\omega_s\gamma_s[\dot{\eta}_s + C_s^2(\eta_s^2\dot{\eta}_s + \eta_s\zeta_s\dot{\zeta}_s)] + C_s^2[\eta_s^2\ddot{\eta}_s + \eta_s\dot{\eta}_s^2 + \eta_s\zeta_s\ddot{\zeta}_s$$

$$+ \eta_s\dot{\zeta}_s^2] + \omega_s^2[1 + \alpha_s(\eta_s^2 + \zeta_s^2)^{n-1}]\eta_s = \Omega^2(y_o/a)\cos\Omega t \tag{2.12}$$

and

$$\ddot{\zeta}_s + 2\omega_s\gamma_s[\dot{\zeta}_s + C_s^2(\zeta_s^2\dot{\zeta}_s + \eta_s\dot{\eta}_s\zeta_s)] + C_s^2[\zeta_s^2\ddot{\zeta}_s + \zeta_s\dot{\zeta}_s^2 + \eta_s\ddot{\eta}_s\zeta_s + \dot{\eta}_s^2\zeta_s]$$

$$+ \omega_s^2[1 + \alpha_s(\eta_s^2 + \zeta_s^2)^{n-1}]\zeta_s = 0 \tag{2.13}$$

These equations govern the motion of the slosh mass due to translatory excitation, $y_o \cos\Omega t$ of the system.

Although the nonlinear spring contributes to the nonlinearity of the above equations, the principal nonlinear terms are those resulting from the vertical motion of the mass point. It can be seen that linearization of these equations yields the results of reference [4] (equation (54)). The linearized equations are

$$\ddot{\eta}_s + 2\omega_s\gamma_s\dot{\eta}_s + \omega_s^2\eta_s = \Omega^2(y_o/a)\cos\Omega t$$

and

$$\ddot{\zeta}_s + 2\omega_s\gamma_s\dot{\zeta}_s + \omega_s^2\zeta_s = 0$$

The first equation represents the motion of the slosh mass in the y-direction of excitation, while the second equation is the free oscillation equation in the z-direction (perpendicular to the excitation direction). As can be seen, the linearized equations are not coupled.

Similar results can be obtained for a rotational excitation mode such as pitching or yawing. For pitching oscillations the velocity components of the mass point (Figure 2) are

$$\begin{aligned} v_x &= \dot{x}_s + y_s\dot{\varphi} \\ v_y &= \dot{y}_s + (\ell_s - x_s)\dot{\varphi} \\ v_z &= \dot{z}_s \end{aligned}$$

The kinetic energy of the mass point during pitching excitation is then

given by

$$(2.14)\qquad T = \frac{m_s}{2}\{[\frac{C_s}{a}(y_s\dot{y}_s+z_s\dot{z}_s) - y_s\dot{\varphi}]^2 + [\dot{y}_s + \ell_s\dot{\varphi} + \frac{C_s}{2a}(y_s^2+z_s^2)\dot{\varphi}]^2 + \dot{z}_s^2\}$$

The potential energy yields

$$V = m_s g[\frac{C_s}{2a}(y_s^2+z_s^2)\cos\varphi - \ell_s(1-\cos\varphi) - y_s\sin\varphi] + \frac{k_s}{2n}(y_s^2+z_s^2)^n]$$

which, for small angular displacements, becomes

$$(2.15)\qquad V = m_s g[\frac{C_s}{2a}(y_s^2+z_s^2)(1-\frac{\varphi^2}{2}) - \frac{\ell_s}{2}\varphi^2 - y_s\varphi] + \frac{k_s}{2n}(y_s^2+z_s^2)^n$$

Introducing these and the previous dissipation function into the Lagrange equation, nondimensionalizing, and neglecting higher order terms such as $\varphi_o^2\eta_s$, $\varphi_o\eta_s\zeta_s$, etc., the equations of motion for pitching excitations, $\varphi=\varphi_o\cos\Omega t$, are

$$(2.16)\qquad \ddot{\eta}_s+2\omega_s\gamma_s[\dot{\eta}_s+C_s^2(\eta_s\dot{\eta}_s+\eta_s\zeta_s\dot{\zeta}_s)]+C_s^2[\eta_s^2\ddot{\eta}_s+\eta_s\dot{\eta}_s^2+\eta_s\zeta_s\ddot{\zeta}_s+\eta_s\dot{\zeta}_s^2]$$
$$+\omega_s^2[1+\alpha_s(\eta_s^2+\zeta_s^2)^{n-1}]\eta_s = \Omega^2\varphi_o\frac{\ell_s}{a}\cos\Omega t+\frac{g}{a}\varphi_o\cos\Omega t$$

and

$$(2.17)\qquad \ddot{\zeta}_s+2\omega_s\gamma_s[\dot{\zeta}_s+C_s^2(\zeta_s\dot{\zeta}_s+\eta_s\zeta_s\dot{\eta}_s)]+C_s^2[\zeta_s^2\ddot{\zeta}_s+\zeta_s\dot{\zeta}_s^2+\eta_s\ddot{\eta}_s\zeta_s+\zeta_s\dot{\eta}_s^2]$$
$$+\omega_s^2[1+\alpha_s(\eta_s^2+\zeta_s^2)^{n-1}]\zeta_s = 0$$

Again it can be seen that the linearized equations reduce to those of

reference [4], (equation (54) for pitching excitation.

$$\ddot{\eta}_s+2\omega_s\gamma_s\dot{\eta}_s+\omega_s^2\eta_s = \Omega^2 \frac{\ell_s}{a} \varphi_o \cos \Omega t+g/a\ \varphi_o \cos \Omega t$$

and

$$\ddot{\zeta}_s+2\omega_s\gamma_s\dot{\zeta}_s+\omega_s^2\zeta_s = 0$$

are the linearized equations and exhibit no coupling.

2.1.2. Solution of the Equations of Motion

Of the various methods used in obtaining an approximate soluttion to a system of nonlinear differential equations the averaging procedure of Ritz seems to be the most appropriate one.

2.1.2.1. Undamped Planar Motion

If the liquid performs planar motion, i.e. if there is a stationary nodal line perpendicular to the direction of excitation, the coordinate ζ_s can be set equal to zero. Therefore, an undamped motion ($\gamma_s = 0$), the equation of motion for translatory excitation reduces to

$$D[\eta_s,t] \equiv \ddot{\eta}_s+C_s^2[\eta_s^2\ddot{\eta}_s+\eta_s\dot{\eta}_s^2]+\omega_s^2[1+\alpha_s\eta_s^{2n-2}]\eta_s-\Omega^2\ y_o/a \cos \Omega t = 0$$

An approximate solution of the steady state motion is given by

$$\bar{\eta}_s = A \cos \Omega t \ , \tag{2.18}$$

and, (with $\Omega t = \tau$), the Ritz condition,

$$\int_o^{2\pi} D[\bar{\eta}_s,\tau]\cdot\cos \tau\ d\tau = 0 \ ,$$

yields

$$\int_0^{2\pi} \{-A\Omega^2 \cos^2\tau + C_s^2[-A^3\Omega^2\cos^4\tau + A^3\Omega^2\cos^2\tau \sin^2\tau] + \omega_s^2[A\cos^2\tau + \alpha_s A^{2n-1}\cos^{2n}\tau]$$

$$-\Omega^2(y_o/a)\cos^2\tau\}d\tau = 0$$

After evaluating the integrals with

$$\int_0^{2\pi} \cos^{2n}\tau \, d\tau = \frac{\pi(2n)!}{2^{2n-1}(n!)^2}$$

and $\eta^2 = \frac{\Omega^2}{\omega_s^2}$, the expression for the frequency response function is

(2.19) $$\eta^2 = A\left\{\frac{1+\alpha_s \frac{A^{2n-2}(2n)!}{2^{2n-1}(n!)^2}}{\{A+\frac{1}{2}C_s^2A^3 \pm y_o/a\}}\right\}$$

where the plus and minus signs in the denominator determine the response curve to the left and right of the backbone curve, respectively (in and out of phase with the excitation function). For a cubic spring, i.e. n = 2, the frequency response function is

(2.20) $$\eta^2 = \frac{A[1+(3/4)\alpha_s A^2]}{A+\frac{1}{2}C_s^2A^3 \pm (y_o/a)} \quad ,$$

while for a spring of fifth order (n = 3), the frequency response function yields the expression

$$\eta^2 = \frac{A[1+(5/8)\alpha_s A^4]}{A+\frac{1}{2}C_s^2A^3 \pm (y_o/a)}$$

The nondimensional spring constant, α_s, must be determined.

For purposes of comparison with experimental data, most of the calculations were performed for the test tank used by Hutton [2] and for an

excitation amplitude, y_o = 0.032 in. The tank has a radius a = 5.938 in., and a fluid depth, h = 8.907 in. With the use of equation (2.7) the fluid amplitude at the wall of the container was determined and graphed versus η^2. Comparison with Hutton's test results reveals that α_s should be about 2/3 for the cubic spring and about 6.5 for the fifth order spring.

The response curves for planar motion are shown in figure (3) using the above values for α_s. The dashed line represents the response function of the linearized fluid theory while the dotted line is the backbone curve of the model with a spring of fifth order. The results of the pendulum are also indicated as the dash-dotten line and exhibit a noticeable deviation.

A better approximation can be achieved by including an additional term in the assumed approximate solution, i.e. employing a more-term-approximation of the form

$$\bar{\eta}_s = A \cos \Omega t + B \cos 3\Omega t$$

With this assumption the Ritz conditions for the determination of the unknowns A and B are

$$\int_o^{2\pi} D[\bar{\eta}_s, \tau] \cos \tau \, d\tau = 0$$

and

$$\int_o^{2\pi} D[\bar{\eta}_s, \tau] \cos 3\tau \, d\tau = 0 ,$$

and yield two simultaneous nonlinear algebraic equations in A and B. For n = 2, i.e. a cubic nonlinear spring, the resulting equations are

$$A\,(1/\eta^2 - 1) - C_s^2[\tfrac{1}{2}A^3+(3/2)A^2B+5AB^2]+\frac{\alpha_s}{\eta^2}\,[(3/4)A^3+(3/4)A^2B+(3/2)AB^2] = y_o/a$$

and

$$B(1/\eta^2 - 9) - C_s^2[\tfrac{1}{2}A^3+5A^2B+(9/2)B^2]+\frac{\alpha_s}{\eta^2}[\tfrac{1}{4}A^3+(3/2)A^2B+(3/4)B^3] = 0$$

These nonlinear algebraic equations for A and B as functions of η^2 were solved by the Newton-Raphson method. The resulting solutions indicated that the maximum magnitude of B is less than 1% of the value of A over the frequency range $0.5 \leq \eta^2 \leq 1.4$. From this we can conclude that the harmonic solution represents a very good approximation and definitely provides an acceptable degree of accuracy. This further substantiated by a comparison with the response wave form obtained with an analog computer (see figure 4).

2.1.2.2. Undamped Nonplanar Motion

As has been mentioned previously, for a narrow exciting frequency range that extends slightly above the linear resonance the liquid exhibits a motion which is characterized by a steady rotation of the nodal diameter of the fluid surface. This is a stable nonplanar motion which is also termed "rotary sloshing." In this case the perpendicular coordinate ζ is no longer zero, and the coupled equations (2.12) and (2.13) must be solved simultaneously. For undamped nonplanar motion, the damping factor $\gamma_s = 0$. Again the Ritz Averaging Method is employed for the solution of this system of two coupled nonlinear equations

$$D_1[\eta_s,\zeta_s,t] = \ddot{\eta}_s+C_s^2[\eta_s^2\ddot{\eta}_s+\eta_s\dot{\eta}_s^2+\eta_s\zeta_s\ddot{\zeta}_s+\eta_s\dot{\zeta}_s^2]+\omega_s^2[1+\alpha_s(\eta_s^2+\zeta_s^2)]\eta_s$$

$$-\Omega^2(y_o/a)\cos\Omega t = 0$$

and

$$D_2[\eta_s,\zeta_s,t] = \ddot{\zeta}_s+C_s^2[\zeta_s^2\ddot{\zeta}_s+\zeta_s\dot{\zeta}_s^2+\zeta_s\eta_s\ddot{\eta}_s+\zeta_s\dot{\eta}_s^2] +\omega_s^2[1+\alpha_s(\eta_s^2+\zeta_s^2)]\zeta_s = 0$$

With an assumed approximate solution

$$\bar{\eta}_s = A\cos\Omega t \tag{2.21}$$

$$\bar{\zeta}_s = E\sin\Omega t \quad ,$$

the Ritz conditions

$$\int_0^{2\pi} D_1[\bar{\eta}_s,\bar{\zeta}_s,\tau]\cdot\cos\tau\, d\tau = 0$$

and

$$\int_0^{2\pi} D_2[\bar{\eta}_s,\bar{\zeta}_s,\tau]\cdot\sin\tau\, d\tau = 0$$

yield the system of simultaneous, nonlinear algebraic equations

$$-A\eta^2-\frac{C_s^2}{2}A\eta^2[A^2-E^2]+A\left[1+\frac{\alpha_s}{\pi}\sum_{\lambda=1}^{n-1}\binom{n-1}{\lambda}A^{2\lambda}E^{2n-2\lambda-2}\int_0^{2\pi}\cos^{2n+2}\tau\sin^{2n-2\lambda-2}\tau\, d\tau\right] = r^2(y_o/a) \tag{2.22}$$

$$-E\eta^2+\frac{C_s^2}{2}E\eta^2[A^2-E^2]+E\left[1+\frac{\alpha_s}{\pi}\sum_{\lambda=1}^{n-1}\binom{n-1}{\lambda}A^{2\lambda}E^{2n-2\lambda-2}\int_0^{2\pi}\cos^{2\lambda}\tau\sin^{2n-2\lambda}\tau\, d\tau\right] = 0 \quad , \tag{2.23}$$

where $\binom{n-1}{\lambda}$ is the binomial coefficient defined by

$$\binom{n-1}{\lambda} = \frac{(n-1)(n-2)\ldots(n-\lambda)}{\lambda!} = \frac{(n-1)!}{\lambda!\,(n-\lambda-1)!}$$

With the following results for the integrals which occur:

$$\int_0^{2\pi}\cos^{2n+2}\tau\sin^{2n-2\lambda-2}\tau\, d\tau = \frac{\pi(2\lambda+1)!(2n-2\lambda-3)!}{2^{2n-3}\,n!(\lambda-1)!(n-\lambda-1)!}$$

$$\int_0^{2\pi} \cos^{2\lambda}\tau \, \sin^{2n-2\lambda}\tau \, d\tau = \frac{\pi(2\lambda-1)!(2n-2\lambda-1)!}{2^{2n-3}\, n!(\lambda-1)!(n-\lambda-1)!}$$

the algebraic equations (2.22) and (2.23) yield

$$(2.24)\quad -A\eta^2 - \frac{C_s^2 A\eta^2}{2}[A^2-E^2] + A\left[1+\alpha_s \sum_{\lambda=1}^{n-1} \frac{(n-1)!\pi(2\lambda+1)!}{(\lambda!)^2(n-\lambda-1)!} A^{2\lambda}E^{2n-2\lambda-2} \frac{(2n-2\lambda-3)!}{2^{2n-3}n!(n-\lambda-2)!}\right.$$

and

$$(2.25)\quad -E\eta^2 + \frac{C_s^2}{2} E\eta^2[A^2-E^2] + E\left[1+\alpha_s \sum_{\lambda=1}^{n-1} \frac{(n-1)!\pi(2\lambda-1)!}{\lambda![(n-\lambda-1)!]^2} A^{2\lambda}E^{2n-2\lambda-2} \frac{(2n-2\lambda-1)!}{2^{2n-3}n!(\lambda-1)!}\right.$$

For n = 2, i.e. a spring of third order, these equations yield the expressions

$$-A\eta^2 - \frac{C_s^2}{2} A\eta^2[A^2-E^2] + A\left[1+\frac{3}{4}\alpha_s A^2 + \frac{1}{4}\alpha_s E^2\right] = \eta^2(y_o/a)$$

$$-E\eta^2 + \frac{C_s^2}{2} E\eta^2[A^2-E^2] + E\left[1+\frac{3}{4}\alpha_s E^2 + \frac{1}{4}\alpha_s A^2\right] = 0$$

These equations may be combined to yield

$$(2.26)\qquad E^2 = A^2 + \frac{\eta^2 (y_o/a)}{A(C_s^2\eta^2 - \frac{1}{2}\alpha_s)}$$

and

$$(2.27)\quad C_s^2(2A+y_o/a)\eta^4 - \alpha_s\left[A+\frac{3}{2}(y_o/a) + \frac{2C_s^2}{\alpha_s} A(1+\alpha_s A^2)\right]\eta^2 + \alpha_s A(1+\alpha_s A^2) = 0$$

The last equation will provide the amplitude - frequency relation in the y-direction, while equation (2.26) yields, with the obtained $A = A(\eta)$ the response amplitude $E = E(\eta)$ in the z-direction.

The response for the rotary motion of the liquid with a fifth order spring is obtained from equations (2.24) and (2.25) for n = 3. These

nonlinear algebraic equations,

$$-A\eta^2-\tfrac{1}{2}C_s{}^2\eta^2A[A^2-E^2]+A[1+\alpha_s(5/8\ A^4+\tfrac{1}{4}A^2E^2+\ 1/8\ E^4)]\ =\ \eta^2\ y_o/a$$

and

$$-E\eta^2+\tfrac{1}{2}C_s{}^2\eta^2E[A^2-E^2]+E[1+\alpha_s(5/8\ E^4+\tfrac{1}{4}A^2E^2+1/8\ A^4)]\ =\ 0\ ,$$

have to be solved for the response functions $A(\eta)$ and $E(\eta)$. For a third order spring and an α_s of 2/3 the rotary response is given in figures 5a and b. Figure 5a shows the fluid amplitude in the direction of excitation, while figure 5b presents those in perpendicular direction. In figure 6 the nonplanar response is also shown and exhibits good agreement with the experimental results. The backbone curve for the rotary response with the fifth order spring is shown in the same figure for comparison (dotted line), and indicates that better agreement can be obtained with the third order spring. The results for the spherical pendulum as a mechanical slosh model are indicated by the dashed line. The pendulum clearly exhibits too much "hardening" for an accurate representation of the rotary fluid motion.

2.1.2.3. Damped Planar Motion

The damped planar response is readily obtained by the solution of the nonlinear differential equation (2.12) which contains the damping term

$$2\omega_s\gamma_s[\dot{\eta}_s+C_s{}^2\dot{\eta}_s\eta_s{}^2]$$

and a third order spring (n = 2). This equation again is treated with

the Ritz Averaging Method by assuming an approximate solution of the form

$$\bar{\eta}_s = A \cos(\Omega t + \psi) \tag{2.28}$$

where ψ is the phase of the motion relative to the excitation function.

The Ritz conditions

$$\int_0^{2\pi} D[\bar{\eta}_s, \tau] \cos \tau \, d\tau = 0$$

and

$$\int_0^{2\pi} D[\bar{\eta}_s, \tau] \sin \tau \, d\tau = 0$$

yield the equations

$$\eta^2 (y_o/a) \cos \varphi = -\eta^2 A(1+\tfrac{1}{2}C_s^2 A^2) + A(1+3/4\ \alpha_s A^2)$$

and

$$\eta^2 (y_o/a) \sin \varphi = -2\eta\gamma_s A(1+\tfrac{1}{4}C_s^2 A^2)$$

The damped frequency response is therefore determined from these equations, which yield for the phase angle, ψ

$$\tan \psi = \frac{2\eta\gamma_s(1+\tfrac{1}{4}C_s^2 A^2)}{\eta^2(1+\tfrac{1}{2}C_s^2 A^2)+(1+3/4\ \alpha_s A^2)}, \tag{2.29}$$

and, for the damped frequency response, the equation

$$\eta^4[A^2(1+\tfrac{1}{2}C_s^2 A^2)^2 - (y_o/a)^2] - \eta^2[2A^2(1+3/4\ \alpha_s A^2)(1+\tfrac{1}{2}C_s^2 A^2) - 4\gamma_s^2 A^2(1+\tfrac{1}{4}C_s^2 A^2)^2] + A^2(1+3/4\ \alpha_s A^2)^2 = 0 \tag{2.30}$$

From this one obtains for η^2 the expression:

$$\eta^2 = \frac{A^2(1+3/4\ \alpha_s A^2)(1+\frac{1}{2}C_s{}^2A^2)-2\gamma_s{}^2A^2(1+\frac{1}{4}C_s{}^2A^2)^2}{A^2(1+\frac{1}{2}C_s{}^2A^2)^2-(y_o/a)^2}$$

$$\pm\left\{\left[\frac{A^2(1+3/4\ \alpha_s A^2)(1+\frac{1}{2}C_s{}^2A^2)-2\gamma_s{}^2A^2(1+\frac{1}{4}C_s{}^2A^2)^2}{A^2(1+\frac{1}{2}C_s{}^2A^2)^2-(y_o/a)^2}\right]^2+\frac{A^2(1+3/4\ \alpha_s A^2)^2}{(y_o/a)^2-A^2(1+\frac{1}{2}C_s{}^2A^2)^2}\right\}^{\frac{1}{2}}$$

For zero damping ($\gamma_s=0$) the planar undamped response (2.20) is obtained. For a nonlinear spring of order (2n-1) the terms $(1+\frac{3}{4}\alpha_s A^2)$ would have to be substituted by $1+\alpha_s\frac{(2n)!}{2^{2n-1}(n!)^2}A^{2n-2}$. The phase angle ψ therefore would yield the expression

$$\tan\psi = \frac{2\eta\gamma_s(1+\frac{1}{4}C_s^2A^2)}{\eta^2(1+\frac{1}{2}C_s{}^2A^2)+1+\alpha_s\frac{(2n)!A^{2n-2}}{2^{2n-1}(n!)^2}}$$

and η^2 would be

$$\eta^2 = \frac{A^2\left(1+\alpha_s\frac{(2n)!}{2^{2n-1}(n!)^2}A^{2n-2}\right)(1+\frac{1}{2}C_s{}^2A^2)-2\gamma_s{}^2A^2(1+\frac{1}{4}C_s{}^2A^2)^2}{A^2(1+\frac{1}{2}C_s{}^2A^2)^2-(y_o/a)^2}$$

$$\pm\left\{\left[\frac{A^2\left(1+\alpha_s\frac{(2n)!}{2^{2n-1}(n!)^2}A^{2n-2}\right)(1+\frac{1}{2}C_s{}^2A^2)-2\gamma_s{}^2A^2(1+\frac{1}{4}C_s{}^2A^2)^2}{A^2(1+\frac{1}{2}C_s{}^2A^2)^2-(y_o/a)^2}\right]^2\right.$$

$$\left.+\frac{A^2\ 1+\alpha_s\frac{(2n)!A^{2n-2}}{2^{2n-1}(n!)^2}}{(y_o/a)^2-A^2(1+\frac{1}{2}C_s{}^2A^2)^2}\right\}^{\frac{1}{2}}$$

2.2.2.4. Damped Nonplanar Motion

The damped nonplanar response of the model can be obtained by applying the Ritz Averaging Method to the two nonlinear differential equations $D_1[\eta_s,\zeta_s,t]$ and $D_2[\eta_s,\zeta_s,t]$ which contain here an additional damping term each. This damping term is for the first equation

in the form of

$$2\omega_s\gamma_s[\dot{\eta}_s+C_s^2(\eta_s^2\dot{\eta}_s+\eta_s\zeta_s\dot{\zeta}_s)]$$

and for the second differential equation describing the motion in z-direction the damping term is

$$2\omega_s\gamma_s[\dot{\zeta}_s+C_s^2(\zeta_s^2\dot{\zeta}_s+\eta_s\dot{\eta}_s\zeta_s)]$$

An assumption of an approximate solution of the form

$$(2.31)\qquad \bar{\eta}_s = A\cos\Omega t + B\sin\Omega t$$

$$\bar{\zeta}_s = D\cos\Omega t + E\sin\Omega t$$

yields, with $\tau = \Omega t$, the Ritz conditions

$$\int_0^{2\pi} D_1[\bar{\eta}_s,\bar{\zeta}_s,\tau]\cos\tau\,d\tau = 0\ ,\quad \int_0^{2\pi} D_1[\bar{\eta}_s,\bar{\zeta}_s,\tau]\sin\tau\,d\tau = 0\ ,$$

$$\int_0^{2\pi} D_2[\bar{\eta}_s,\bar{\zeta}_s,\tau]\cos\tau\,d\tau = 0\ ,\quad \text{and}$$

$$\int_0^{2\pi} D_2[\bar{\eta}_s,\bar{\zeta}_s,\tau]\sin\tau\,d\tau = 0$$

from which, by introduction of the approximate solution, four simultaneous nonlinear algebraic equations for the determination of A, B, D, and E are obtained. For n = 2, i.e. a cubic spring the algebraic equations are

$$(2.32)\quad -\eta^2A+2\eta\gamma_sB+\eta^2C_s^2(-\tfrac{1}{2}A^3-\tfrac{1}{2}AB^2-\tfrac{1}{2}AD^2+\tfrac{1}{2}AE^2-BDE)+\eta\gamma_s\frac{C_s^2}{2}(A^2B+B^3-BD^2+2EAD+BE^2)$$

$$+[A+3/4\ \alpha(A^3+AB^2)+\tfrac{1}{4}\alpha(3AD^2+AE^2+2BDE)]-\eta^2(y_o/a) = 0$$

$$(2.33)\quad -\eta^2 B-2\eta\gamma_s A+\eta^2 C_s{}^2(-\tfrac{1}{2}B^3-\tfrac{1}{2}A^2B+\tfrac{1}{2}BD^2-\tfrac{1}{2}BE^2-ADE)-\eta\gamma_s\frac{C_s{}^2}{2}(A^3+AB^2+AD^2+2BDE$$
$$-E^2A)+[B+3/4\ \alpha(B^3+A^2B)+\tfrac{1}{4}\alpha(2ADE+BD^2+3BE^2)] = 0$$

$$(2.34)\quad -\eta^2 D+2\eta\gamma_s E+\eta^2 C_s{}^2(-\tfrac{1}{2}D^3-\tfrac{1}{2}DE^2-\tfrac{1}{2}DA^2+\tfrac{1}{2}DB^2-EAB)+\eta\gamma_s\frac{C_s{}^2}{2}(E^2+D^2E-EA^2+2BDA$$
$$+EB^2)+[D+3/4\ \alpha(D^3+DE^2)+\tfrac{1}{4}\alpha(3DA^2+DB^2+2EAB)] = 0$$

$$(2.35)\quad -\eta^2 E-2\eta\gamma_s D+\eta^2 C_s{}^2(-\tfrac{1}{2}E^3-\tfrac{1}{2}D^2E+\tfrac{1}{2}EA^2-\tfrac{1}{2}EB^2-DAB)-\eta\gamma_s\frac{C_s{}^2}{2}(D^3+DE^2+DA^2+2EAB$$
$$-B^2D)+[E+3/4\ \alpha(E^3+D^2E)+\tfrac{1}{4}\alpha(2DAB+EA^2+3EB^2)] = 0$$

The solution of this system may be accomplished with the Newton-Raphson Method, using the undamped rotary response as a starting point for the iteration procedure. This was performed, but no new aspects entered into the results.

For pitching excitation the solution procedure of the equations of motion is identical to that performed above. Their derivation is therfore omitted and only the main results are presented here. No experimental data for nonlinear pitching oscillations are available, but it can be expected that the model will describe the motion of the liquid due to pitching motion as has been seen and checked for linear models.

The undamped planar response is given by the expression

$$\bar{\eta}_s = A \cos \Omega t \qquad \bar{\zeta}_s = 0$$

and yields for a cubic spring

$$\eta^2 = \frac{A(1+3/4\ \alpha A^2)-(\varphi_o/C_s)}{A+\frac{1}{2}C_s^2A^2+\varphi_o(\ell_s/a)}$$

The undamped nonplanar response is given for n = 2 by

$$C_s^2[2A+\varphi_o(\ell_s/a)]\eta^4-\alpha[A+3/2\ \varphi_o(\ell_s/a)+\frac{2C_s^2}{\alpha}\ A(1+\alpha A^2)-\frac{C_s}{\alpha}\ \varphi_o]\eta^2$$

$$+\alpha[A(1+\alpha A^2)-3/2\ (\varphi_o/a)] = 0$$

and

$$E^2 = A^2+\frac{(\eta^2\ \ell_s/a + 1/C_s)\ \varphi_o/A}{C_s^2\eta^2-\frac{1}{2}\alpha}$$

2.2. Stability Analysis of Undamped Planar and Nonplanar Motion

The determination of the character of the solutions of (2.12) and (2.13) in the neighborhood of linear resonance requires an analysis of the stability of these solutions with respect to small perturbations. A stability analysis which is not restricted to small excitation amplitudes and frequencies of excitation in the neighborhood of linear resonance leads to rather lengthy and cumbersome calculations and stability polynomials of eighth order. However, the method of analysis employed by Miles [7] and Hutton [2] is readily adaptable to the model equations, and yields a considerably less complicated analysis than results from

other methods. This method takes advantage of the fact that unstable motions occur in the neighborhood of linear resonance, and yields a stability polynomial of fourth order.

In the following analysis, it is convenient to introduce the parameters ϵ, ν, and τ given by

$$(2.36) \qquad \epsilon = y_o/a \ , \quad \nu = \epsilon^{-2/3}(\eta^2-1) \ , \quad \text{and} \quad \tau = \tfrac{1}{2}\epsilon^{2/3}\Omega t$$

Thus, ϵ, ν, and τ are excitation, frequency, and time parameters, respectively. It is assumed [7] that in the neighborhood of $r = 1$, the amplitudes of $\bar{\eta}_s$ and $\bar{\zeta}_s$ are of order $\epsilon^{1/3}$, $\eta^2 = 1 + 0(\epsilon^{2/3})$, and that terms of $0(\epsilon^{5/3})$ may be neglected.

With these assumptions, the solution to equations (2.12) and (2.13) is taken in the form

$$(2.37) \qquad \bar{\eta}_s = \epsilon^{1/3}[f_1(\tau) \cos \Omega t + f_2(\tau) \sin \Omega t]$$

and

$$(2.38) \qquad \bar{\zeta}_s = \epsilon^{1/3}[g_1(\tau) \cos \Omega t + g_2(\tau) \sin \Omega t]$$

On substituting (2.37) and (2.38) into the differential euqations (2.12) and (2.13) and collecting coefficients of $\cos \Omega\tau$ and $\sin \Omega\tau$, the following four first order differential equations are obtained:

$$(2.39a) \quad f_2' = 1+\nu f_1+\frac{C_s^2}{2}[f_1^3+f_1 f_2^2+f_1 g_1^2+2f_2 g_1 g_2-f_1 g_2^2]-\frac{\alpha}{4}[3f_1^3+3f_1 f_2^2 + 3f_1 g_1^2 + f_1 g_2^2+2f_2 g_1 g_2]$$

$$(2.39b) \quad f_1' = -\nu f_2-\frac{C_s^2}{2}[f_1^2 f_2+f_2^3-f_2 g_1^2+f_2 g_2^2+2f_1 g_1 g_2]+\frac{\alpha}{4}[3f_1^2 f_2+3f_2^3+2f_1 g_1 g_2 + f_2 g_1^2+3f_2 g_2^2]$$

(2.39c) $g_2' = \nu g_1 + \frac{C_s^2}{2}[g_1^3 + g_1 g_2^2 + g_1 f_1^2 - g_1 f_2^2 + 2g_2 f_1 f_2] - \frac{\alpha}{4}[3g_1^3 + 3g_1 g_2^2 + 3g_1 f_1^2 + 2g_1 f_2^2 + 2g_2 f_1 f_2]$

(2.39d) $g_1' = -\nu g_2 - \frac{C_s^2}{2}[g_1^2 g_2 + g_2^3 - g_2 f_1^2 + g_2 f_2^2 + 2g_1 f_1 f_2] + \frac{\alpha}{4}[3g_1^2 g_2 + 3g_2^3 + 2g_1 f_1 f_2 + g_2 f_1^2 + 3g_2 f_2^2]$

Prime indicates differentiation with respect to τ.

Steady-state amplitude-frequency relations are determined from equations (2.39) with $f_1' = f_2' = g_1' = g_2' = 0$. For planar motion, the steady-state response is assumed in the form

(2.40) $$\bar{\eta}_s = \epsilon^{1/3} \bar{f} \cos \Omega t \quad , \quad \bar{\zeta}_s = 0$$

On substitution $f_1(\tau) = \bar{f}$, $f_2(\tau) = g_1(\tau) = g_2(\tau) = 0$ into equations (2.39), only the first equation is not identically satisfied, and yields the amplitude frequency relation

(2.41) $$\nu = -1/f - \tfrac{1}{2}(C_s^2 - 3/2\ \alpha)\ \bar{f}^2$$

The planar response given by equations (2.20) and (2.41) can be compared on substituting relations (2.36) and

$$1/\eta^2 = 1 - \epsilon^{2/3}\ \nu + 0(\epsilon^{4/3})$$

into equation (2.41), yielding

(2.42) $$\eta^2 = \frac{A}{A + \frac{1}{2} C_s^2 A^3 + y_0/a - 3/4\ \alpha A^3}$$

with

$$A = \epsilon^{1/3}\ \bar{f}$$

Therefore, the amplitude frequency relation obtained with the Ritz Averaging procedure and equation (2.42) are approximately equivalent in

the neighborhood of resonance. In order to investigate the stability of the steady-state solution given by equations (2.40) and (2.41), a perturbation of the steady-state amplitudes,

$$
\begin{aligned}
f_1(\tau) &= \bar{f} + c_1 e^{\lambda\tau} \\
f_2(\tau) &= c_2 e^{\lambda\tau} \\
f_3(\tau) &= c_3 e^{\lambda\tau} \\
f_4(\tau) &= c_4 e^{\lambda\tau}
\end{aligned} \tag{2.43}
$$

was assumed, where terms of $O(c_i^2)$ are negligible. Substitution of equations (2.43) into equations (2.39) yields the following homogeneous equation in the coefficients c_i:

$$
\begin{array}{cccc|c}
[\nu+\frac{3}{2}(C_s^2-\frac{3}{2}\alpha)\bar{f}^2]C_1 & -\lambda C_2 & 0 & 0 & = 0 \\
-\lambda C_1 & -[\nu+\frac{1}{2}(C_s^2-\frac{3}{2}\alpha)\bar{f}^2]C_2 & 0 & 0 & = 0 \\
0 & 0 & [\nu+\frac{1}{2}(C_s^2-\frac{3}{2}\alpha)\bar{f}^2]C_3 & -\lambda C_4 & = 0 \\
0 & 0 & -\lambda C_3 & -[\nu-\frac{1}{2}(C_s^2+\frac{1}{2}\alpha)\bar{f}^2]C_4 & = 0
\end{array}
$$

On setting the determinant of the coefficients equal to zero, the fourth order polynomial in λ,

$$[\lambda^2+\beta_1][\lambda^2+\beta_2] = 0$$

is obtained, where

$$\beta_1 = [\nu - (C_s^2/2 + \tfrac{1}{4}\alpha)\bar{f}^2][\nu + (C_s^2/2 - 3/4\alpha)\bar{f}^2]$$

and

$$\beta_2 = [\nu + 3/2\ (C_s^2 - 3/2\ \alpha)\bar{f}^2][\nu + \tfrac{1}{2}(C_s^2 - 3/2\ \alpha)\bar{f}^2]$$

The regions of unstable planar motion are those portions of the planar response (2.41) for which λ is real, i.e. $\beta_1 < 0$ or $\beta_2 < 0$. Substituting equation (2.41) into the expressions for β_1 and β_2 shows that planar motion is unstable if

$$(2.44) \qquad \bar{f}^3 > \frac{1}{C_s^2 - 3/2\alpha} \qquad \text{or} \qquad \bar{f}^3 < -\frac{1}{C_s^2 - \frac{1}{2}\alpha}$$

The stability boundaries are determined by

$$\bar{f}_L^3 = \frac{1}{C_s^2 - 3/2\ \alpha} \qquad \text{and} \qquad \bar{f}_R^3 = -\frac{1}{C_s^2 - \frac{1}{2}\ \alpha}$$

yielding

$$(2.45) \qquad \eta_L^3 = \frac{y_o/a}{C_s^2 - 3/2\ \alpha} \qquad \text{and} \qquad \eta_R^3 = -\frac{y_o/a}{C_s^2 - \frac{1}{2}\ \alpha}$$

where η_L and η_R indicate the stability boundaries below and above linear resonance, respectively. The corresponding frequencies follow from equation (2.41).

Figure (3) shows the stable and unstable portions of the planar response and the corresponding stability boundaries as determined by relations (2.44) and (2.45).

Equations (2.37) and (2.38) with $f_1(\tau)=\bar{f}$, $g_2(\tau)=\bar{g}$ and $f_2(\tau)=g_1(\tau)=0$ represent the steady-state nonplanar motion,

$$(2.46) \qquad \bar{\eta}_s = \epsilon^{1/3}\ \bar{f} \cos \Omega t$$
$$\zeta_s = \epsilon^{1/3}\ \bar{g} \sin \Omega t$$

Equations (2.39b) and (2.39c) are satisfied identically, and equation (2.39a) and (2.39d) become

$$1 + \nu\bar{f} + C_s^2/2\ \bar{f}\ (\bar{f}^2 - \bar{g}^2) - \alpha/4\ (3\bar{f}^3 + \bar{f}\ \bar{g}^2) = 0$$

and

$$-\nu\bar{g} + \frac{C_s^2}{2}\,\bar{g}(\bar{f}^2 - \bar{g}^2) + \frac{\alpha}{4}\,(3\bar{g}^3 + \bar{f}^2\bar{g}) = 0$$

These equations combine to give

$$(2.47) \qquad \nu = \alpha\,\bar{f}^2 - \frac{(C_s^2 - 3/2\,\alpha)}{2C_s^2 - \alpha}\,\frac{1}{\bar{f}}$$

and

$$(2.48) \qquad \bar{g}^2 = \bar{f}^2 + \frac{2}{2C_s^2 - \alpha}\,\frac{1}{\bar{f}}$$

Equation (2.47) relates the amplitude and frequency of the motion in the plane of excitation, while equation (2.48) determines the amplitude in the direction perpendicular to the excitation plane. These equations agree well with equations (2.26) and (2.27) in the neighborhood of resonance.

The perturbation of the steady-state nonplanar solution was assumed in the form

$$f_1(\tau) = \bar{f} + c_1\,e^{\lambda\tau} \qquad f_2(\tau) = c_2\,e^{\lambda\tau}$$

$$g_1(\tau) = c_3\,e^{\lambda\tau} \qquad g_2(\tau) = \bar{g} + c_4\,e^{\lambda\tau}$$

and on substitution into equations (2.39) yields the following four homogeneous equations in the coefficients c_i.

$$\left[\nu + \frac{C_s^2}{2}\,(3\bar{f}^2 - \bar{g}^2) - \frac{\alpha}{4}\,(9\bar{f}^2 + \bar{g}^2)\right]c_1 - \lambda c_2 - (C_s^2 + \frac{\alpha}{2})\bar{f}\,\bar{g}\,c_4 = 0$$

$$\lambda c_1 + \left[\nu + \frac{C_s^2}{2}\,(\bar{f}^2 + \bar{g}^2) - 3/4\,\alpha\,(\bar{f}^2 + \bar{g}^2)\right]c_2 + (C_s^2 - \frac{\alpha}{2})\bar{f}\,\bar{g}\,c_3 = 0$$

$$(C_s^2 - \frac{\alpha}{2})\bar{f}\,\bar{g}\,c_2 + \left[\nu + \frac{C_s^2}{2}\,(\bar{f}^2 + \bar{g}^2) - 3/4\,\alpha\,(\bar{f}^2 + \bar{g}^2)\right]c_3 - \lambda c_4 = 0$$

$$(C_s^2 + \frac{\alpha}{2})\bar{f}\,\bar{g} \qquad -\lambda c_3 \qquad -[\nu + \frac{C_s^2}{2}(3\bar{g}^2 - \bar{f}) - \frac{\alpha}{4}(9\bar{g}^2 + \bar{f}^2)]c_4 = 0$$

Setting the determinant of the coefficients of the c_i equal to zero yields the equation

$$\lambda^4 + p\,\lambda^2 + q = 0 \tag{2.49}$$

where

$$p = [2\nu + (C_s^2 - 5/2\ \alpha)(\bar{f}^2 + \bar{g}^2)][\nu + (\frac{C_s^2}{2} - 3/4\ \alpha)(\bar{f}^2 + \bar{g}^2)] + 2(C_s^4 - \frac{\alpha^2}{4})\bar{f}^2\bar{g}^2$$

and

$$q = \{[\nu + \frac{C_s^2}{2}(3\bar{f}^2 - \bar{g}^2) - \frac{\alpha}{4}(9\bar{f}^2 + \bar{g}^2)][\nu + \frac{C_s^2}{2}(3\bar{f}^2 - \bar{g}^2) - \frac{\alpha}{4}(9\bar{f}^2 + \bar{g}^2)] - (C_s^2 + \frac{\alpha}{2})^2\bar{f}^2\bar{g}^2\}$$
$$\cdot\{[\nu + \tfrac{1}{2}(C_s^2 - 3/2\ \alpha)(\bar{f}^2 + \bar{g}^2)]^2 - (C_s^2 - \alpha/2)^2\bar{f}^2\bar{g}^2\}$$

with equations (2.47) and (2.48), p and q become

$$p = 4(C_s^2 - \alpha/2)^2\,\bar{f}^4 + 2C_s^2\,\bar{f} \tag{2.50}$$

and

$$q = 4\alpha(C_s^2 - \alpha/2)^2\bar{f}^5 + (C_s^2 + 5/2\ \alpha)(C_s^2 - \tfrac{1}{2}\alpha)\bar{f}^2 + 1/\bar{f}\ (C_s^2 - 3/2\ \alpha) \tag{2.51}$$

The unstable portions of the nonplanar response are those parts for which $\mathrm{Re}(\lambda)>0$. Therefore, the nonplanar response will be unstable if $p < 0$, $q < 0$, or $p^2 < 4q$. The minimum amplitude at which stable nonplanar motion can occur is given by the stability boundary $p^2 = 4q$.

With equation (2.50) and (2.51), this condition yields the polynomial

$$(2.52) \quad 4(C_s^2 - \alpha/2)^4 \bar{f}^9 + 4(C_s^2 - \alpha)(C_s^2 - \alpha/2)^2 \bar{f}^6 + \alpha(3C_s^2 - 5/4\ \alpha)\bar{f}^3 - (C_s^2 - 3/2\ \alpha) = 0$$

The one positive root of equation (2.52) corresponds to the minimum stable nonplanar amplitude. The corresponding amplitudes of $\bar{\eta}_s$ and $\bar{\zeta}_s$ are determined from the relations

$$(2.53) \quad \bar{\eta}_s = (y_o/a)^{1/3}\ \bar{f} \cos \Omega t \qquad \bar{\zeta}_s = (y_o/a)^{1/3}\ \bar{g} \sin \Omega t$$

where $\bar{f}$ and $\bar{g}$ are related by equation (2.48).

Figures (5a) and (5b) show the nonplanar response amplitudes in the plane of excitation and in the direction perpendicular to the excitation plane, respectively. The regions of stable and unstable motion and the stability boundaries are indicated.

The stability analysis for the pitching case is identical to the above if the definition for ϵ is $\varphi_o \ell_s/a$ and the equations (2.16) and (2.17) are used. If the term $1/C_s(a/\ell_s$ is added to the right-hand side of equation (2.39a) the corresponding equations for the pitching case result.

The relation between ν and $\bar{f}$ for the planar motion due to pitching is

$$\nu = -\frac{1 + 1/C_s\ (a/\ell_s)}{\bar{f}} - \tfrac{1}{2}(C_s^2 - 3/2\ \alpha)\bar{f}^2$$

For the nonplanar pitching response, the following relations are obtained:

$$\nu = \alpha\,\bar{f}^2 - \frac{(C_s^2 - 3/2\,\alpha)}{2C_s^2 - \alpha}\left[1 + 1/C_s\,(a/\ell_s)\right] 1/\bar{f}$$

and

$$\bar{g}^2 = \bar{f}^2 + \frac{\left[1 + 1/C_s\,(a/\ell_s)\right]}{C_s^2 - \alpha/2}\,1/\bar{f}$$

If these equations are substituted into β_1 and β_2 for the translational case, the stability boundaries of the response due to pitching excitation may be determined. The resulting expression for the planar stability boundaries are:

$$\bar{f}_L^3 = \frac{1 + 1/C_s(a/\ell_s)}{C_s^2 - 3/2\,\alpha} \qquad \text{and} \qquad f_R^3 = -\frac{1 + 1/C_s(a/\ell_s)}{C_s^2 - \tfrac{1}{2}\,\alpha}$$

and the corresponding amplitude of $\bar{\eta}_s$ is determined from the planar response,

$$\bar{\eta}_s = (\varphi_o\,\ell_s/a)^{1/3}\,\bar{f}\cos\Omega t$$

2.3. Comparison with Spherical Pendulum

The results obtained by Miles [7] for the response and stability boundaries of a spherical pendulum subjected to harmonic excitation of the point of suspension were compared with the results of the paraboloid model. On choosing the pendulum length as

$$\ell = g/\omega_1^2$$

where ω_1 is the first mode frequency of the fluid, and with $\epsilon = y_o/a$, the pendulum planar solution becomes

$$\bar{\eta}_s = \ell/a\,\sin\alpha\,\cos\Omega t$$

where α is related to the excitation frequency by

$$\eta^2 = 1 - \frac{y_o/a}{\alpha} - 1/8\ \alpha^2$$

The stability boundaries for the planar motion are:

$$\alpha_L = (y_o/a)^{1/3}\ 2^{2/3} \qquad \text{and} \qquad \alpha_R = (y_o/a)^{1/3}\ (4/3)^{1/3}$$

The nonplanar solution is

$$\bar{\eta}_s = \ell/a \sin\alpha \cos\Omega t \qquad \text{and} \qquad \bar{\zeta}_s = \ell/a \sin\beta \sin\Omega t$$

where

$$\eta^2 = 1 - 1/6\ \frac{y_o/a}{\alpha} + \tfrac{1}{2}\ \alpha^2$$

and

$$\beta^2 = \alpha^2 + 4/3\ \frac{y_o/a}{\alpha}$$

Figure (7) shows the results of planar response calculations for the pendulum and the paraboloid models, experimental data, and the results of linear fluid theory. Equation (2.7) was used in relating the displacement of the pendulum and the fluid amplitudes. Although the paraboloid and pendulum models agree closely for small amplitudes, the amplitudes of the stability boundary below resonance are significantly different. This is partly due to the fact that the relation of the horizontal and vertical displacement of the pendulum mass is not a pure quadratic one as in the liquid and the previously derived model. The results for the nonplanar response of the two models are compared in figure (6). It is clear that the pendulum predicts considerably smaller

nonplanar amplitudes than those predicted by the paraboloid model.

3. Derivation of the Nonlinear Mechanical Model of the total Liquid System.

The analytical mechanical analogy is designed in such a fashion that it describes the observed nonlinear phenomena and presents the results of the linear model in a limit consideration for small amplitudes.

The liquid in the lower part of the container follows the motion like a rigid body, and is chosen to have a mass m_o and a moment of inertia I_o. The sloshing masses are denoted by m_n and the spring stiffnesses by k_n. The nonsloshing mass m_o is rigidly connected at a height h_o below the center of gravity of the quiescent liquid. To make the mechanical model equivalent to the fluid system, the sum of the model masses must be equal to the total liquid mass. It is therefore

$$m = m_o + \sum_{n=1}^{\infty} m_n \tag{3.1}$$

For pitching or yawing excitation about the origin, not all of the fluid participates in the motion, but a part remains completely at rest. For this reason a frictionlessly mounted, massless sphere with a moment of inertia, I_s, has been introduced at the center of gravity of the quiescent liquid.

Assuming that the sloshing masses are subjected to a damping force proportional to their velocity relative to the paraboloid, the dissipation function for the n^{th} sloshing mass point is

$$D_n(\dot{x}_n, \dot{y}_n, \dot{z}_n) = \tfrac{1}{2} C_n(\dot{x}_n^2 + \dot{y}_n^2 + \dot{z}_n^2)$$

where $C_n = 2m_n\omega_n\gamma_n$. In addition, a damper is introduced with damping coefficients C_{S1} and C_{S2} between the sphere and the container bottom. The reason for this is the fact that for rotational excitation of a viscous liquid, more fluid participates in the motion than for frictionless liquid.

The equations of motion of the mechanical model are now derived with the help of the Lagrange equations. For this reason one determines the kinetic and potential energy as well as the dissipation function of the system (see figure 8). With x_n, y_n, z_n as the displacement of the n^{th} sloshing mass, m_n, with respect to the container, with $y(t)$ the tank displacement in y-direction, with φ the rotation about the z-axis and with ψ_1 and ψ_2 the rotation angle in perpendicular directions of the sphere with respect to the container bottom, the kinetic energy is given by:

$$(3.2) \qquad T = \frac{m_o}{2}(\dot{y}-h_o\dot{\varphi})^2 + \tfrac{1}{2}I_o\dot{\varphi}^2 + \tfrac{1}{2}I_s[(\dot{\varphi}+\dot{\psi}_1)^2 + \dot{\psi}_2^2] + \tfrac{1}{2}\sum_{n=1}^{\infty} m_n\left[[(\dot{y}_n+\dot{y})+(h_n-x_n)\dot{\varphi}]^2 + \dot{z}_n^2 + [\dot{x}_n+y_n\dot{\varphi}]^2\right]$$

The first two terms represents the kinetic energy of the nonsloshing mass, m_o, which is regidly connected with the tank. The second term is the kinetic energy of the sphere, while the series describes the kinetic energy of the sloshing mass points. It may be remarked here that the pitching motion $\varphi(t)$ was assumed to exhibit small angles φ such that $\cos\varphi \approx 1$ and $\sin\varphi \approx \varphi$.

The dissipation function is with $C_{S1} = C_{S2}$ give by

$$(3.3) \qquad D = \tfrac{1}{2}\sum_{n-1}^{\infty} C_n(\dot{x}_n^2 + \dot{y}_n^2 + \dot{z}_n^2) + \tfrac{1}{2}C_s(\dot{\psi}_1^2 + \dot{\psi}_2^2)$$

where the infinite series represents the contribution of the damping of the sloshing masses m_n and the last term is due to the dampers c_s between sphere and container bottom.

The potential energy is composed of the lifting of the sloshing and nonsloshing mass and the energy stored in the springs. It is for small φ values

$$(3.4) \qquad V = \frac{m_o}{2} gh_o \varphi^2 - \frac{g}{2}\sum_{n=1}^{\infty} m_n(h_n - x_n)\varphi^2 - g\varphi\sum_{n=1}^{\infty} m_n y_n - \sum_{n=1}^{\infty} m_n g x_n + \tfrac{1}{4}\sum_{n=1}^{\infty} k_n(y_n^2 + z_n^2)^2$$

The first term represents the potential energy due to the lifting of the nonsloshing mass, m_o, during rotation $\varphi(t)$, while the second, third, and fourth term describe the same fact for the sloshing masses. The last term represents the accumulated energy in the springs. The coordinates y, φ, ψ_1, ψ_2, y_n, z_n, and x_n are related by one equation of constraint, which expresses that the mass point m_n has to move on a paraboloid. The equation of constraint is therefore

$$(3.5) \qquad f = x_n + \bar{\alpha}_n(y_n^2 + z_n^2) = 0$$

where α_n was found to be

$$(3.6) \qquad \bar{\alpha}_n = \frac{\epsilon_n \tanh(\epsilon_n \frac{h}{a})}{2a}$$

Defining a Lagrange function L^*, such that it is

$$L^* = L - \lambda f$$

and L being the Lagrange $L = T-V$ and λ a Lagrange multiplier, the equations of motion can be derived with the Lagrange equation

$$\frac{d}{dt}\left(\frac{dL^*}{d\dot{q}_v}\right) - \frac{\partial L^*}{\partial q_v} + \frac{\partial D}{\partial \dot{q}_v} = Q_v$$

where D is the dissipation function and Q_v are the forces with respect to the coordinates $\bar{q}_v$. Another method for the derivation of the equations of motion from the Lagrange Equation is based on the generalized coordinates q_v which are, by elimination of the equation of constraint, made independent of each other. The kinetic energy and dissipation function in these generalized coordinates are:

$$(3.7)\quad T = \frac{m_o}{2}(\dot{y}-h_o\dot{\varphi})^2 + \tfrac{1}{2}I_o\dot{\varphi}^2 + \tfrac{1}{2}I_s[(\dot{\varphi}+\dot{\psi}_1)^2 + \dot{\psi}_2^2] + \tfrac{1}{2}\sum_{n=1}^{\infty} m_n[\dot{y}_n + \dot{y} + (h_n + \bar{\alpha}_n^2(y_n^2+z_n^2))\dot{\varphi}]^2 + \dot{z}_n^2 + [2\bar{\alpha}_n(\dot{y}_n y_n + \dot{z}_n z_n) - y_n\dot{\varphi}]^2]$$

$$(3.8)\quad D = \tfrac{1}{2}\sum_{n=1}^{\infty} C_n[\dot{y}_n^2 + \dot{z}_n^2 + (2\bar{\alpha}_n(\dot{y}_n y_n + \dot{z}_n z_n))^2] + \frac{C_s}{2}(\dot{\psi}_1^2 + \dot{\psi}_2^2)$$

The potential energy is given by

$$(3.9)\quad V = \frac{m_o}{2} g h_o\varphi^2 - \frac{g}{2}\varphi^2\sum_{n=1}^{\infty} m_n[h_n + \bar{\alpha}_n(y_n^2+z_n^2)] - g\varphi\sum_{n=1}^{\infty} m_n y_n + \tfrac{1}{4}\sum_{n=1}^{\infty} k_n(y_n^2+z_n^2)^2 + \sum_{n=1}^{\infty} m_n g\bar{\alpha}_n(y_n^2+z_n^2)$$

The equations of motion are derived from the Lagrange equations

$$(3.10)\quad \frac{d}{dt}\left(\frac{\partial T}{\partial \dot{q}_v}\right) + \frac{\partial D}{\partial \dot{q}_v} - \frac{\partial T}{\partial q_v} + \frac{\partial V}{\partial q_v} = Q_v$$

where the generalized coordinates q_v are y, φ, ψ_1, ψ_2, y_n and z_n, and $Q_y = F_y$, $Q_\varphi = -M_z$, $Q_{\psi_1} = Q_{\psi_2} = 0$ and $Q_{yn} = Q_{zn} = 0$ are the generalized forces. The equations of motion are then

$$(3.11)\quad m_o(\ddot{y} - h_o\ddot{\varphi}) + \sum_{n=1}^{\infty} m_n[\ddot{y}_n + \ddot{y} + [h_n + \bar{\alpha}_n(y_n^2+z_n^2)]\ddot{\varphi} + 2\bar{\alpha}_n\dot{\varphi}(\dot{y}_n y_n + \dot{z}_n z_n)] = -F_y$$

$$(3.12)\quad (m_o h_o^2 + I_o)\ddot{\varphi} - m_o h_o \ddot{y} + I_s(\ddot{\varphi} + \ddot{\psi}_1) + \sum_{n=1}^{\infty} m_n \ddot{y}[h_n + \bar{\alpha}_n(y_n^2 + z_n^2)] + \sum_{n=1}^{\infty} m_n \ddot{y}_n[h_n +$$

$$+ \bar{\alpha}_n(z_n^2 + y_n^2)] - 2\sum_{n=1}^{\infty} m_n \ddot{z}_n \bar{\alpha}_n y_n z_n + \ddot{\varphi}\sum_{n=1}^{\infty} m_n[2h_n\bar{\alpha}_n(y_n^2+z_n^2) + \bar{\alpha}_n^2(y_n^2 + z_n^2)^2$$

$$+ h_n^2 + y_n^2] + 2\sum_{n=1}^{\infty} m_n \bar{\alpha}_n[2(y_n^2 + z_n^2)\bar{\alpha}_n\dot{\varphi} + 2h_n\dot{\varphi} + \dot{y}] \cdot [\dot{y}_n y_n + \dot{z}_n z_n]$$

$$-2\sum_{n=1}^{\infty} m_n y_n \bar{\alpha}_n(\dot{y}_n^2 + \dot{z}_n^2) + 2\sum_{n=1}^{\infty} m_n y_n \dot{y}_n \dot{\varphi}$$

$$+ m_o g h_o \varphi - g\varphi\sum_{n=1}^{\infty} m_n[h_n + \bar{\alpha}_n(y_n^2 + z_n^2)] - g\sum_{n=1}^{\infty} m_n y_n = -M_z$$

$$(3.13)\quad I_s(\ddot{\psi}_1 + \ddot{\varphi}) + C_s\dot{\psi}_1 = 0$$

$$(3.14)\quad I_s\ddot{\psi}_2 + C_s\dot{\psi}_2 = 0$$

$$(3.15)\quad \ddot{y} + \ddot{y}_n + h_n\ddot{\varphi} + 4\bar{\alpha}_n^2 y_n(\dot{y}_n^2 + \dot{z}_n^2 + \ddot{y}_n y_n + \ddot{z}_n z_n)$$

$$+ \frac{C_n}{m_n}[\dot{y}_n + 4\bar{\alpha}_n^2 y_n(y_n\dot{y}_n + z_n\dot{z}_n)]$$

$$+ \frac{k_n}{m_n} y_n(y_n^2 + z_n^2) - g\varphi + 2\alpha_n g y_n = 0$$

$$n = (1, 2, \ldots.)$$

$$(3.16)\quad \ddot{z}_n + 4\bar{\alpha}_n^2 z_n(\dot{y}_n^2 + \dot{z}_n^2 + \ddot{y}_n y_n + \ddot{z}_n z_n)$$

$$+ \frac{C_n}{m_n}\dot{z}_n + \frac{4C_n}{m_n}\bar{\alpha}_n^2 z_n(y_n\dot{y}_n + \dot{z}_n z_n) + \frac{k_n}{m_n} z_n(y_n^2 + z_n^2)$$

$$+ 2\bar{\alpha}_n g z_n = 0$$

$$(n = 1, 2, \ldots.)$$

The first equation is the force equation, and it was obtained with the generalized coordinate y. The second equation, as obtained with the generalized coordinate φ, is the moment equation, while the third and fourth equation represent the equation of motion of the sphere and were obtained

with the generalized coordinates ψ_1 and ψ_2, respectively. The last two equations are the sloshing equations in y and z-direction and are obtained by using the generalized coordinates y_n and z_n respectively, in the Lagrange equation.

Linearization of this system yields the equations of motion of the linear model which agrees with the result of the linear model equations (51) through (54) of Reference [4]. They are:

$$(3.17) \qquad m_o(\ddot{y}-h_o\ddot{\varphi}) + \sum_{n=1}^{\infty} m_n(\ddot{y}_n + \ddot{y} + h_n\ddot{\varphi}) = -F_y$$

$$(3.18) \qquad (m_o h_o^2 + I_o)\ddot{\varphi} + I_s(\ddot{\varphi} + \ddot{\psi}_1) + \sum_{n=1}^{\infty} m_n h_n(\ddot{y}_n + h_n\ddot{\varphi}) - g\sum_{n=1}^{\infty} m_n y_n$$
$$+(\ddot{y} - g\varphi)\left[\sum_{n=1}^{\infty} m_n h_n - m_o h_o\right] = -M_y$$

$$(3.19) \qquad I_s(\ddot{\psi}_1 + \ddot{\varphi}) + c_s\dot{\psi}_1 = 0$$

$$(3.20) \qquad I_s\ddot{\psi}_2 + c_s\dot{\psi}_2 = 0$$

$$(3.21) \qquad \ddot{y} + \ddot{y}_n + h_n\ddot{\varphi} + \frac{c_n}{m_n}\dot{y}_n - g\varphi + 2\bar{\alpha}_n g y_n = 0 \qquad (n = 1, 2, \ldots)$$

$$(3.22) \qquad \ddot{z}_n + \frac{c_n}{m_n}\dot{z}_n + 2\bar{\alpha}_n g z_n = 0 \qquad (n = 1, 2, \ldots)$$

It can be seen that (by observing equation (3.6)) these equations agree exactly with the linear spring-mass-model of Reference [4]. In the linearized moment equation the expression

$$m_o h_o = \sum_{n=1}^{\infty} m_n h_n$$

which expresses that the mass center of the liquid shifts only horizontally. The slosh equation (3.21) describes the motion of the model mass in

y-direction, while equation (3.22) represents the free oscillation equation in z-direction. (Figure 9). In the linearized form there is no coupling between these motions.

4. Equivalent linearization of the nonlinear mechanical model

For the introduction of the nonlinear effects of the mechanical analogy into the linearized equations of motion of the space vehicle an equivalent linear system is of advantage in order to preserve the powerful methods for the solution of linear systems of differential equations. The nonlinear equations of the propellant sloshing model should therefore be described by equivalent linear ones which exhibit both linear restoring characteristic and linear damping. We must expect, of course, that the equivalent damping coefficient and equivalent spring constant are depending on the amplitude of the motion.

Since due to symmetry the equations of motion of a space vehicle are usually treated for a motion of the vehicle in a plane, we restrict ourselves to the planar motion of the liquid in such a plane. The equation of motion of the n^{th} Sloshing mass is therefore for translational excitation

$$(4.1) \qquad m_n\ddot{y}_n + c_n\dot{y}_n(1 + 4\bar{\alpha}_n^2 y_n^2) + k_n y_n^3 + k_{on}y_n + 4\bar{\alpha}_n^2 m_n(y_n\dot{y}_n^2 + y_n^2\ddot{y}_n) = -\ddot{y}\cdot m_n$$

where $k_{on}/m_n = \omega_n^2$ represents the square of the linear circular natural frequency. We search in the equivalent linear equation

$$(4.2) \qquad m_n\ddot{y}_n + \bar{c}_n\dot{y}_n + \bar{k}_n y_n = -\ddot{y}\cdot m_n$$

the equivalent damping coefficient $\bar{c}_n$ and the equivalent spring stiffness $\bar{k}_n$. This is performed by considering the energy dissipation of the system. The energy dissipated over a period by the damping force $\bar{c}_n\dot{y}_n$

must equal that of the damping force $c_n\dot{y}_n\,(1 + 4\overline{\alpha}_n^2 y_n^2)$. It is therefore with $y_n = Y\sin\,(\Omega t - \alpha)$ the dissipated energy of the equivalent linear damper

$$\overline{E}_D = \overline{c}_n \int_o^T \dot{y}_n^2\, dt = \overline{c}_n Y^2 \Omega\pi \tag{4.3}$$

while the energy of the nonlinear system is

$$E_D = c_n \int_o^T \dot{y}_n^2\,(1 + 4\overline{\alpha}_n^2 y_n^2)\, dt = c_n \Omega\pi Y^2 [1 + \overline{\alpha}_n^2\, Y^2] \tag{4.4}$$

The equivalent damping factor is therefore obtained by setting these dissipated energies equal and yields the expression $\overline{c}_n$ for the equivalent linear damping coefficient:

$$\overline{c}_n = c_n(1 + \overline{\alpha}_n^2 Y^2) \tag{4.5}$$

To find a equivalent spring constant $\overline{k}_n$ we apply the method of Kryloff-Bogoliuboff with which the square of the frequency yields

$$\omega^2 = \frac{\overline{k}_n}{m_n} = \frac{k_{on}}{m_n} + \frac{k_n}{\pi m_n Y} \int_o^{2\pi} Y^3 \sin^4 \psi d\psi + \frac{4\overline{\alpha}_n^2 m_n}{\pi Y m_n} \int_o^{2\pi} [Y^3\Omega^2 \sin^2\psi\cos^2\psi - \Omega^2 Y^3 \sin^4 \psi]\, d\psi \tag{4.6}$$

This yields the equivalent spring constant

$$\overline{k}_n = k_{on} + \frac{3\, k_n Y^2}{4} - 2\,\overline{\alpha}_n^2 Y^2 \Omega^2 m_n \tag{4.7}$$

The equivalent linear sloshing equation reads therefore

$$m_n\ddot{y}_n + c_n\,(1 + \overline{\alpha}_n^2 Y^2)\,\dot{y}_n + [k_{on} + (\frac{3}{4}\, k_n - 2\alpha_n^2 \Omega^2 m_n)\, Y^2\,]\, y_n = -\ddot{y}\, m_n \tag{4.8}$$

and is in the first order approximation equivalent to the nonlinear system (4.1). The basic condition for the applicability of such a method of equivalent linearization is the approximate harmonic character of the vibration, which is the case with fluid oscillations. As can be seen the coefficients of the oscillator are some definite functions of the amplitude of the oscillations, and the integration of the equations of motion of a space vehicle has to be performed for a sufficiently large number of amplitudes, Y.

5. Equations of Motion of a Space Vehicle

For missiles and space vehicles it is necessary to consider the general problem of dynamics and stability of the total vehicle under thrust. This is best described by the two essential investigations of stability and response. Stability expresses how effectively the vehicle achieves a state of motion and how rapidly it occurs. In a control feedback analysis of a space vehicle one is usually satisfied to determine just the roots of stability instead of solving the motion of the whole system. The shifting of roots to more optimal positions represents then a major part of the investigation. If this is accomplished, however, the response of the space vehicle is needed to determine if the design of the system, i.e. the structural design and/or design of the control system, is adequate for certain given inputs such as control maneuvers or encountered winds. The design values are the available engine deflection, its rate, maximum bending moments, wave height of the oscillating propellants in the fuel containers, etc., due to a given probable wind increase and gust, through which the vehicle may have to pass during the ascent phase. The dynamic characteristic of the vehicle differ in complexity depending, of course, upon the complexity of the space vehicle itself. They are reduced here to a less complex system by truncating the equations of motion in such a

fashion that a more lucid presentation can be provided without loss of the more general features of the system.

The largest amount of the total weight of a space vehicle is in form of liquid propellant, thus indicating that the problem of interaction of the sloshing propellant with the motion of the space vehicle remains throughout powered flight.

The general problem of concern is the motion of the center of mass, the vehicle attitude, the motion of the propellants in the fuel containers and the lateral bending of the vehicle under the action of a control system. For the purpose of the following derivation of the equations of motion, the rate of mass, the moment of inertia and longitudinal acceleration variations are considered small enough to be negligible. It is furthermore assumed that the motion of the vehicle can be considered small, enabling one to linearize them, and that only the nonlinear effects of propellant sloshing and the control system are dominant. This is quite justified since only the propellant amplitude and the engine deflection, interaction of amplifiers and limited output of velocity, etc. may exhibit large deviations from linear theory. The equations of motion are quite simple and are adequate to illustrate gross effects of the interaction of structure, propellant sloshing and control. The control moments will be produced by swivel engines and the main energy is fed into the system by the feedback loops between the structure of the space vehicle and its control system.

The coordinate system (figure 10) has its origin in the center of mass of the undisturbed vehicle [8, 9]. The accelerated coordinate system is replaced by an inertial system such that the space vehicle is subjected to an equivalent field of acceleration. Centrifugal and Coriolis forces which result from a rotation are considered negligible, and the acceleration of

the vehicle is in direction of the trajectory.

Since the space vehicle is assumed to possess rotational symmetry about its longitudinal axis, there will be no coupling through the structure in the pitch-and yaw plane, and one can consider the motion of a flexible body in one plane perpendicular to the trajectory. The body fixed coordinates x, y, z, are defined with the origin coinciding with the center of mass. We denote the translatory motion of the vehicle by y and z, the pitching and the yaw motion about the center of mass by φ and χ respectively, the propellant motion by y_n and z_n, and the bending vibrations by η_n and ζ_n. Considering motion in one plane, say the xy plane, ζ and χ are not present. We follow the conventional path of deriving the equations of motion from Lagrange's equations. It is assumed that the motion of the space vehicle can be described by a superposition of a finite number of preassigned bending mode shapes and the translatory and rotational motions of the vehicle. The elastic mode shapes are introduced as normal modes of vibration of the structure of the space vehicle.

5.1. Equations of Motion for Nonlinear System

For the derivation of the equations of motion, Lagrange's equation is employed in the form

$$(5.1)\qquad \frac{d}{dt}\frac{\partial T}{\partial \dot{q}_i} - \frac{\partial T}{\partial q_i} + \frac{\partial D}{\partial \dot{q}_i} + \frac{\partial V}{\partial q_i} = Q_i + \sum_{\nu} \left\{ \lambda_{\nu 1} \frac{\partial \Psi_{\nu 1}}{\partial q_i} + \lambda_{\nu 2} \frac{\partial \Psi_{\nu 2}}{\partial q_i} \right\} \qquad (i = 1,2\ldots)$$

where T is the kinetic energy of the system, D the dissipation function, and V the potential energy. Q_i are the generalized forces corresponding to those external forces which cannot be derived from a potential. The coordinates, q_i, specify the configuration of the system at any time. The second term and third term on the right hand side represent the influence

of the constraints on the system, λ_ν being the Lagrange multipliers. ψ_ν is the equation of constraint of the ν^{th} swivel engine. This constraint is imposed by the control system which prescribes the angular deflection of the swivel engines.

It is

y, the lateral translation of the center of mass, or center line of the undeformed space vehicle, in y-direction

z, the lateral translation of the center of mass, or center line of the undeformed space vehicle, in z-direction

φ, the pitching motion of the center line of the undeformed vehicle about the center of mass, with respect to the y-axis

$y_{n\lambda}, z_{n\lambda}$, the displacement of the n^{th} sloshing mass relative to the container wall in y-and z-direction respectively (for the λ^{th} container)

η_n, ζ_n, the elastic deflection of the n^{th} normalized bending mode shape, in y- andz-direction respectively.

ψ_{1n}, ψ_{2n}, the non-sloshing sphere motion in the n^{th} container with respect to the tank bottom

$\varepsilon_\nu = \beta_\nu - \beta_{c\nu}$, the compliance of the ν^{th} swivel engine, expressing the difference of the actual engine deflection and the angle due to the control signal.

Toll motion has been neglected. It is of major importance only if the propellant tanks are clusteres. Circular cylindrical propellant containers have been considered in the derivation of the equations of motion. If some tanks are spherical another $\bar{\alpha}_n$-value has to be chosen in the mechanical model.

Kinetic energy. The kinetic energy is composed of those parts due to the empty structure of the space vehicle, that of the liquid propellant, and that of the swivel engines. The kinetic energy, T_s, of the empty structure is obtained by summation of the translational and rotational kinetic energy of each segment. The translational velocity v due to

translation, rotation and bending displacement, and the angular velocity ω are

$$v^2 = [\dot{y} - x\dot{\varphi} + \sum_{\nu=1}^{\infty} \dot{\eta}_\nu Y_\nu]^2 + [\dot{z} - x\dot{\chi} + \sum_{\nu=1}^{\infty} \dot{\zeta}_\nu Z_\nu]^2$$

$$\omega^2 = (\dot{\varphi} - \sum_{\nu=1}^{\infty} \dot{\eta}_\nu Y_\nu')^2 + (\dot{\chi}^2 - \sum_{\nu=1}^{\infty} \dot{\zeta}_\nu Z_\nu')^2 \qquad (*)$$

where x is the distance of the considered element from the center of mass of the space vehicle and Y_ν, Z_ν are the normalized bending deflections of the νth lateral bending mode. The kinetic energy T_s of the structure is therefore

$$(5.2) \qquad T_s = \tfrac{1}{2}\int m_s' \{(\dot{y} - x\dot{\varphi} + \sum_{\nu=1}^{\infty} \dot{\eta}_\nu Y_\nu)^2 + (\dot{z} - x\dot{\chi} + \sum_{\nu=1}^{\infty} \dot{\zeta}_\nu Z_\nu)^2\} dx$$

$$+ \tfrac{1}{2}\int I_s' \{(\dot{\varphi} - \sum_{\nu=1}^{\infty} \dot{\eta}_\nu Y_\nu')^2 + (\dot{\chi} - \sum_{\nu=1}^{\infty} \dot{\zeta}_\nu Z_\nu')^2\} dx$$

Here, m_s' is the mass of the structure per unit length and I_s' is the mass moment of inertia per unit length about the center of mass of the elemental segment. The integration is performed along the total vehicle length, and the bending mode deflection curves Y_ν, Z_ν are normalized (to unity) at the swivel point of the engines of the space vehicle.

The kinetic energy T_p of the liquid propellant is obtained by using the mechanical model (spring-mass-system, see section 3). This model describes the liquid motion, and consists of a fixed mass, m_o, and an infinite set of oscillating masses, m_n, which are rolling on paraboloids and are connected with springs of "stiffness", k_n, to the longitudinal vehicle axis. With the mechanical analogy, the kinetic energy of the propellant

*The dot indicated differentiation with respect to time, while the prime stands for differentiation with respect to x.

can be written as

$$
\begin{aligned}
(5.3)\qquad T_p = {} & \tfrac{1}{2}\sum_{\lambda=1}^{\ell} m_{o\lambda}\{[\dot{y} - x_{o\lambda}\dot{\varphi} + \sum_{\nu=1}^{\infty}\dot{\eta}_\nu Y_\nu(x_{o\lambda})]^2 + [\dot{z} - x_{o\lambda}\dot{\chi} + \sum_{\nu=1}^{\infty}\dot{\zeta}_\nu Z_\nu(x_{o\lambda})]^2 \\
& + \tfrac{1}{2}\sum_{\lambda=1}^{\ell} I_{o\lambda}\{[\dot{\varphi} - \sum_{\nu=1}^{\infty}\dot{\eta}_\nu Y'_\nu(x_{o\lambda})]^2 + [\dot{\chi} - \sum_{\nu=1}^{\infty}\dot{\zeta}_\nu Z'_\nu(x_{o\lambda})]^2\} \\
& + \tfrac{1}{2}\sum_{\lambda=1}^{\ell} I_{s\lambda}[\dot{\varphi} + \dot{\psi}_{1\lambda})^2 + (\dot{\chi} + \dot{\psi}_{2\lambda})^2] \\
& + \tfrac{1}{2}\sum_{\lambda=1}^{\ell}\sum_{n=1}^{\infty} m_{\lambda n}\{[\dot{y} - x_{\lambda n}\dot{\varphi} + \bar{\alpha}_{\lambda n}\dot{\varphi}(y_{\lambda n}^2 + z_{\lambda n}^2) + \sum_{\nu=1}^{\infty}\dot{\eta}_\nu Y_\nu(x_{\lambda n}) + \dot{y}_{n\lambda}]^2 \\
& + [\dot{z} - x_{\lambda n}\dot{\chi} + \bar{\alpha}_{\lambda n}\dot{\chi}(y_{\lambda n}^2 + z_{\lambda n}^2) + \sum_{\nu=1}^{\infty}\dot{\zeta}_\nu Z_\nu(x_{\lambda n}) + \dot{z}_{n\lambda}]^2 \\
& + [2\bar{\alpha}_{\lambda n}(y_{\lambda n}\dot{y}_{\lambda n} + z_{\lambda n}\dot{z}_{\lambda n}) - y_{\lambda n}\dot{\varphi} - z_{\lambda n}\dot{\chi}]^2\}
\end{aligned}
$$

where ℓ indicates the number of propellant containers, $m_{o\lambda}$, the fixed (non-sloshing) mass in the λth propellant tank, $m_{n\lambda}$ the mass of the nth sloshing mode in the λth container, $x_{o\lambda}$ the distance of the non-sloshing mass in the λth container to the center of mass of the vehicle and $x_{\lambda n}$ the distance of the nth sloshing mass in the λth container to the center of mass of the vehicle. The value $I_{o\lambda}$ is the moment of inertia of the non-sloshing mass in the λth container about its own center of mass. The displacement of the mass of the nth sloshing mode in the λth container relative to the tank wall is denoted in y-direction by $y_{n\lambda}$ and in z-direction by $z_{n\lambda}$.

The kinetic energy of the engines consists of their translational and rotational energy about their centers of gravity. For a stationary

(fixed) engine it is therefore

$$T_{FE} = \tfrac{1}{2} m_E \{[\dot{y} - x_E\dot{\omega} - \ell_E\dot{\varphi} + \sum_{\nu=1}^{\infty} \dot{\eta}_\nu Y_\nu(x_E)]^2 + [\dot{z} - x_E\dot{\chi} - \ell_E\dot{\chi} + \sum_{\nu=1}^{\infty} \dot{\zeta}_\nu Z_\nu(x_E)]^2\}$$

$$\tfrac{1}{2} I_E \{[\dot{\varphi} - \sum_{\nu=1}^{\infty} \dot{\eta}_\nu Y_\nu'(x_E)]^2 + [\dot{\chi} - \sum_{\nu=1}^{\infty} \dot{\zeta}_\nu Z_\nu'(x_E)]^2\}$$

where ℓ_E is the distance of the mass center of the engine to the swivel point and x_E is the distance of the swivel point to the mass center of the vehicle. The value I_E is the moment of inertia about the mass center of the engine.

If the vehicle has p stationary engines, the kinetic energy of these is

$$(5.4)\quad T_{EF} = \tfrac{1}{2} \sum_{\lambda=1}^{p} m_{E\lambda}\{[\dot{y} - (x_{E\lambda} + \ell_{E\lambda})\dot{\varphi} + \sum_{\nu=1}^{\infty} \dot{\eta}_\nu Y_\varphi(x_{E\lambda})]^2$$
$$+ [\dot{z} - (x_{E\nu} + \ell_{E\lambda})\dot{\chi} + \sum_{\nu=1}^{p} \dot{\zeta}_\nu Z_\nu(x_{E\lambda})]^2\}$$
$$+ \tfrac{1}{2} \sum_{\lambda=1}^{p} I_{E\lambda}\{[\dot{\varphi} - \sum_{\nu=1}^{\infty} \dot{\eta}_\nu Y_\nu'(x_E)] + [\dot{\chi} - \sum_{\nu=1}^{\infty} \dot{\zeta}_\nu Z_\nu'(x_E)]^2\}$$

The kinetic energy of a swivel engine is given by

$$T_{SE} = \tfrac{1}{2} m_E \{[\dot{y} - x_E\dot{\varphi} - \ell_E\dot{\Phi}_1 + \sum_{\nu=1}^{\infty} \dot{\eta}_\nu Y_\nu(x_E)]^2 + [\dot{z} - x_E\dot{\chi} - \ell_E\dot{\Phi}_2 + \sum_{\nu=1}^{\infty} \dot{\zeta}_\nu Z_\nu(x_E)]^2\}$$

$$\tfrac{1}{2} I_E (\dot{\Phi}_1^2 + \dot{\Phi}_2^2)$$

where Φ_1 and Φ_2 are the rotations of the swivel engine in the xy and xz-plane relative to an inertial system.

It is

$$\Phi_1 = \varphi + \beta_1 - \sum_{\nu=1}^{\infty} \eta_\nu Y_\nu'(x_E)$$

and

$$\Phi_2 = \chi + \beta_2 - \sum_{\nu=1}^{\infty} \zeta_\nu Z'_\nu(x_E)$$

where β_1 and β_2 are the engine deflections in xy and xz-plane respectively. If the space vehicle has q swivel engines, the kinetic energy is then

$$(5.5)\quad T_{SE} = \tfrac{1}{2} \sum_{\lambda=1}^{\infty} m_{E\lambda}\{[\dot{y} - x_{E\lambda}\dot{\Phi} - \ell_{E\lambda}\dot{\Phi}_{1\lambda} + \sum_{\nu=1}^{\infty} \dot{\eta}_\nu Y_\nu(x_{E\lambda})]^2 + [\dot{z} - x_{E\lambda}\dot{\chi} - \ell_{E\lambda}\dot{\Phi}_{2\lambda} + \sum_{\nu=1}^{\infty} \dot{\zeta}_\nu Z_\nu(x_{E\lambda})]^2\} + \tfrac{1}{2} \sum_{\lambda=1}^{\infty} I_{E\lambda}(\dot{\Phi}^2_{1\lambda} + \dot{\Phi}^2_{2\lambda})$$

In most practical cases the masses of the engines, their moments of inertia and the distances $x_{E\lambda}$ and $\ell_{E\lambda}$ can be considered equal among each other.

Potential Energy. The potential energy consists again of three main parts, namely that of the structure, engines and that of the propellant. The potential energy of the structure is made up by two parts, one of which representing the elastic energy of deformation

$$(5.6)\quad V_{SE} = \tfrac{1}{2} \sum_{\nu=1}^{\infty} \{\eta_\nu^2 [\int \frac{M_\nu^2}{EI}\, dx + \int \frac{Q_\nu^2}{A_S G}] + \zeta_\nu^2 [\int \frac{M_\nu^2}{EI}\, dx + \int \frac{Q_\nu^2}{A_S G}\, dx]\}$$

$$= \tfrac{1}{2} \sum_{\nu=1}^{\infty} V_\nu(\eta_\nu^2 + \zeta_\nu^2)$$

and the other, the work performed by raising the center of mass of the empty vehicle in the gravitational field due to rotation. This part becomes in linearized form

$$(5.7) \qquad V_s = m_s g x_s \left(\frac{\varphi^2 + \chi^2}{2}\right)$$

Equation (5.6) can also be expressed by

$$(5.8)\ V_{SE} = \tfrac{1}{2} \sum_{\nu=1}^{\infty} \{\omega_\nu^2 \eta_\nu^2 [\int m_s' Y_\nu^2 \, dx + \int I_s' Y_\nu'^2 dx] + \omega_\nu^2 \zeta_\nu^2 [\int m_s' Z_\nu^2 dx + \int I_s' Z_\nu'^2 dx]\}$$

$$= \tfrac{1}{2} \sum_{\nu=1}^{\infty} M_{B\nu} \, \omega_\nu^2 \, (\eta_\nu^2 + \zeta_\nu^2)$$

Here, M_ν represents the bending moment, and Q_ν the shear force acting on an elemental cross section. The flexural stiffness is EI, G is the shear modulus, and A_s represents the shear area of the cross section. The bending frequency of the νth lateral bending mode is w_ν and $M_{B\nu}$ represents the generalized mass of the space vehicle. It may be mentioned here that the values $M_{B\nu}$, Y_ν, ω_ν^2 are obtained from a lateral bending analysis with non-sloshing propellant. The value m_s' therefore, represents the mass per unit length of the structure and non-sloshing propellant. m_s represents the mass of the empty structure.

The potential energy of the propellant is obtained by using again the mechanical analogy, and it is composed of the energy stored in springs and the lifting of the model masses in the gravitational field. It is

$$(5.9)\ V_p = \tfrac{1}{4} \sum_{\lambda=1}^{\ell} \sum_{n=1}^{\infty} k_{\lambda n} (y_{n\lambda}^2 + z_{n\lambda}^2)^2 + \tfrac{1}{2} g \varphi^2 \left\{ \sum_{\lambda=1}^{\ell} m_{o\lambda} x_{o\lambda} + \sum_{\lambda=1}^{\infty} \sum_{n=1}^{\infty} m_{n\lambda} \, x_{n\lambda} \right\}$$

$$- \frac{g}{z} (\varphi^2 + \chi^2) \sum_{\lambda=1}^{\ell} \sum_{n=1}^{\infty} m_{n\lambda} \alpha_{n\lambda} (y_{n\lambda}^2 + z_{n\lambda}^2) + \sum_{\lambda=1}^{\ell} \sum_{n=1}^{\infty} m_{n\lambda} g \alpha_{n\lambda} (y_{n\lambda}^2 + z_{n\lambda}^2)$$

$$- g \sum_{\lambda=1}^{\ell} \sum_{n=1}^{\infty} m_{\lambda n} y_{n\lambda} \{\varphi - \sum_{\nu=1}^{\infty} \eta_\nu Y_\nu'(x_{\lambda n})\} - g \sum_{\lambda=1}^{\ell} \sum_{n=1}^{\infty} m_{n\lambda} z_{\lambda n} \{\chi - \sum_{\nu=1}^{\infty} \zeta_\nu Z_\nu'(x_{\lambda n}) \}$$

In order to derive the potential energy of the engines, they are considered as masses $m_{E\lambda}$ with a moment of inertia $I_{E\lambda}$. At the swivel engines

the gimballing system is considered as a simple spring-damper-system.

The work performed due to pitching and yawing in the gravitational field g is for p stationary engines given by

$$(5.10)\quad V_{EGF} = \tfrac{1}{2}\sum_{\lambda=1}^{p} m_{E\lambda}\, g(x_{E\lambda} + \ell_{E\lambda})\,(\varphi^2 + \chi^2)$$

and for q swivel engines, it is

$$(5.11)\quad V_{EGS} = \tfrac{1}{2}\sum_{\lambda=1}^{q} m_{E\lambda} g\, x_{E\lambda}(\varphi^2 + \chi^2) + \tfrac{1}{2}\sum_{\lambda=1}^{q} m_{E\lambda} g \ell_{E\lambda}(\Phi_{1\lambda}^2 + \Phi_{2\lambda}^2)$$

The actual engine deflection will be determined by an effective spring constant and damping coefficient of the gimbal system. The potential energy therefore is

$$(5.12)\quad V_{EKS} = \tfrac{1}{2}\sum_{\lambda=1}^{q} k_{E\lambda}(\epsilon_{1\lambda}^2 + \epsilon_{2\lambda}^2)$$

where $\epsilon_{i\lambda} = \beta_{i\lambda} - \beta_{ic\lambda}$. $\beta_{i\lambda}$ is the actual engine deflection of the λth engine, while $\beta_{ic\lambda}$ is the angle due to the control signal. $\omega_{E\lambda}$ is the natural frequency of the λth gimbal engine system and $\bar{I}_{E\lambda} = m_{E\lambda}\ell_{E\lambda}^2 + I_{E\lambda}$. The subscript $i = 1, 2$ indicates the plane in which the engine gimbals. $i = 1$ indicates the xy-plane, while $i = 2$, indicates the xz-plane.

Dissipation function. The dissipation function of the structure arises from its structural damping which is considered proportional to the amplitude of the elastic system and in phase with its velocity. This, unfortunately, would lead to complex elements, which would complicate the analysis considerably. To avoid this computational complication, a dissipation function is employed which is based on an equivalent linear viscous damping. This is justified as long as the damping forces are small and only of importance in the neighborhood of the bending frequencies.

The dissipation function of the structure is therefore given by

$$(5.13) \qquad D_s = \tfrac{1}{2} \sum_{\nu=1}^{\infty} \omega_\nu M_{B\nu} g_\nu (\dot{\eta}_\nu^2 + \dot{\zeta}_\nu^2)$$

where g_ν is the dimensionless structural damping coefficient of the νth lateral bending vibration mode, and ranges in the neighborhood of $0.001 \leq g \leq 0.05$.

The dissipation function of the liquid propellant arises from the equivalent linear viscous damping as it was introduced in the mechanical model (see section 4). It is with $C_{\lambda n} = 2\, \zeta_{n\lambda}\, \omega_{n\lambda}\, m_{n\lambda}$

$$(5.14) \quad D_p = \tfrac{1}{2} \sum_{\lambda=1}^{\ell} \sum_{n=1}^{\infty} C_{n\lambda} (\dot{x}_{\lambda n}^2 + \dot{y}_{\lambda n}^2 + \dot{z}_{\lambda n}^2) + \tfrac{1}{2} \sum_{\lambda=1}^{\ell} C_{s\lambda} (\dot{\psi}_{1\lambda}^2 + \dot{\psi}_{2\lambda}^2)$$

$$= \sum_{\lambda=1}^{\ell} \sum_{n=1}^{\infty} \zeta_{n\lambda} \omega_{n\lambda} m_{n\lambda} \{\dot{y}_{\lambda y}^2 + \dot{z}_{\lambda n}^2 + 4\alpha_{n\lambda}^2 (y_{\lambda n} \dot{y}_{\lambda n} + z_{\lambda n} \dot{z}_{\lambda n})^2\} + \tfrac{1}{2} \sum_{\lambda=1}^{\ell} C_{s\lambda} (\dot{\psi}_{1\lambda}^2 + \dot{\psi}_{2\lambda}^2)$$

where $\zeta_{n\lambda}$ is the damping factor and $\omega_{n\lambda}$ the circular natural frequency of the nth sloshing mode in the λth container. The second series represents the damping of the spheres.

The dissipation concerned with the swivel engines arises from the friction of the gimballing system at the swivel points and the viscous damping in their actuators. The friction at the swivel point is assumed to be small and independent of the load. It will therefore be neglected. The viscous damping of the actuators is described by the dashpot of the equivalent mechanical gimballing system and is proportional to the difference of the velocities of the command signal and the actual velocity of the swivel engine. It is therefore

$$(5.15) \qquad D_E = \tfrac{1}{2} \sum_{\lambda=1}^{q} C_{\lambda E} (\dot{\epsilon}_{1x}^2 + \dot{\epsilon}_{2\lambda}^2)$$

The equations of motion are obtained by performing the differentiations for each generalized coordinate in the Lagrange equation, where the

following relations have to be observed.

The total mass m of the vehicle is given by

$$(5.16)\quad m = \int m_s' dx + \sum_{\lambda=1}^{\ell} m_{o\lambda} + \sum_{\lambda=1}^{\ell} \sum_{n=1}^{\infty} m_{n\lambda} + \sum_{\lambda=1}^{p+q} m_{E\lambda}$$

The origin of the coordinate system is at the equilibrium position of the center of mass of the total space vehicle, which is expressed by the equation

$$(5.17)\quad \int m_s' x dx + \sum_{\lambda=1}^{\ell} m_{o\lambda} x_{o\lambda} + \sum_{\lambda=1}^{\ell} \sum_{n=1}^{\infty} m_{n\lambda} x_{n\lambda} + \sum_{\lambda=1}^{p+q} m_{E\lambda} (x_{E\lambda} + \ell_{E\lambda}) = 0$$

Furthermore the linear momentum for the normal modes of vibration is conserved and expressed by

$$(5.18)\quad \int m_s' \begin{Bmatrix} Y_\nu \\ Z_\nu \end{Bmatrix} dx + \sum_{\lambda=1}^{\ell} m_{o\lambda} \begin{Bmatrix} Y_\nu(x_{o\lambda}) \\ Z_\nu(x_{o\lambda}) \end{Bmatrix} + \sum_{\lambda=1}^{\ell} \sum_{n=1}^{\infty} m_{n\lambda} \begin{Bmatrix} Y_\nu(x_{n\lambda}) \\ Z_\nu(x_{n\lambda}) \end{Bmatrix} = 0$$

where the integrations are to be performed along the total vehicle length.

Generalized forces of thrust. Before proceeding to the derivation of the equations of motion some of the generalized forces that cannot be represented from a potential are derived. They are obtained by calculating the virtual work done by the external forces through virtual increments of the generalized coordinate δq_i. It is

$$\delta W = \Sigma\, Q_i\, \delta q_i$$

where W is the work and Q_i are the generalized forces. We shall derive here that due to the space vehicle's thrust F. If only a part F_2 of the thrust $F = F_1 + F_2$ is employed for control purposes, i.e., if only

this part of the total thrust can be gimballed, while the remainder F_1 of the thrust is stationary then the derivation of the generalized forces with respect to the thrust is as follows.

The generalized force of the lateral translation due to the thrust vector of the vehicle is given by the thrust component in y-direction. The virtual work is

$$\delta W_y = F[\varphi - \sum_{\nu=1}^{\infty} \eta_\nu Y'_\nu(x_E)]\delta y + F_2 \beta_1 \delta y$$

from which the generalized force Q_y is obtained. It is

$$Q_y = F[\varphi - \sum_{\nu=1}^{\infty} \eta_\nu Y'_\nu(x_E)] + F_2 \beta_1 \tag{5.19}$$

where β_1 is the engine deflection as measured from the center line of the space vehicle. A similar expression is obtained in z-direction. It is

$$Q_z = F[\chi - \sum_{\nu=1}^{\infty} \zeta_\nu Z'_\nu(x_E)] + F_2 \beta_2 \tag{5.20}$$

The generalized force of rotation is presented by the moment of the thrust force about the center of mass of the vehicle, and yields with

$$\delta W_\varphi = F\{x_E \sum_{\nu=1}^{\infty} \eta_\nu Y'_\nu(x_E) - \sum_{\nu=1}^{\infty} \eta_\nu Y_\nu(x_E)\}\delta\varphi - F_2 x_E \beta_1 \delta\varphi$$

the expression

$$Q_\varphi = F\{x_E \sum_{\nu=1}^{\infty} \eta_\nu Y'_\nu(x_E) - \sum_{\nu=1}^{\infty} \eta_\nu Y_\nu(x_E)\} - F_2 x_E \beta_1 \tag{5.21}$$

and

$$(5.22)\quad Q_\chi = F\left\{x_E \sum_{\nu=1}^{\infty} \zeta_\nu Z'_\nu(x_E) - \sum_{\nu=1}^{\infty} \zeta_\nu Z_\nu(x_E)\right\} - F_2 x_E \beta_1$$

Finally the generalized force of the thrust with respect to the generalized coordinates arising from the lateral bending of the space vehicle are obtained in a similar way be observing that the thrust force is always perpendicular to the lateral bending motion and that the virtual work through a virtual displacement of the generalized coordinate η_ν is

$$\delta W_{\eta\nu} = F_2 \beta_1 Y_\nu(x_E)\ \delta\eta_\nu$$

The generalized force is therefore

$$(5.23)\qquad Q_{\eta\nu} = F_2 \beta_1 Y_\nu(x_E)$$

and

$$(5.24)\qquad Q_{\zeta\nu} = F_2 \beta_2 Z_\nu(x_E)$$

The generalized forces of the thrust with respect to the sloshing displacement is zero, i.e., $Q_{y_n} = 0$ and $Q_{z_n} = 0$. Furthermore $Q_{\varepsilon i} = 0$.

The equations of constraint are obtained for the νth engine from

$$\Psi_{\nu 1} = \varphi + \beta_{\nu 1} - \sum_{\mu=1}^{\infty} \eta_\mu Y'_\mu(x_E) - \Phi_{1\nu} = 0$$

$$\Psi_{\nu 1} = \chi + \beta_{\nu 2} - \sum_{\mu=1}^{\infty} \zeta_\mu Z'_\mu(x_E) - \Phi_{2\nu} = 0$$

which can be expressed with $\beta_{\nu\lambda} = \beta_{\nu\lambda c} + \epsilon_{\nu\lambda}$ as

$$(5.25)\quad \Psi_{\nu 1} = \varphi + \beta_{c\nu 1} + \epsilon_{\nu 1} - \sum_{\mu=1}^{\infty} \eta_\mu Y'_\mu(x_E) - \Phi_{1\nu} = 0$$

$$(5.26)\qquad \Psi_{\nu 2} = \chi + \beta_{c\nu 2} + \epsilon_{\nu 2} - \sum_{\mu=1}^{\infty} \zeta_\mu Z'_\mu(x_E) - \Phi_{2\nu} = 0$$

The equation of motion for the translation y of the space vehicle is obtained from equation (5.1) with equations (6.2) through (5.15) by employing the results (5.16) through (5.17). It is

$$(5.27)\quad m\ddot{y} + \sum_{\lambda=1}^{\infty}\sum_{n=1}^{\infty} m_{n\lambda}\,\ddot{y}_{n\lambda} - m_{sE}\ell_E\Big[\ddot{\beta}_1 - \sum_{\nu=1}^{\infty}\ddot{\eta}_\nu Y'_\nu(x_E)\Big]$$
$$m_E\sum_{\nu=1}^{\infty}\ddot{\eta}_\nu Y_\nu(x_E) = F\Big\{\varphi - \sum_{\nu=1}^{\infty}\eta_\nu Y'_\nu(x_E)\Big\} + F_2\beta_1 + Q_y$$

where Q_y is the generalized force due to aerodynamics forces (drag, etc.). $m_{sE}\ell_E$ is the total first moment of the swivel engines about swivel point, and m_E is the total mass of all engines.

$$m_E = \sum_{\lambda=1}^{p} m_{\lambda_E} + \sum_{\lambda=1}^{q} m_{\lambda E}$$

The equation of motion for the translation z of the space vehicle is given by

$$(5.28)\quad m\ddot{z} + \sum_{\lambda=1}^{\ell}\sum_{n=1}^{\infty} m_{\lambda n}\,\ddot{z}_{\lambda n} - m_{sE}\ell_E\Big[\ddot{\beta}_2 - \sum_{\nu=1}^{\infty}\ddot{\zeta}_\nu Z'_\nu(x_E)\Big]$$
$$+ m_E\sum_{\nu=1}^{\infty}\ddot{\zeta}_\nu Z_\nu(x_E) = F\Big\{\chi - \sum_{\nu=1}^{\infty}\zeta_\nu Z'_\nu(x_E)\Big\} + F_2\beta_2 + Q_z$$

The reaction moments about the swivel points are obtained by differentiating the Lagrange equation with respect to the rotation angle ψ_ν

and observing that $Q_{\psi_\nu} = 0$. It is

$$-\lambda_1 = \bar{I}_{SE}\Big[\ddot{\varphi} + \ddot{\beta}_1 - \sum_{\nu=1}^{\infty} \ddot{\eta}_\nu Y'_\nu(x_E)\Big] + m_{SE}\, g\ell_E \Big[\varphi + \beta_1 - \sum_{\nu=1}^{\infty} \eta_\nu Y'_\nu(x_E)\Big]$$

$$-m_{SE}\,\ell_{SE}\Big[\ddot{y} - x_E\ddot{\varphi} + \sum_{\nu=1}^{\infty} \ddot{\eta}_\nu Y_\nu(x_E)\Big]$$

and $$-\lambda_2 = \bar{I}_{SE}\Big[\ddot{\chi} + \ddot{\beta}_2 - \sum_{\nu=1}^{\infty} \ddot{\zeta}_\nu Z'_\nu(x_E)\Big] + m_{SE}\, g\ell_E \Big[\chi + \beta_2 - \sum_{\nu=1}^{\infty} \zeta_\nu Z'_\nu(x_E)\Big]$$

$$-m_{SE}\,\ell_{SE}\Big[\ddot{Z} - x_E\chi + \sum_{\nu=1}^{\infty} \ddot{\zeta}_\nu Z_\nu(x_E)\Big]$$

The equation of motion for <u>pitching motion</u>, φ, of the space vehicle is obtained from equation (5.1) with $q_i = \varphi$ and with the result of the equations (5.2) through (5.26). It is

(5.29)

$$I\ddot{\varphi} + \sum_{\lambda=1}^{\ell} I_{s\lambda}\ddot{\psi}_{1\lambda} - \sum_{\lambda=1}^{\ell}\sum_{n=1}^{\infty} m_{n\lambda} x_{n\lambda}\ddot{y}_{n\lambda} + \sum_{\lambda=1}^{\ell}\sum_{n=1}^{\infty} m_{n\lambda}\bar{\alpha}_{n\lambda}(y_{n\lambda}^2 + z_{n\lambda}^2).\Big\{\ddot{y} + \ddot{y}_{n\lambda}\sum_{\nu=1}^{\infty}\ddot{\eta}_\nu Y_\nu(x_{n\lambda})\Big\}$$

$$+ 2\sum_{\lambda=1}^{\ell}\sum_{n=1}^{\infty} m_{n\lambda}\bar{\alpha}_{n\lambda}(y_{n\lambda}\dot{y}_{n\lambda} + z_{n\lambda}\dot{z}_{n\lambda})\Big\{\dot{y} + \dot{y}_{n\lambda} + \sum_{\nu=1}^{\infty}\dot{\eta}_\nu Y_\nu(x_{n\lambda})\Big\} - g\sum_{\lambda=1}^{\ell}\sum_{n=1}^{\infty} m_{n\lambda} y_{n\lambda}$$

$$+ m_{SE}\, g\,\ell_E\Big[\beta_1 - \sum_{\nu=1}^{\infty}\eta_\nu Y'_\nu(x_E)\Big] + \Big[\bar{I}_{SE} + m_{SE}\, x_E\,\ell_E\Big]\Big[\ddot{\beta}_1 - \sum_{\nu=1}^{\infty}\ddot{\eta}_\nu Y'_\nu(x_E)\Big] - m_{SE}\,(x_E+\ell_E)\sum_{\nu=1}^{\infty}\ddot{\eta}_\nu Y_\nu(x_E)$$

$$- m_{FE}\,(x_E+\ell_E)\sum_{\nu=1}^{\infty}\ddot{\eta}_\nu Y_\nu(x_E) - I_{FE}\sum_{\nu=1}^{\infty}\ddot{\eta}_\nu Y'_\nu(x_E) = Q_\varphi + F\Big\{x_E\sum_{\nu=1}^{\infty}\eta_\nu Y'_\nu(x_E) - \sum_{\nu=1}^{\infty}\eta_\nu Y_\nu(x_E)\Big\}$$

$$- F_2\, x_E\,\beta_1 .$$

where the effective moment of inertia of the space vehicle is given by

$$(5.30)\quad I \equiv mk^2 = \int m_s' x^2\,dx + \int I_s'\,dx + \sum_{\lambda=1}^{\ell} m_{o\lambda} x_{o\lambda}^2 + \sum_{\lambda=1}^{\ell} I_{o\lambda} + \sum_{\lambda=1}^{\ell} \sum_{n=1}^{\infty} m_{n\lambda} x_{n\lambda}^2 + \sum_{\lambda=1}^{p+q} \{ I_{E\lambda} + m_{E\lambda}(x_{E\lambda} + \ell_{E\lambda})^2 \} + \sum_{\lambda=1}^{\ell} I_{s\lambda}$$

and the equation for the conservation of the angular moment has been observed:

$$(5.31)\quad \int m_s' x Y_\nu(x)\,dx + \int I_s' Y_\nu'(x)\,dx + \sum_{\lambda=1}^{\ell} m_{o\lambda} x_{o\lambda} Y_\nu(x_{o\lambda}) - \sum_{\lambda=1}^{\ell} I_{o\lambda} Y_\nu'(x_{o\lambda}) + \sum_{n=1}^{\infty} \sum_{\lambda=1}^{\ell} m_{n\lambda} x_{n\lambda}\, Y_\nu(x_{n\lambda}) = 0$$

The value x_E is the distance of the swivel point of the engines from the origin and k is the radius of gyration of the space vehicle. The first term on the right hand side of equation (5.29) represents the generalized force of the thrust with respect to lateral bending and Q_y in the generalized force due to aerodynamics, drag, etc. The values $Y_\nu(x_E)$ and $Y_\nu'(x_E)$ are the lateral displacement and slope (in y-direction) of the νth bending mode at the location of the swivel point, respectively.

The equation of motion for <u>yawing</u>, χ, is given by

(5.32)

$$I\ddot{\chi} + \sum_{\lambda=1}^{\ell} I_{s\lambda}\ddot{\psi}_{2\lambda} - \sum_{\lambda=1}^{\ell}\sum_{n=1}^{\infty} m_{n\lambda}x_{n\lambda}\ddot{z}_{n\lambda} + \sum_{\lambda=1}^{\ell}\sum_{n=1}^{\infty} m_{n\lambda}\overline{\alpha}_{n\lambda}(y_{n\lambda}+z_{n\lambda})\{\ddot{z}+\ddot{z}_{n\lambda}+\sum_{\nu=1}^{\infty}\ddot{\zeta}_{\nu}Z_{\nu}(x_{n\lambda})\}$$

$$+ 2\sum_{\lambda=1}^{\ell}\sum_{n\ 1}^{\infty} m_{n\lambda}\overline{\alpha}_{n\lambda}(y_{n\lambda}\dot{y}_{n\lambda}+ z_{n\lambda}\dot{z}_{n\lambda})\{\dot{z}+\dot{z}_{n\lambda}+\sum_{\nu=1}^{\infty}\dot{\zeta}_{\nu}Z_{\nu}(x_{n\lambda})\} - g\sum_{\lambda=1}^{\ell}\sum_{n=1}^{\infty} m_{n\lambda}z_{n\lambda}$$

$$+ m_{SE}\,g\,\ell_E[\beta_2 - \sum_{\nu=1}^{\infty}\zeta_{\nu}Z'_{\nu}(x_E)] + [\overline{I}_{SE}+m_{SE}x_E\ell_E][\ddot{\beta}_2 - \sum_{\nu=1}^{\infty}\ddot{\zeta}_{\nu}Y'_{\nu}(x_E)] - m_{SE}(x_E+\ell_E)\sum_{\nu=1}^{\infty}\ddot{\zeta}_{\nu}Z_{\nu}(x_E)$$

$$- m_{FE}(x_E+\ell_E)\sum_{\nu=1}^{\infty}\ddot{\zeta}_{\nu}Z_{\nu}(x_E) - I_{FE}\sum_{\nu=1}^{\infty}\ddot{z}_{\nu}Z'_{\nu}(x_E) = Q_{\chi}+F\{x_E\sum_{\nu=1}^{\infty}\zeta_{\nu}Z'_{\nu}(x_E) - \sum_{\nu=1}^{\infty}\zeta_{\nu}Z_{\nu}(x_E)\}$$

$$- F_2x_E\beta_2 .$$

where the equation of conservation of angular momentum

$$(5.33)\quad \int m'_s x\, Z_{\nu}(x)dx + \int I'_s Z'_{\nu}(x)dx + \sum_{\lambda=1}^{\infty} m_{o\lambda}x_{o\lambda}Z_{\nu}(x_{o\lambda}) + \sum_{\lambda=1}^{\ell} I_{o\lambda}Z'_{\nu}(x_{o\lambda}) + \sum_{n=1}^{\infty}\sum_{\lambda=1}^{\ell} m_{n\lambda}x_{n\lambda}\,Z_{\nu}(x_{n\lambda}) = 0$$

has been observed.

The equation of motion of the moving <u>propellant</u> in the containers of the space vehicle is based on the mechanical model and is obtained by applying the Lagrange equation to the generalized coordinate $y_{n\lambda}$. Observing that the generalized force $Q_{yn\lambda}$ vanishes yields the equation of the modal sloshing mass

$$(5.34)\quad \ddot{y}_{n\lambda} + 2\omega_{n\lambda}\zeta_{n\lambda}[\dot{y}_{n\lambda} + 4\overline{\alpha}^2_{n\lambda}y_{n\lambda}(y_{n\lambda}\dot{y}_{n\lambda}+z_{n\lambda}\dot{z}_{n\lambda})] + 4\overline{\alpha}^2_{n\lambda}y_{n\lambda}[\dot{y}^2_{n\lambda} + \dot{z}^2_{n\lambda} + y_{\lambda n}\ddot{y}_{n\lambda}+z_{n\lambda}\ddot{z}_{n\lambda}] + \omega^2_{n\lambda}y_{n\lambda} + \frac{k_{n\lambda}}{m_{n\lambda}}y_{n\lambda}(y^2_{n\lambda}+z^2_{n\lambda}) + \ddot{y} - x_{n\lambda}\ddot{\varphi} - g\varphi + \sum_{\nu=1}^{\infty}\ddot{\eta}_{\nu}Y_{\nu}(x_{n\lambda}) + g\sum_{\nu=1}^{\infty}\eta_{\nu}Y'_{\nu}(x_{n\lambda}) = 0$$

The subscript n indicates the number of the propellant mode under consideration while λ indicates the container number. $\zeta_{n\lambda}$ is the damping factor of the propellant and $\omega_{\lambda n}$ its undamped circular natural frequency. In z-direction it is

$$(5.35)\quad \ddot{z}_{n\lambda} + 2\omega_{n\lambda}\,\zeta_{n\lambda}[\dot{z}_{n\lambda} + 4\bar{\alpha}^2_{n\lambda} z_{n\lambda}(y_{n\lambda}\dot{y}_{n\lambda} + z_{n\lambda}\dot{z}_{n\lambda})] + 4\bar{\alpha}^2_{n\lambda} z_{n\lambda}[\dot{y}^2_{n\lambda} + \dot{z}^2_{n\lambda} + y_{n\lambda}\ddot{y}_{n\lambda} + z_{n\lambda}\ddot{z}_{n\lambda}] + \omega^2_{n\lambda} z_{n\lambda} + \frac{k_{n\lambda}}{m_{n\lambda}} z_{n\lambda}(y^2_{n\lambda} + z^2_{n\lambda}) + \ddot{z} - x_{n\lambda}\ddot{\chi} - g\chi + \sum_{\nu=1}^{\infty} \ddot{\zeta}_\nu z_\nu(x_{n\lambda}) + g\sum_{\nu=1}^{\infty} \zeta_\nu z'_\nu(x_{n\lambda}) = 0$$

$\begin{Bmatrix} Y_\nu(x_{n\lambda}) \\ Z_\nu(x_{n\lambda}) \end{Bmatrix}$ and $\begin{Bmatrix} Y'_\nu(x_{n\lambda}) \\ Z'_\nu(x_{n\lambda}) \end{Bmatrix}$ are displacement and slope respectively of the νth lateral bending mode at the location of the nth sloshing mass in the λth container.

As space vehicles increase in size the lateral fundamental bending frequency approaches more and more the control frequency and the lower natural frequencies of the propellant. This indicates that in many cases the bending vibrations of the space vehicle can no longer be neglected in a dynamic analysis of the vehicle with the inclusion of propellant sloshing and control system.

The equation of motion of the <u>νth bending mode</u> is obtained from equation (6.1) with the equations (6.2) through (6.16) by observing the results of equations (6.17), (6.26) and the orthogonality relations between normal modes, as expressed by

$$(5.36)\quad \int m'_s \begin{Bmatrix} Y_\nu(x)Y_\mu(x) \\ Z_\nu(x)Z_\mu(x) \end{Bmatrix} dx + \int I'_s \begin{Bmatrix} Y'_\nu(x)Y'_\mu(x) \\ Z'_\nu(x)Z'_\mu(x) \end{Bmatrix} dx + \sum_{\lambda=1}^{\ell} m_{o\lambda} \begin{Bmatrix} Y_\nu(x_{o\lambda})Y_\mu(x_{o\lambda}) \\ Z_\nu(x_{o\lambda})Z_\mu(x_{o\lambda}) \end{Bmatrix} + \sum_{\lambda=1}^{\ell} I_{o\lambda} \begin{Bmatrix} Y'_\nu(x_{o\lambda})Y'_\mu(x_{o\lambda}) \\ Z'_\nu(x_{o\lambda})Z'_\mu(x_{o\lambda}) \end{Bmatrix} + \sum_{\lambda=1}^{\ell}\sum_{n=1}^{\infty} m_{n\lambda} \begin{Bmatrix} Y_\nu(x_{n\lambda})Y_\mu(x_{n\lambda}) \\ Z_\nu(x_{n\lambda})Z_\mu(x_{n\lambda}) \end{Bmatrix}$$

It is therefore

(5.37)

$$M_{B\nu}\{\ddot{\eta}_\nu + g_\nu\omega_\nu\dot{\eta}_\nu + \omega_\nu^2\eta_\nu\} + \sum_{\lambda=1}^{\ell}\sum_{n=1}^{\infty} m_{n\lambda}\,\ddot{y}_{n\lambda}\,Y_\nu(x_{n\lambda}) + g\sum_{\lambda=1}^{\ell}\sum_{n=1}^{\infty} m_{n\lambda}y_{n\lambda}Y_\nu'(x_{n\lambda})$$

$$-m_{ES}\,g\ell_E\,Y_\nu'(x_E)\,[\varphi + \beta_1 - \sum_{\mu=1}^{\infty}\eta_\mu Y_\mu'(x_E)]$$

$$+m_E Y_\nu(x_E)\{\ddot{y} - (x_E + \ell_E)\,\ddot{\varphi} - \ell_E\ddot{\beta}_1 + \sum_{\mu=1}^{\infty}\ddot{\eta}_\mu Y_\mu(x_E)\} - m_{SE}\ell_E Y_\nu(x_E)\sum_{\mu=1}^{\infty}\ddot{\eta}_\mu Y_\mu'(x_E)$$

$$+m_{ES}\ell_E Y_\nu'(x_E)\{\ddot{y} - x_E\ddot{\varphi} + \sum_{\mu=1}^{\infty}\ddot{\eta}_\mu Y_\mu(x_E)\}$$

$$+\bar{I}_{SE}Y_\nu'(x_E)\{\sum_{\mu=1}^{\infty}\ddot{\eta}_\mu Y_\mu'(x_E) - \ddot{\beta}_1 - \ddot{\varphi}\}$$

$$+I_{FE}Y_\nu'(x_E)\{\sum_{\mu=1}^{\infty}\ddot{\eta}_\mu Y_\mu'(x_E) - \ddot{\varphi}\} = Q_{\eta\nu} + F_2\beta_1 Y_\nu(x_E)$$

Here ω_ν represents the natural circular frequency of the νth lateral bending mode and g_ν is the corresponding structural damping. The generalized mass of the νth lateral bending mode, $M_{B\nu}$ is given by the expression

$$(5.38)\quad M_{B\nu} = \int m_s'\begin{Bmatrix} Y_\nu^2(x) \\ Z_\nu^2(x)\end{Bmatrix} dx \quad \int I_s'\begin{Bmatrix} Y_\nu'^2(x) \\ Z_\nu'^2(x)\end{Bmatrix} dx \sum_{\lambda=1}^{\ell} m_{o\lambda}\begin{Bmatrix} Y_\nu^2(x_{o\lambda}) \\ Z_\nu^2(x_{o\lambda})\end{Bmatrix}$$

$$\sum_{\lambda=1}^{\ell} I_{o\lambda}\begin{Bmatrix} Y_\nu'^2(x_{o\lambda}) \\ Z_\nu'^2(x_{o\lambda})\end{Bmatrix} + \sum_{n=1}^{\infty}\sum_{\lambda=1}^{\ell} m_{n\lambda}\begin{Bmatrix} Y_\nu^2(x_{n\lambda}) \\ Z_\nu^2(x_{n\lambda})\end{Bmatrix}$$

In z-direction it is

(5.39)

$$M_B \nu \{\ddot{\zeta}_\nu + g_\nu \omega_\nu \dot{\zeta}_\nu + \omega_\nu^2 \zeta_\nu\} + \sum_{\lambda=1}^{\ell} \sum_{n=1}^{\infty} m_{n\lambda} \ddot{z}_{n\lambda} Z_\nu(x_{n\lambda}) + g \sum_{\lambda=1}^{\ell} \sum_{n=1}^{\infty} m_{n\lambda} z_{n\lambda} Z_\nu'(x_{n\lambda})$$

$$-m_{ES} g \ell_E Z_\nu'(x_E) [\chi + \beta_2 - \sum_{\mu=1}^{\infty} \zeta_\mu Z_\mu'(x_E)] + m_E Z_\nu(x_E) \{\ddot{z} - (x_E + \ell_E)\ddot{\chi} - \ell_E \ddot{\beta}_2 + \sum_{\mu=1}^{\infty} \ddot{\zeta}_\mu Z_\mu(x_E)\}$$

$$-m_{SE} \ell_E Z_\nu(x_E) \sum_{\mu=1}^{\infty} \ddot{\zeta}_\mu Z_\mu'(x_E) + m_{ES} \ell_E Z_\nu'(x_E) \{\ddot{z} - x_E \ddot{\chi} + \sum_{\mu=1}^{\infty} \ddot{\zeta}_\mu Z_\mu'(x_E)\}$$

$$+\bar{I}_{SE} Z_\nu'(x_E) \{\sum_{\mu=1}^{\infty} \ddot{\zeta}_\mu Z_\mu'(x_E) - \ddot{\beta}_2 - \ddot{\chi}\} + I_{FE} Z_\nu'(x_E) \{\sum_{\mu=1}^{\infty} \ddot{\zeta}_\mu Z_\mu'(x_E) - \ddot{\chi}\}$$

$$= Q_{\zeta\nu} + F_2 \beta_2 Z_\nu(x_E)$$

The values $\begin{Bmatrix} Y_\nu(x_{o\lambda}) \\ Z_\nu(x_{o\lambda}) \end{Bmatrix}$ and $\begin{Bmatrix} Y_\nu'(x_{o\lambda}) \\ Z_\nu'(x_{o\lambda}) \end{Bmatrix}$ represent the displacement and slope of the νth lateral bending mode at the location of the non-sloshing mass in the λth propellant tank.

Besides the sloshing of the propellant, only the control equation is a pronounced nonlinear equation. However, translational and rotational motions of the space vehicle usually occur at small frequencies where, in many cases, the control elements can be considered as essentially linear. Nonlinearities usually occur at higher frequencies in the form of saturation of amplifiers, limited output of velocities, etc. Therefore the control equation is written in the form $f_1(\beta_1, \beta_2) = f_2(\varphi_i, \chi_i, A_{i1}, A_{i2})$ where the operators f_1 and f_2 are functions depending on the character of the system. A_{i1} is the indicated acceleration as measured by an accelerometer normal to the longitudinal axis of the vehicle in y-direction, while A_{i2} is the indicated acceleration in z-direction.

φ_i and χ_i are the indicated angular deviation from the trajectory as indicated by the gyroscope.

It is $$\varphi_i = \varphi - \sum_{\nu=1}^{\infty} \eta_\nu Y'_\nu(x_G)$$

and $$\chi_i = \chi - \sum_{\nu=1}^{\infty} \zeta_\nu Z'_\nu(x_G)$$

where $\left\{ \begin{matrix} Y'_\nu(x\ ) \\ Z'_\nu(x\ ) \end{matrix} \right\}$ is the derivative of the νth lateral bending mode at the location of the gyroscope. If the fundamental lateral bending frequency is well above the control and propellant sloshing frequencies, of which the corresponding sloshing masses create pronounced dynamic effects, the flexibility of the space vehicle can be usually neglected. The equation of control sensors such as rate gyroscope angle-of-attack-meter and accelerometer are omitted here, but can be found in reference [10].

The equations of motion for the "nonsloshing spheres" are obtained by using for $q_i = \psi_{1n}$ and ψ_{2n}. They are

$$(5.40)\quad I_{sn}(\ddot{\varphi} + \ddot{\psi}_{1n}) + c_{sn}\dot{\psi}_{1n} = 0$$

and

$$(5.41)\quad I_{sn}(\ddot{\chi} + \ddot{\psi}_{2}\ ) + c_{sn}\dot{\psi}_{2n} = 0$$

$$(n = 1, 2, \ldots\ ).$$

The swivel engine equations are obtained by introducing into the Lagrange equations the coordinates $q_i = \epsilon_{1\nu}, \epsilon_{1\nu}$ and observing $Q_{\epsilon\nu} = 0$. They are

$$(5.42)\quad \bar{I}_{SE}\left[\ddot{\varphi} + \ddot{\beta}_1 - \sum_{\nu=1}^{\infty} \ddot{\eta}_\nu Y'_\nu(x_E)\right] + m_{SE}\, g\ell_E\left[\varphi + \beta_1 - \sum_{\nu=1}^{\infty} \eta_\nu Y'_\nu(x_E)\right]$$

$$-m_{SE}\,\ell_{SE}\left[\ddot{y} - x_E\ddot{\varphi} + \sum_{\nu=1}^{\infty} \ddot{\eta}_\nu Y_\nu(x_E)\ \right] + c_E(\dot{\beta}_1 - \dot{\beta}_{1C}) + k_E(\beta_1 - \beta_{1C}) = 0$$

and

$$(5.43)\ \bar{I}_{S\varepsilon}\left[\ddot{\chi}+\ddot{\beta}_2-\sum_{\nu=1}^{\infty}\ddot{\zeta}_\nu Z_\nu'(x_\varepsilon)\right]+m_{S\varepsilon}\,g\,\ell_\varepsilon\left[\chi+\beta_2-\sum_{\nu=1}^{\infty}\zeta_\nu Z_\nu'(x_\varepsilon)\right]$$

$$-m_{S\varepsilon}\,\ell_{S\varepsilon}\left[\ddot{z}-x_\varepsilon\ddot{\chi}+\sum_{\nu=1}^{\infty}\ddot{\zeta}_\nu Z_\nu(x_\varepsilon)\right]+c_\varepsilon(\dot{\beta}_2-\dot{\beta}_{2c})+k_\varepsilon(\beta_2-\beta_{2c})=0$$

5.2. Equations of Motion for Equivalently Linearized System

In many practical cases a dynamic analysis in one plane, say the xy-plane, is sufficient to indicate stability or instability of the system. Since linear theory can easily be treated with the usual methods applied to a system of linear equations, and since a computer program of such a system is available at the Aero-Astro-Laboratory of the Marshall Space Flight Center, NASA, in Huntsville, Alabama, an equivalently linearized mechanical model is used here for the description of the propellant motion. In this way, the solution of a system of linear and nonlinear equations is avoided and the presently available computer programs can be used. The integration of the equations of motion, however, has to be performed for a sufficiently large number of amplitudes.

The equations of motion are obtained from section 6.1. by omitting the equations in z-direction, χ, ζ_ν, $z_{n\lambda}$ and setting z, χ, ζ_ν and $z_{n\lambda}$ equal to zero. The equation of motion for <u>translation</u> is then

$$m\ddot{y}+\sum_{\lambda=1}^{\ell}\sum_{n=1}^{\infty}m_{n\lambda}\,\ddot{y}_{n\lambda}+m_\varepsilon\sum_{\nu=1}^{\infty}\ddot{\eta}_\nu Y_\nu(x_\varepsilon)-m_{S\varepsilon}\,\ell_\varepsilon\left[\ddot{\beta}_1-\sum_{\nu=1}^{\infty}\ddot{\eta}_\nu Y_\nu'(x_\varepsilon)\right]$$

$$=F\left\{\varphi-\sum_{\nu=1}^{\infty}\eta_\nu Y_\nu'(x_\varepsilon)\right\}+F_2\beta_1+Q_y$$

The equation for pitching motion is

$$I\ddot{\varphi} + \sum_{\lambda=1}^{\ell} I_{s\lambda}\ddot{\psi}_{\lambda} - \sum_{\lambda=1}^{\ell}\sum_{n=1}^{\infty} m_{n\lambda}\, x_{n\lambda}\, \ddot{y}_{n\lambda} - g \sum_{\lambda=1}^{\ell}\sum_{n=1}^{\infty} m_{n\lambda}\, y_{n\lambda} + m_E g \ell_E \left[\beta_1 - \sum_{\nu=1}^{\infty} \eta_\nu Y'_\nu(x_E)\right]$$

$$+ \left[\bar{I}_{SE} + m_{S_E} x_E \ell_E\right]\left[\ddot{\beta}_1 - \sum_{n=1}^{\infty} \ddot{\eta}_\nu Y'_\nu(x_E)\right] - m_{SE}(x_E + \ell_E)\sum_{\nu=1}^{\infty} \ddot{\eta}_\nu Y_\nu(x_E) - m_{FE}(x_E+\ell_E)\sum_{\nu=1}^{\infty} \ddot{\eta}_\nu Y_\nu(x_E)$$

$$-I_{FE}\sum_{\nu=1}^{\infty} \ddot{\eta}_\nu Y'_\nu(x_E) = Q_\varphi + F\{x_E \sum_{\nu=1}^{\infty} \eta_\nu Y'_\nu(x_E) - \sum_{\nu=1}^{\infty} \eta_\nu Y_\nu(x_E)\} - F_2 \beta_1 x_E$$

The sloshing of the propellant is now described by the equivalent linear equations.

$$m_{n\lambda}\, \ddot{y}_{n\lambda} + c_{n\lambda}(1 + \bar{\alpha}^2_{n\lambda} Y^2_{n\lambda})\, \dot{y}_{n\lambda} + [k_{on\lambda} + (\tfrac{3}{4} k_{n\lambda} - 2\bar{\alpha}^2_{n\lambda}\, \Omega^2 m_{n\lambda})\ Y^2_{n\lambda}]\, y_{n\lambda} =$$

$$= m_{n\lambda}\left[x_{n\lambda}\, \ddot{\varphi} - \ddot{y} + \sum_{\nu=1}^{\infty} \ddot{\eta}_\nu Y_\nu(x_{n\lambda})\right] + m_{n\lambda}\, g\left[\varphi - \sum_{\nu=1}^{\infty} \eta_\nu Y'_\nu(x_{n\lambda})\right]$$

$(n = 1, 2, \ldots.; \lambda = 1, 2, \ldots \ell)$.

The equation of motion of the "sphere" is given by

$$I_{sn}(\ddot{\varphi} + \ddot{\Psi}_n) + c_{sn}\dot{\Psi}_n = 0 \qquad (n = 1, 2, \ldots \ell)$$

The equation of bending vibrations is given by equation (5.37). The equation of the swivel engines are the same as in the previous case (see equation 5.42).

6. Comparison With Experimental Data

Of the small amount of experimental data available, especially amplitude frequency nonplanar data, that presented by Hutton [2] appeared most useful for purposes of comparison. Fluid amplitude versus excitation frequency measurements are given there for both the planar and nonplanar motions for several excitation amplitudes. These experimental values are compared with the response amplitudes determined from the model equations (2.20) and (2.27) in figures (6), (7a) and (7b). The value $\alpha_s = 2/3$ for the dimensionless spring constant was determined for agreement with the nonplanar data for excitation amplitude $x_o = 0.032$ in., since the nonplanar measurements for this excitation are more numerous and seemed more consistent. Figure (7b) indicates, however, that $\alpha_s = 2/3$ may be too large based on a comparison of the model values with the data for $x_o = 0.0195$ in. Although not shown in this figure, the model nonplanar response will agree well with the experimental point for $x_o = 0.0195$ in. if $\alpha_s = \frac{1}{2}$ is chosen. All comparisons with experimental data were made with $\alpha_s = 2/3$, since this value appears to be an upper bound. A decrease in the value of α_s will predict larger nonplanar amplitudes and bring the planar response into ever closer agreement with experimental values. Since the theoretical amplitudes and frequencies for the planar stability boundaries decrease with a decrease in α_s; $\alpha_s < 2/3$ will be a more conservative choice.

Figure (11) is a comparison of the fluid force determined for the model equations and experimental measurements obtained from [3]. The large amplitude planar measurements were obtained through the use of a vertical splitter plate plate which prevented the occurrence of nonplanar motion. The model force with $\alpha_s = 0$ and $\alpha_s = 2/3$ are shown along with the

theoretical values given in [3]. A value of α_s less than $\alpha_s = 2/3$ is indicated.

The effect of damping on the amplitudes of planar response is shown in figure (12) while the phase is shown in figure (13).

Figure (14) shows the regions of stable planar and nonplanar motions determined from the model equations for a 105" diameter tank with $x_o = \frac{1}{2}$ in. and $h/a = 1.5$.

7. Conclusions

The nonlinear mechanical model as it was derived gives a good description of the liquid behavior off and near resonance. Planar and nonplanar motion of the liquid are well described. Points of instability are obtained with good accuracy as has been seen by comparison with available experimental data. A model consisting of a mass point constrained to a paraboloid and a nonlinear spring that is capable of moving up and down the longitudinal axis seems to describe the liquid motion quite adequately. The results show better agreement than those of other models, such as a spherical pendulum, the mass of which does not exhibit the same relation between horizontal and vertical motion as the mass center of the sloshing liquid. Due to insufficient data on the pressure distribution, the liquid forces and torques, one value (α) of the model had to be obtained from experimental results [2] . The magnitude of this value seems to lie in the range $\frac{1}{2} \leq \alpha \leq 2/3$ for a circular cylindrical container. A change of this value may well describe fluid motions in other tank configurations, but has to be determined from experimental data.

Since, in most vehicles, only the propellant motion and control system exhibit dominant nonlinearities, the equations of motion of a space vehicle have been derived for lateral translation, pitching and yawing motion, propellant sloshing, swivel engine compliances and lateral bending. For the convenience of using available linear computer programs, the motion of the space vehicle was confined to the trajectory phane and the equations of motion have been equivalently linearized.

8. References

[1] Abramson, H. N., "Amazing Motion of Liquid Propellants", Astronautics, 6, pp. 35-37, March 1961.

[2] Hutton, R. W., "An Investigation of Resonant, Nonlinear, Nonplanar Free Surface Oscillations of a Fluid", NASA-TN-D-1870, May 1963.

[3] Abramson, H. N., Chu, W. H., Kana, D. D., "Some Studies of Nonlinear Lateral Sloshing in Rigid Containers", Southwest Research Institute, Final Report No. 02-1329 (Dec. 1964)

[4] Bauer, H. F., "Fluid Oscillations in the Container of a Space Vehicle and Their Influence Upon the Stability", NASA-TR-R-187 (1964)

[5] Berlot, R. R., "Production of Rotation in a Confined Liquid Through Translational Motion of the Boundaries", Journal of Applied Mechanics, 26, No. 4, pp. 513-516 (1959).

[6] Freed, L. E., "Stability of Motion of Conical Pendulums", Ramo-Woolridge Co., Report GM-45.3-434 (1957)

[7] Miles, J. W., "Stability of Forced Oscillations of a Spherical Pendulum", Quarterly Applied Mathematics, 20, 1, pp. 21-32 (1962)

[8] Rheinfurth, M. H., "Control-Feedback Stability Analysis," Army Ballistic Missile Agency, Redstone Arsenal, Alabama, Report No. DA-TR-2-60 (1960).

[9] Bauer, H. F., Rheinfurth, M. H.,: "Flutter and Stability Analysis", Army Ballistic Missile Agency, Redstone Arsenal, Alabama, Report No. DA-TM-4-60 (1960)

[10] Rheinfurth, M. H., "The Influence of Control Sensors on the Stability of Space Vehicles", NASA, Marshall Space Flight Center, MTR-61-65 (1961).

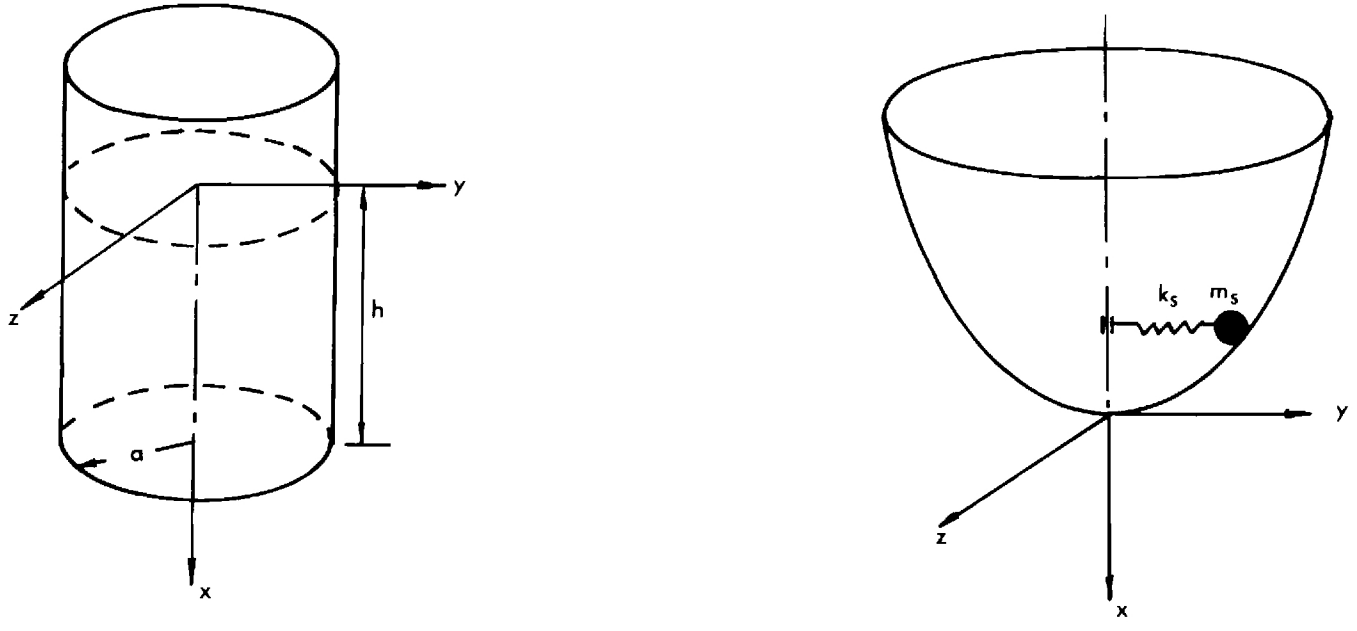

FIGURE 1: MECHANICAL MODEL AND COORDINATE SYSTEM

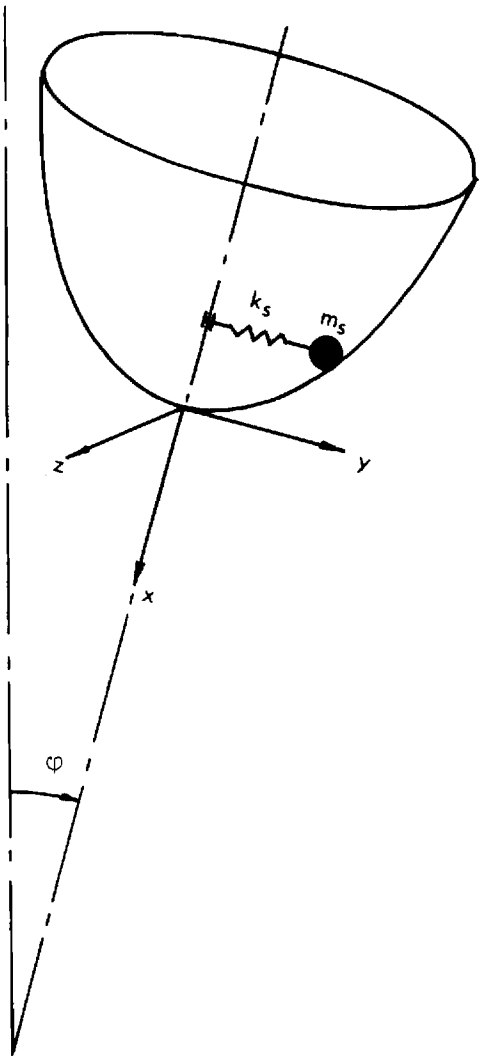

FIGURE 2: COORDINATES FOR PITCHING MOTION

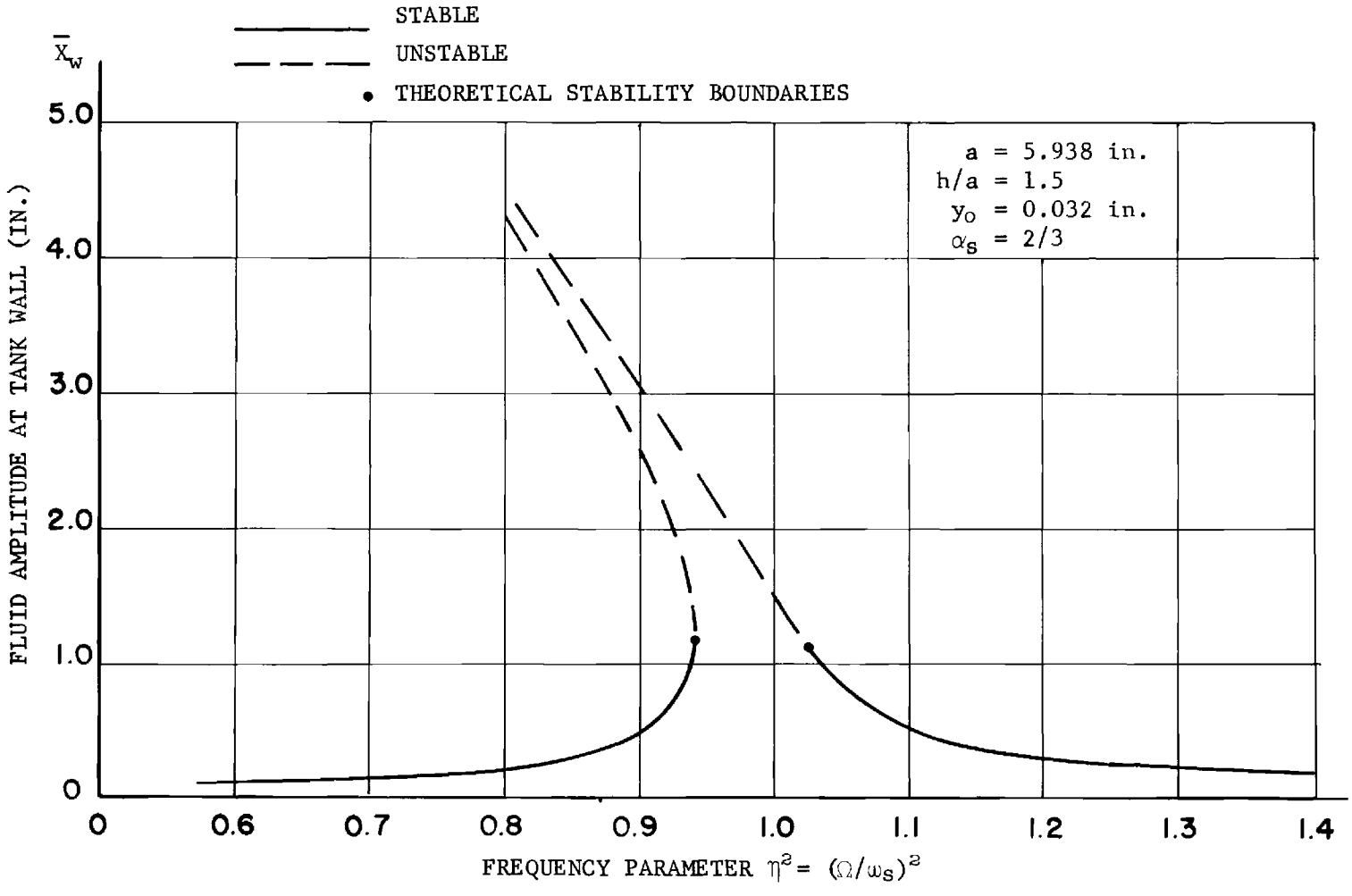

FIGURE 3: PLANAR FLUID MOTION RESPONSE

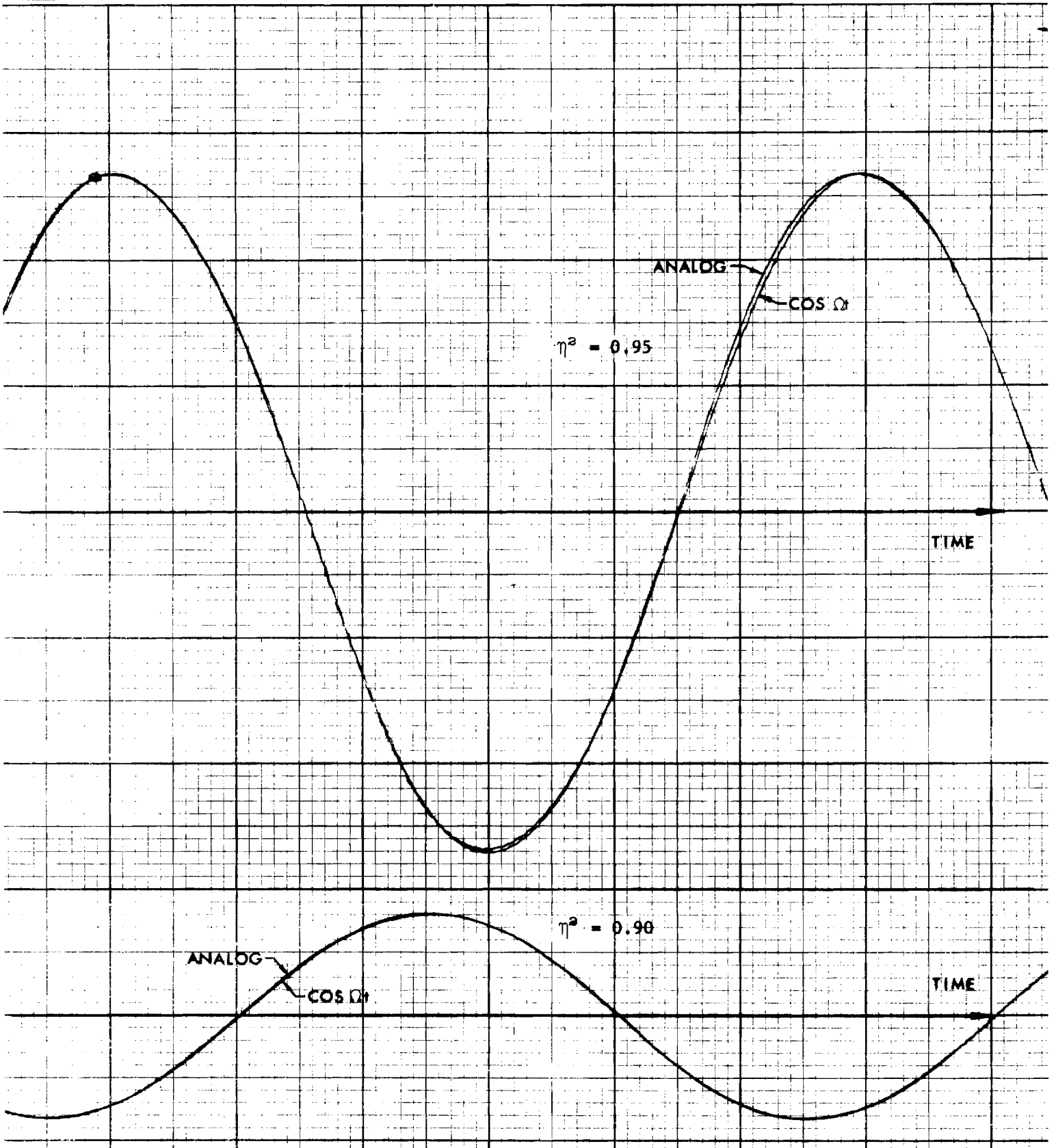

FIGURE 4: COMPARISON OF WAVE FORM OF ANALOG COMPUTER SOLUTION WITH HARMONIC, COS Ωt

(PLANAR)

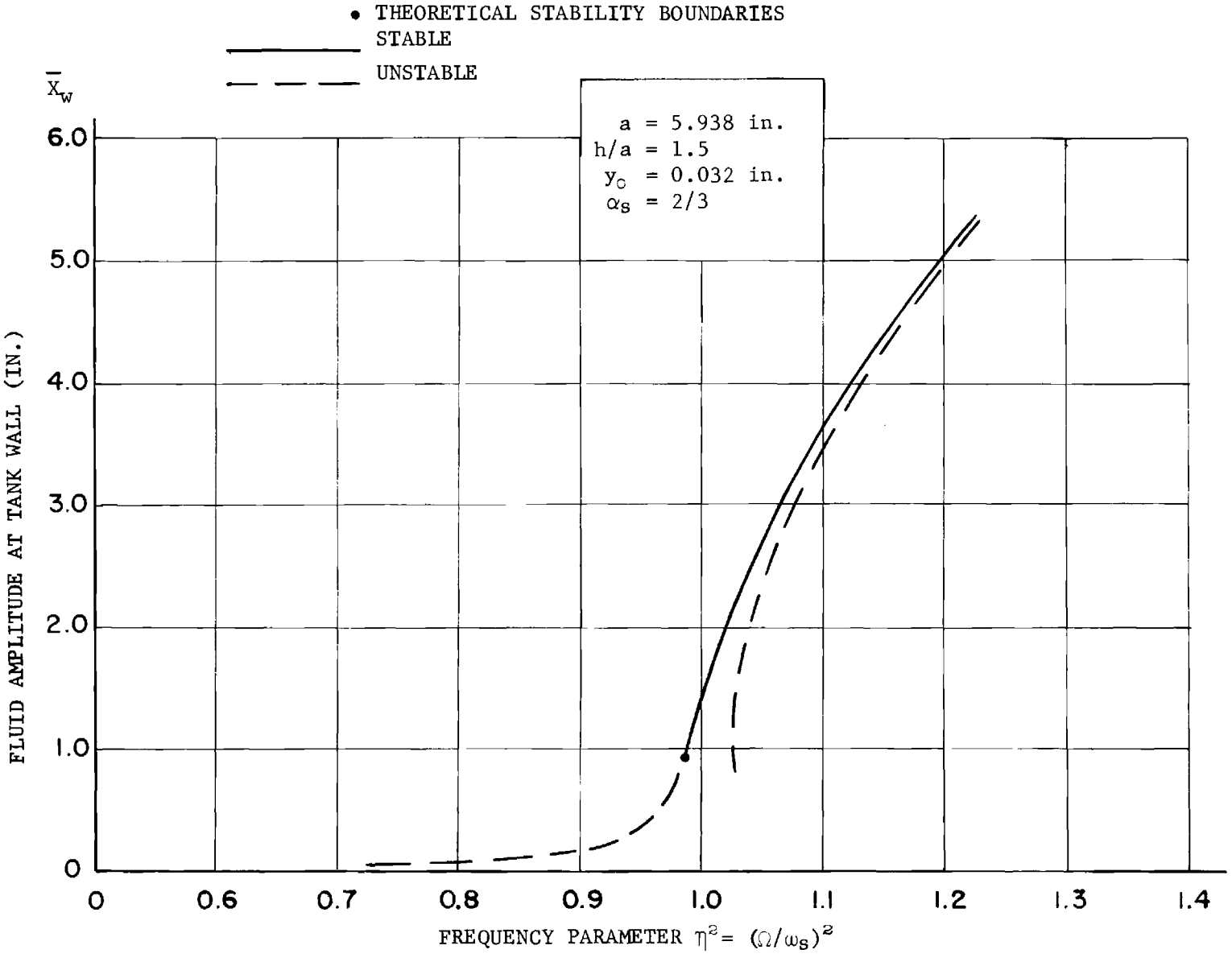

FIGURE 5a: NONPLANAR RESPONSE IN DIRECTION OF EXCITATION

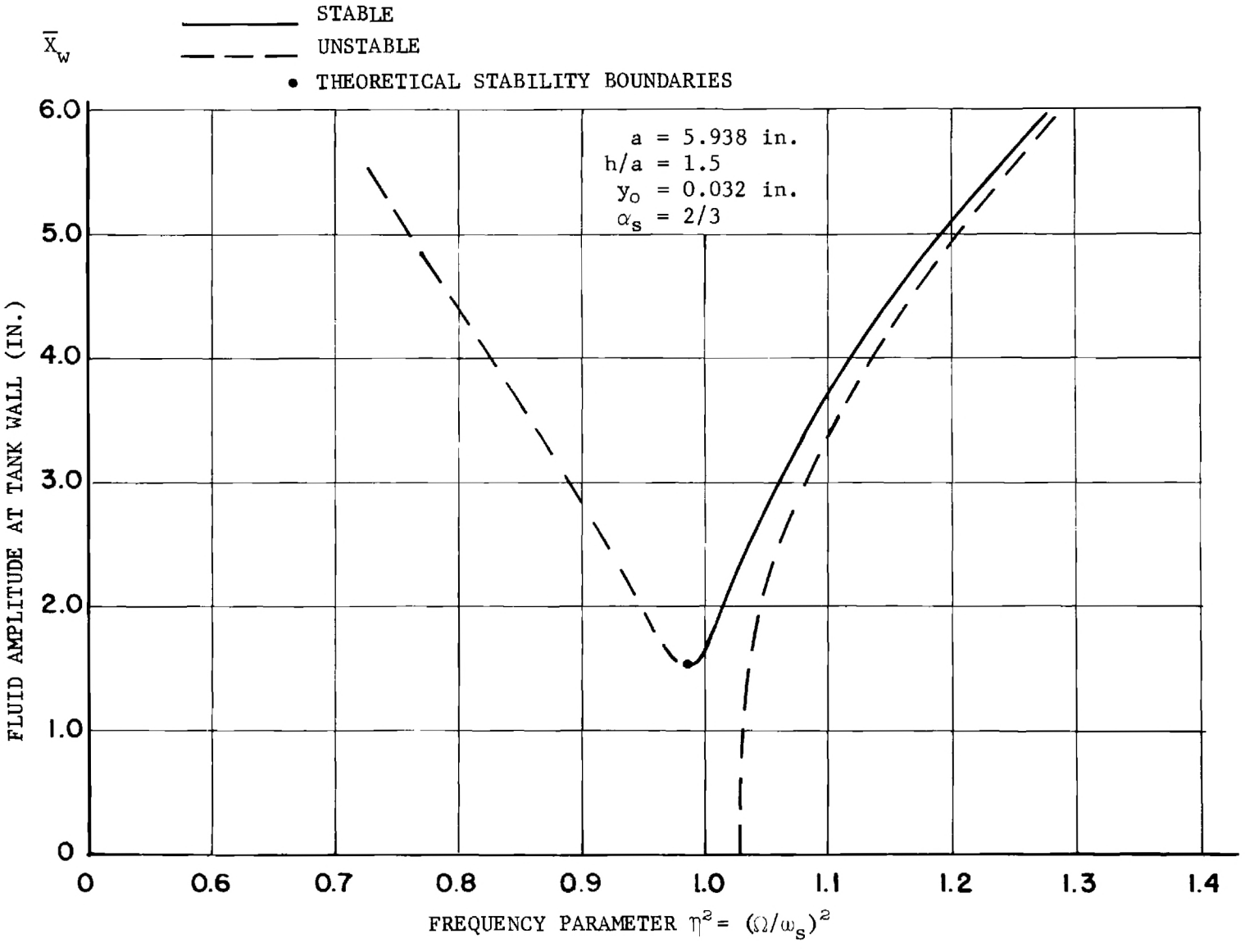

FIGURE 5b: NONPLANAR RESPONSE PERPENDICULAR TO EXCITATION

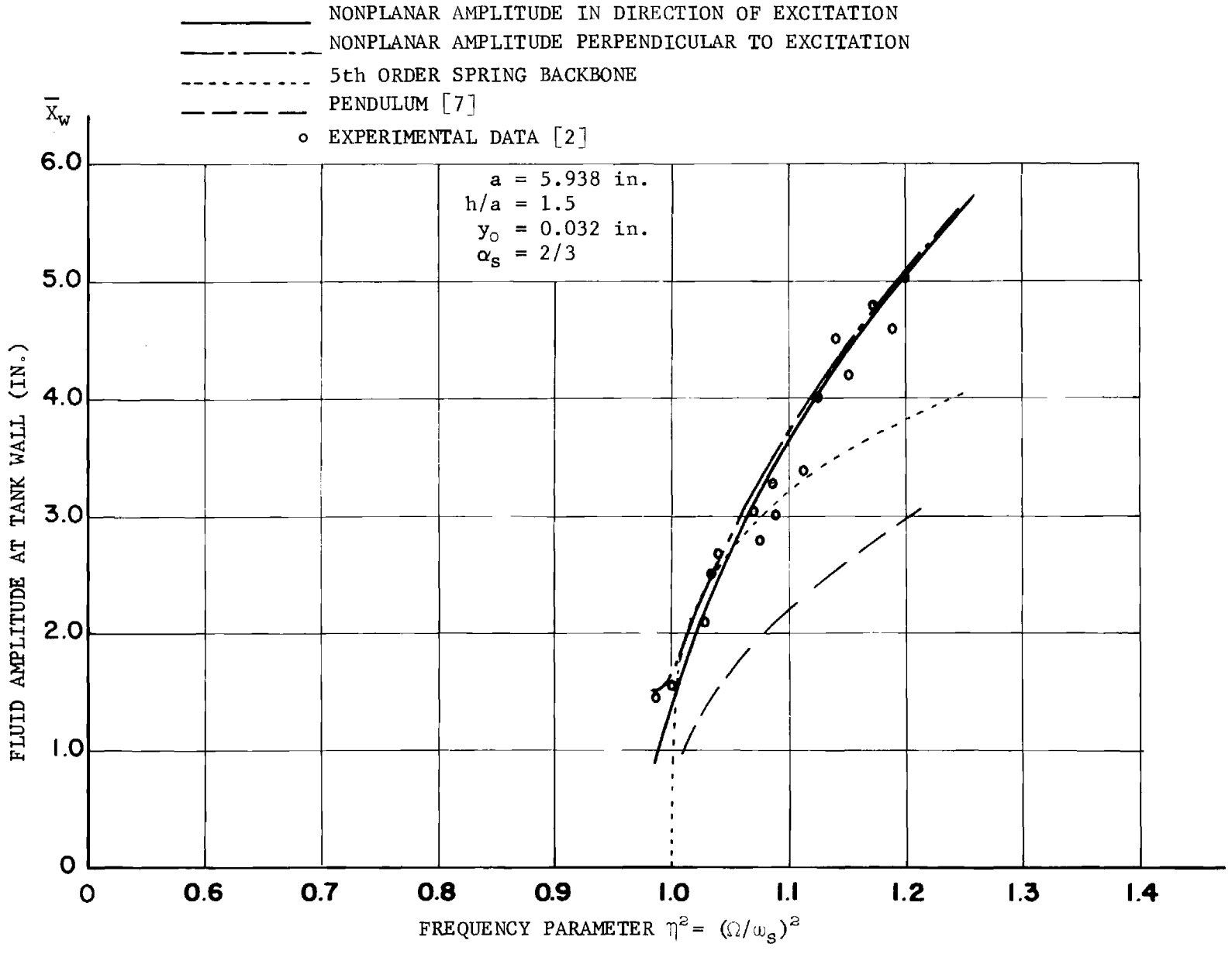

FIGURE 6: COMPARISON OF THEORETICAL AND EXPERIMENTAL FLUID AMPLITUDES

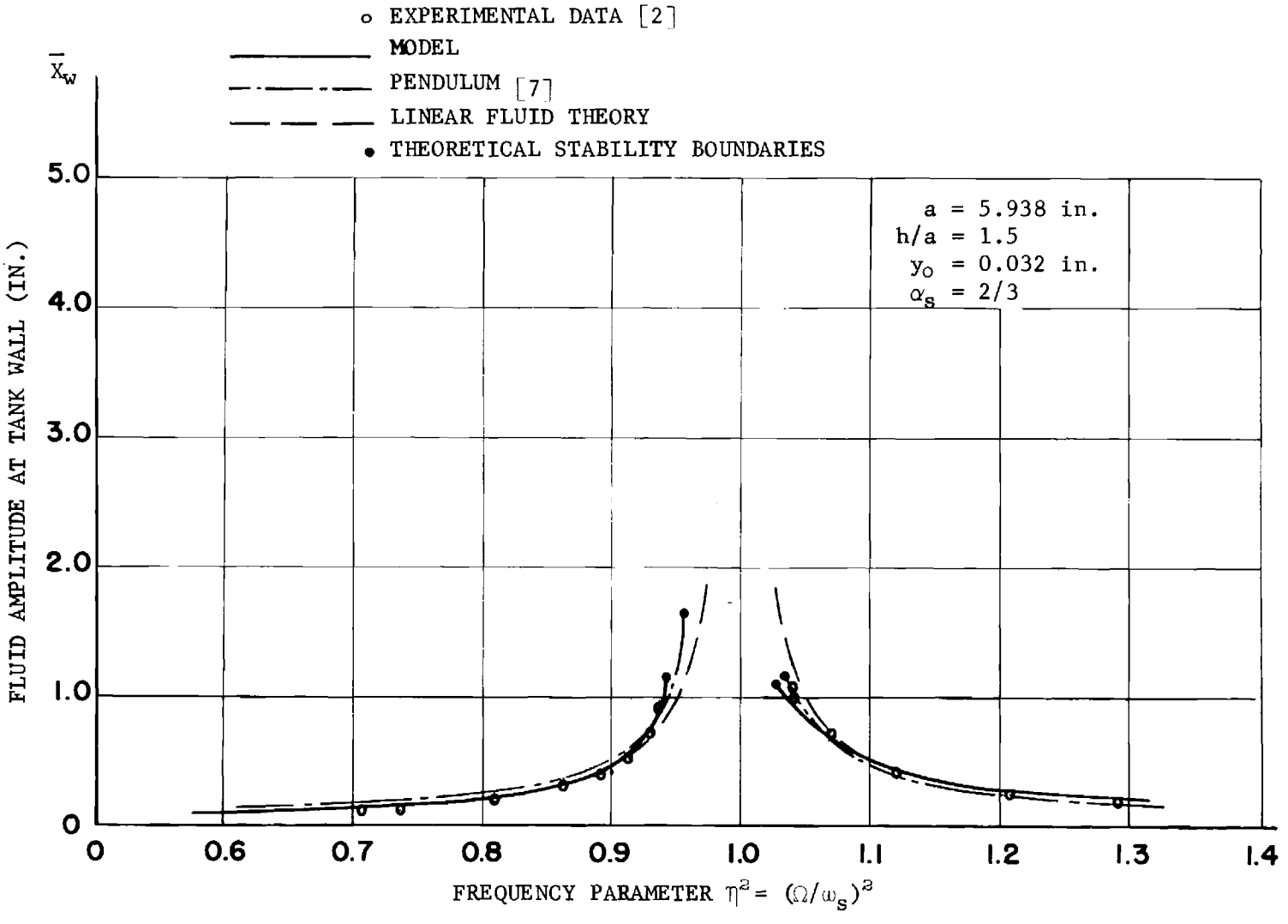

FIGURE 7a: COMPARISON OF THEORETICAL AND EXPERIMENTAL FLUID AMPLITUDES

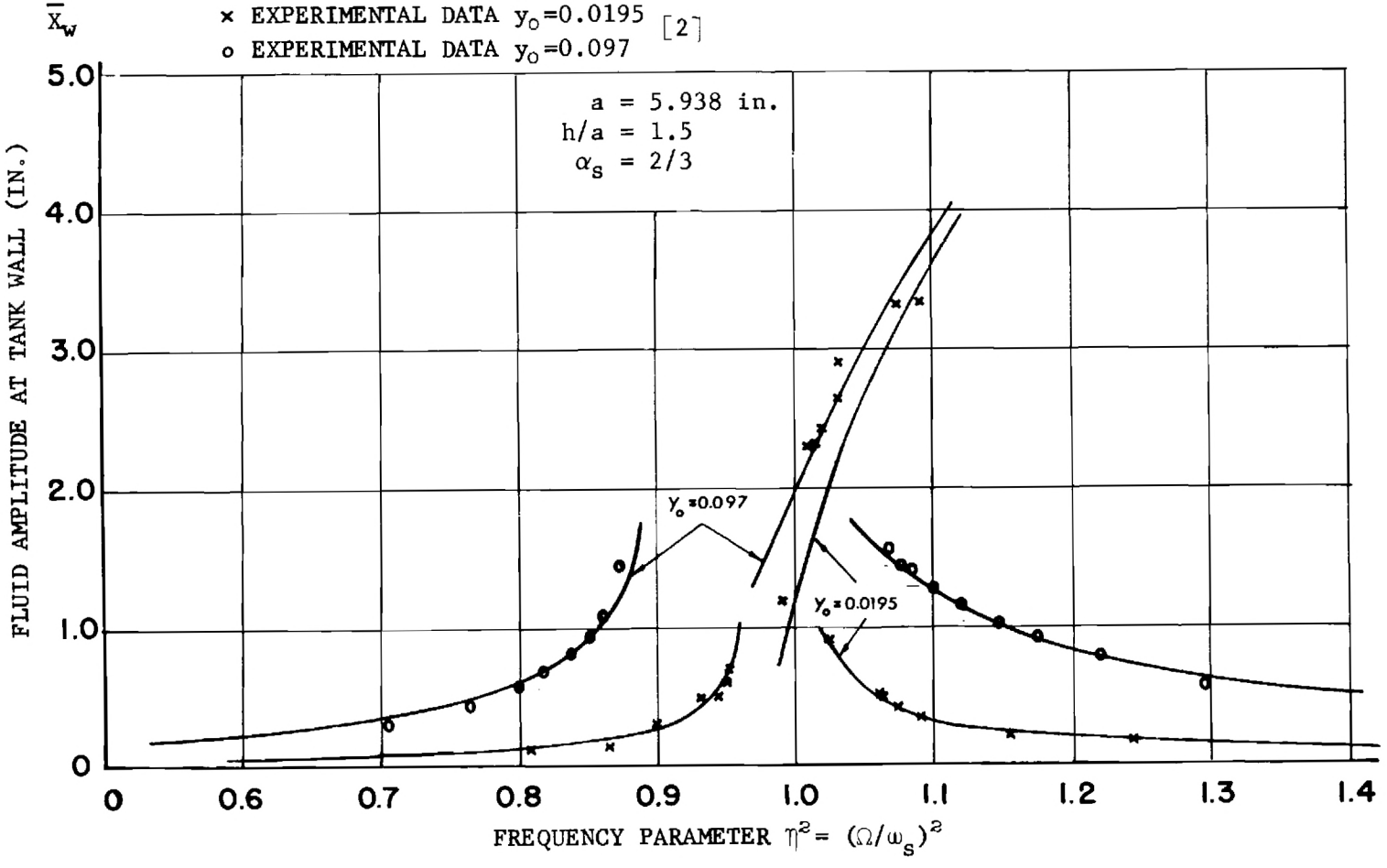

FIGURE 7b: COMPARISON OF THEORETICAL AND EXPERIMENTAL FLUID AMPLITUDES

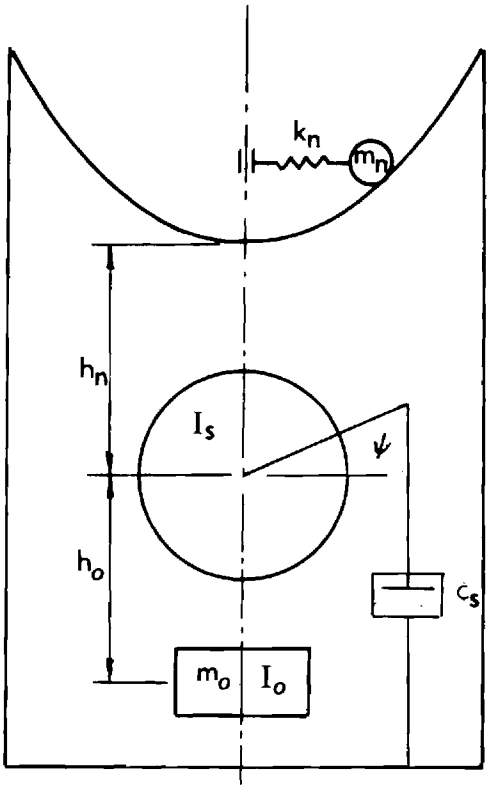

FIGURE 8: MECHANICAL MODEL FOR TOTAL FLUID SYSTEM

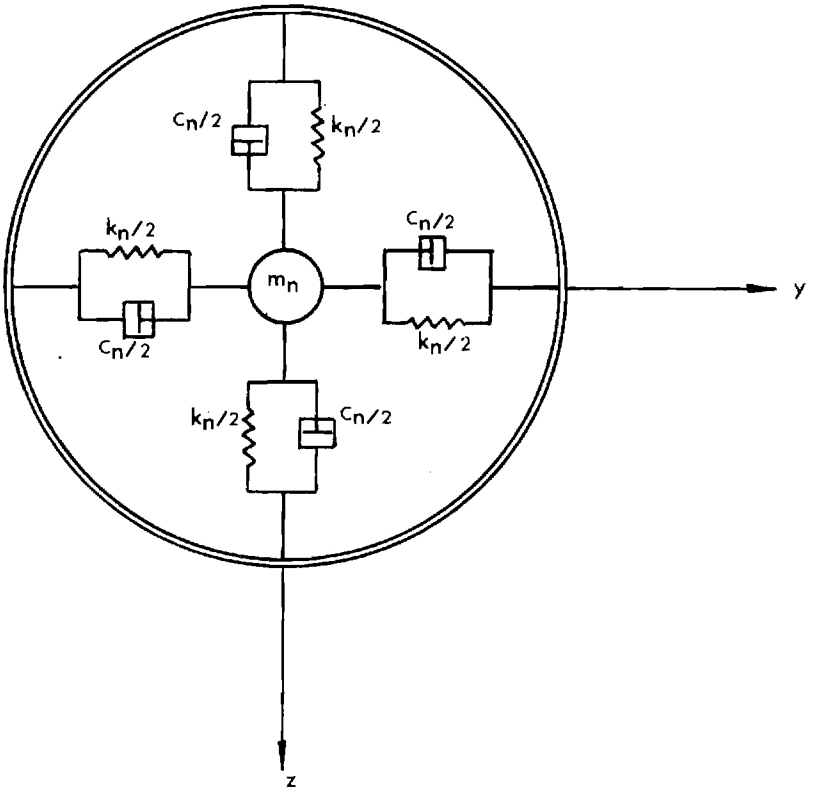

FIGURE 9: LINEAR MECHANICAL MODEL

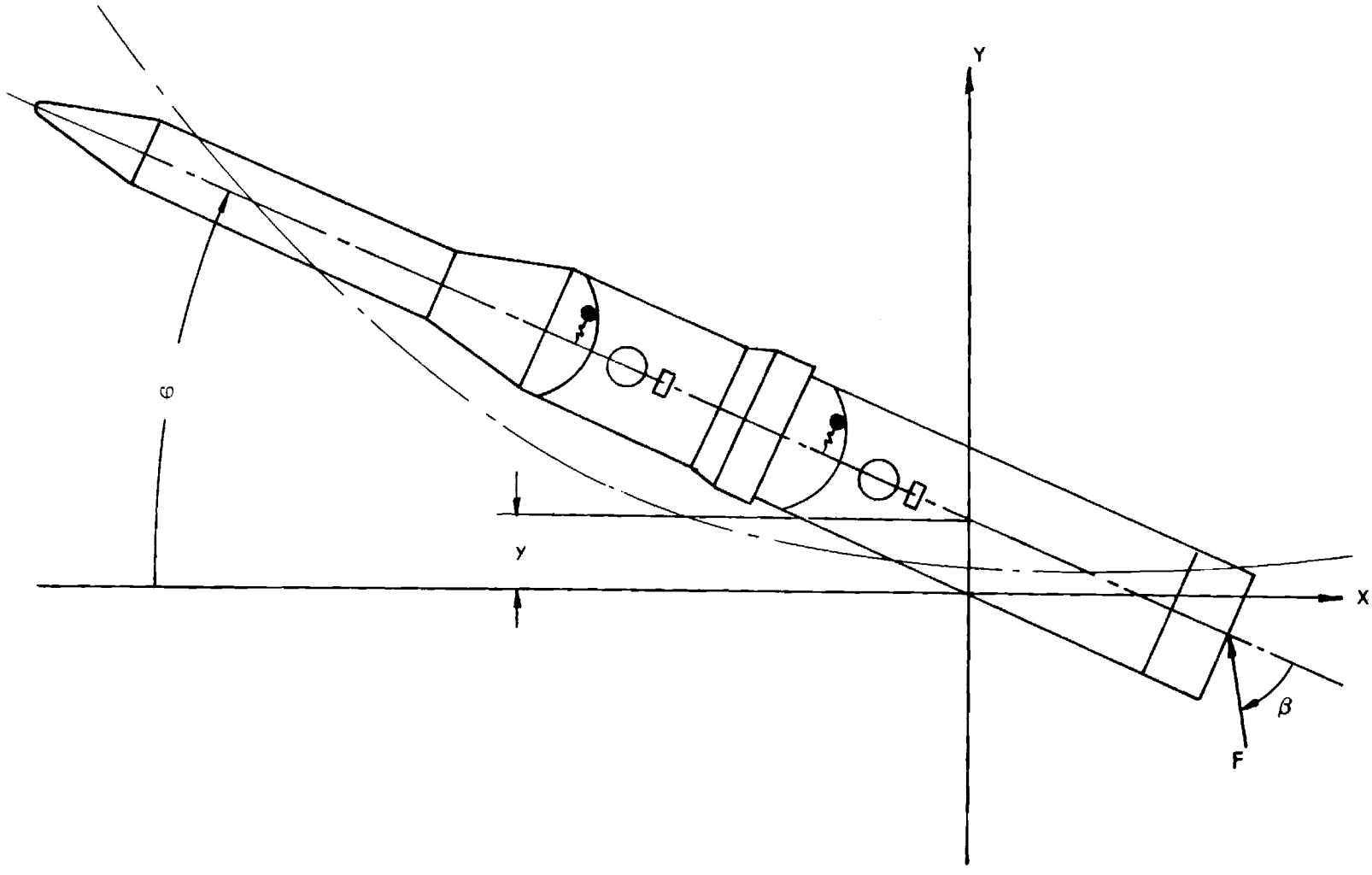

FIGURE 10: COORDINATE SYSTEM OF SPACE VEHICLE

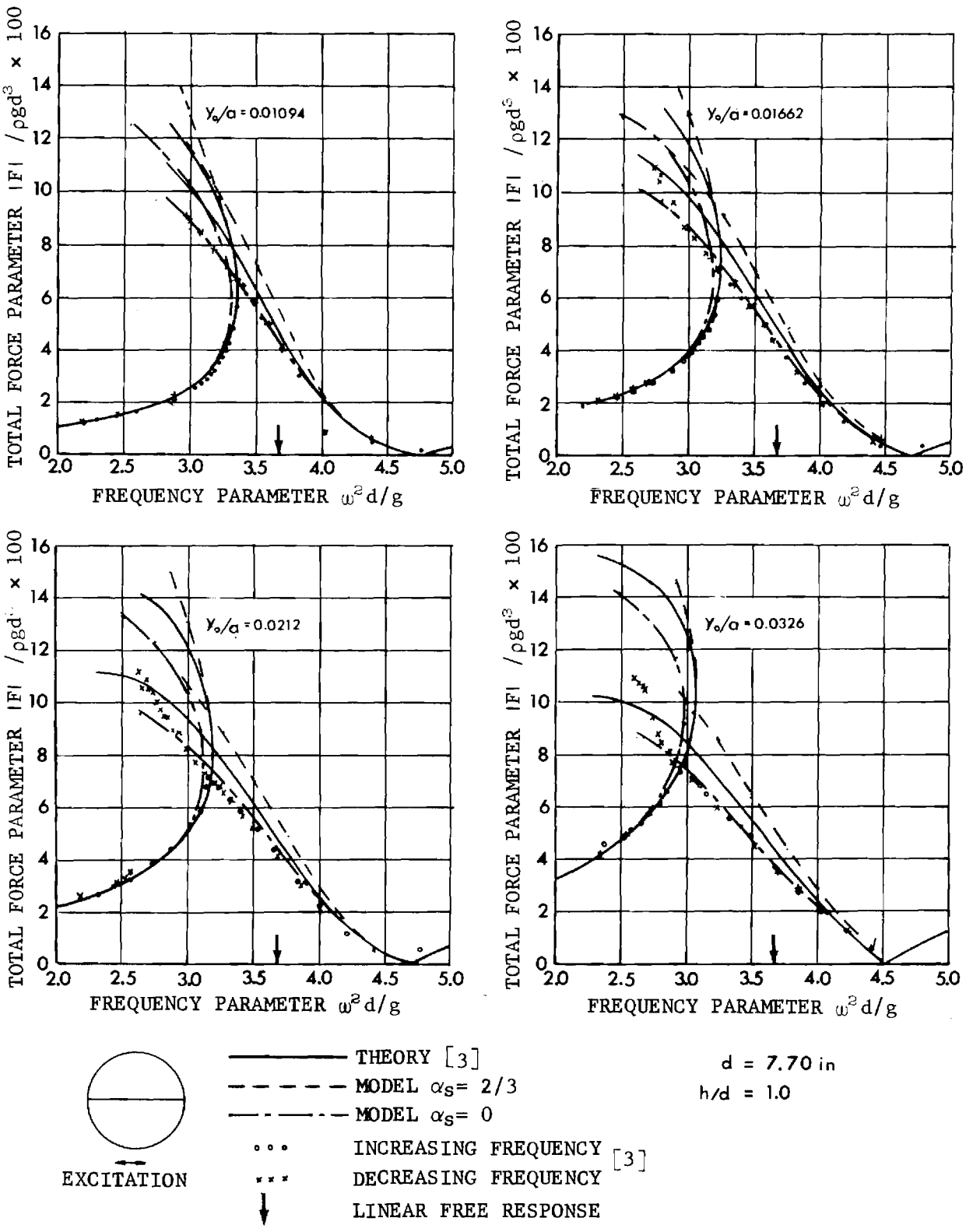

FIGURE 11: COMPARISON OF FLUID FORCE WITH EXPERIMENTAL DATA

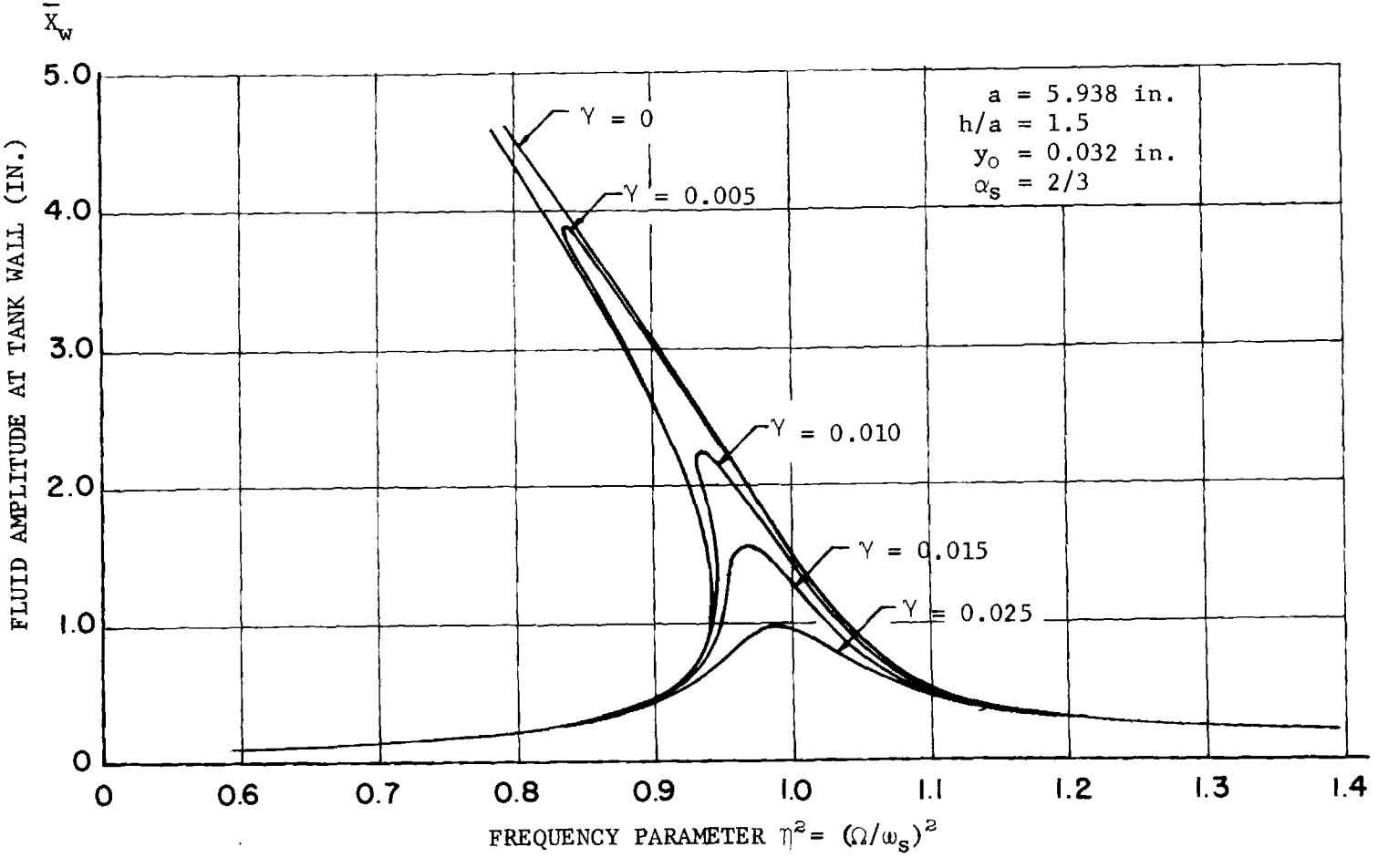

FIGURE 12: DAMPED PLANAR RESPONSE

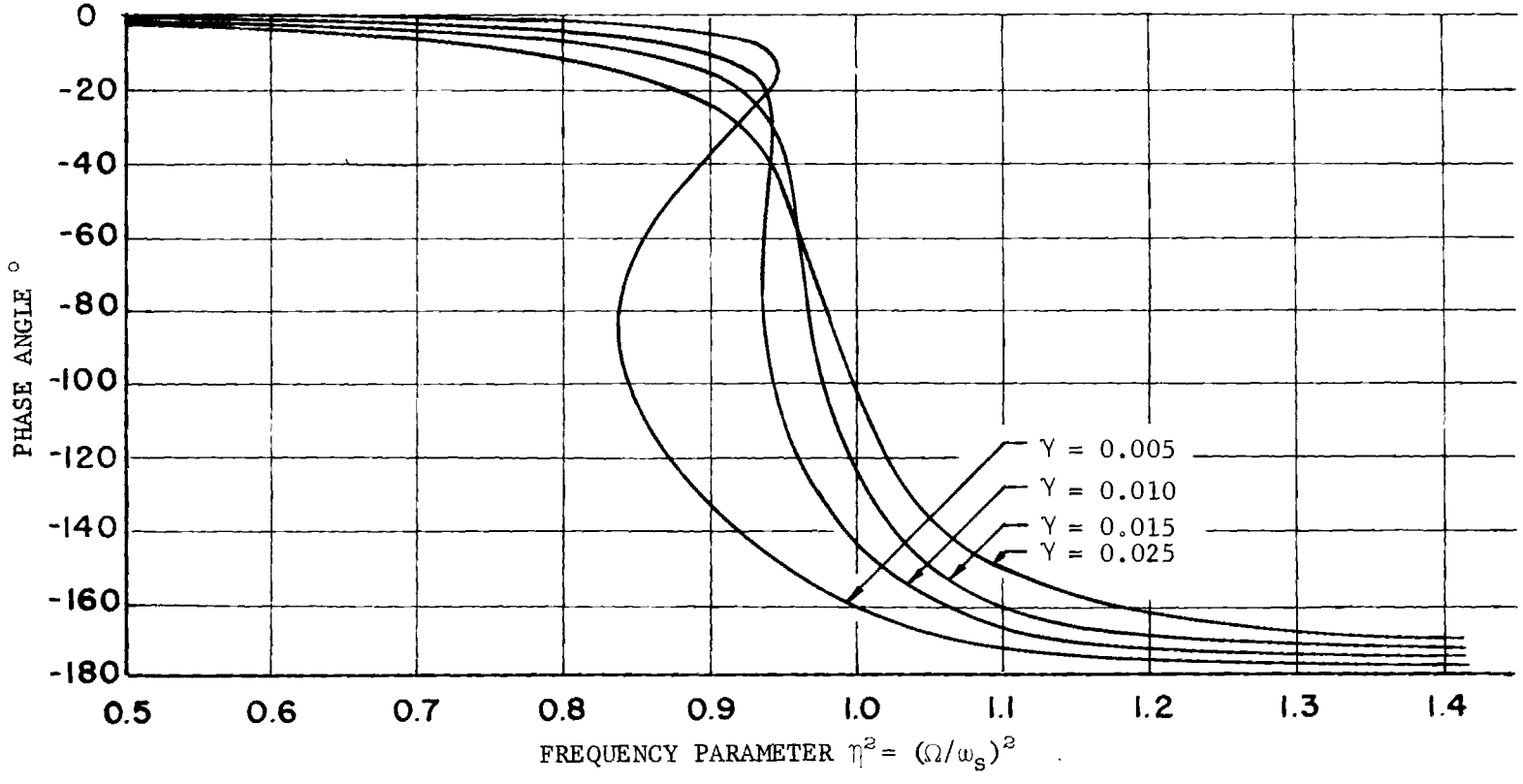

FIGURE 13: DAMPED PLANAR PHASE ANGLE

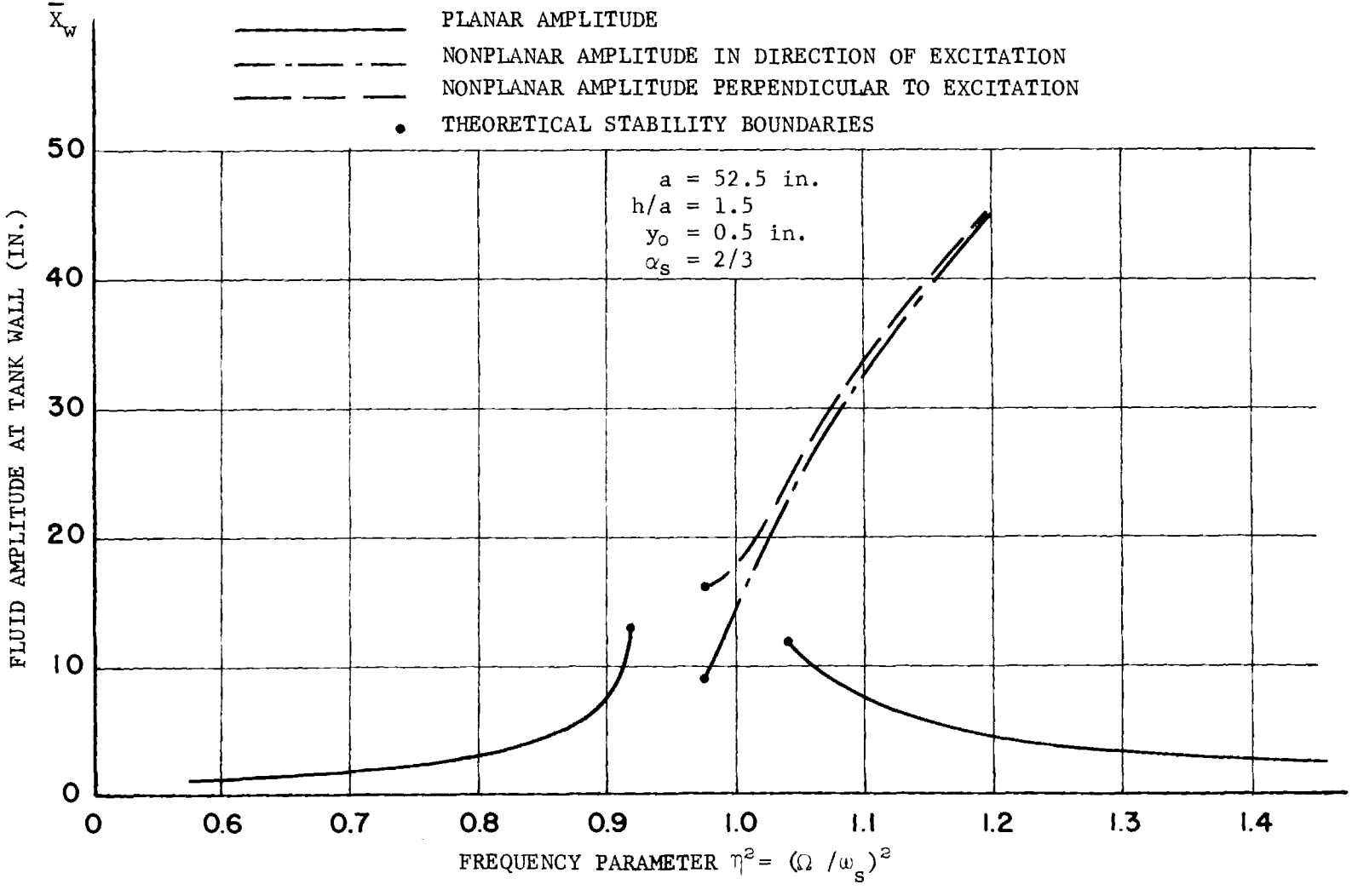

FIGURE 14: STABLE PLANAR AND NONPLANAR RESPONSE FOR JUPITER TANK